DEPARTMENT OF PHYSICS
INDIAN INSTITUTE OF TECHNOLOGY MADRAS
CHENNAI – 600036

Inflation and primordial perturbations in modified theories of gravitation

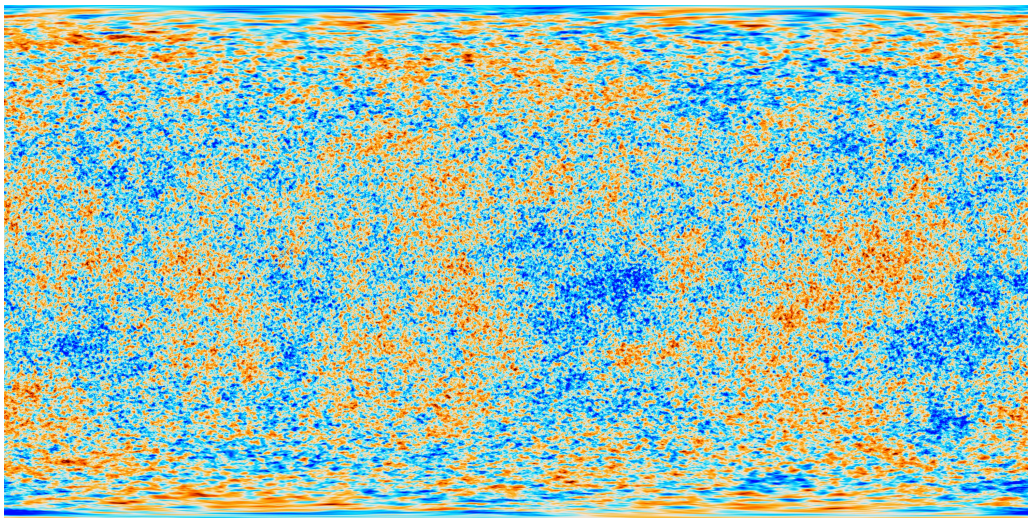

A Thesis

Submitted by

PULKIT BANSAL

For the award of the degree

Of

MASTER OF TECHNOLOGY

May 2023

DEPARTMENT OF PHYSICS
INDIAN INSTITUTE OF TECHNOLOGY MADRAS
CHENNAI – 600036

Inflation and primordial perturbations in modified theories of gravitation

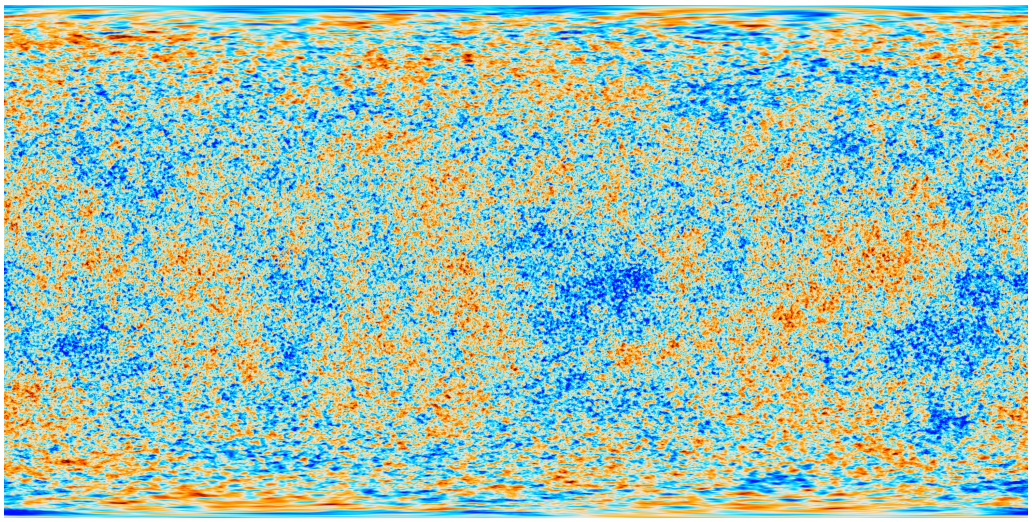

A Thesis

Submitted by

PULKIT BANSAL

For the award of the degree

Of

MASTER OF TECHNOLOGY

May 2023

Study hard what interests you the most in the most undisciplined, irreverent and original manner possible.

– Richard Feynman

THESIS CERTIFICATE

This is to undertake that the report on the dual degree project titled ***Inflation and primordial perturbations in modified theories of gravitation***, submitted by me to the Indian Institute of Technology Madras, for the award of **Master of Technology**, is a bona fide record of the research work done by me under the supervision of **Dr. L. Sriramkumar**. The contents of this Thesis, in full or in parts, have not been submitted to any other Institute or University for the award of any degree or diploma.

Chennai 600036 **Pulkit Bansal**

Date: 13 May 2023

Dr. L. Sriramkumar
Research advisor
Professor
Department of Physics
IIT Madras

ACKNOWLEDGEMENTS

I am very grateful to Prof. L. Sriramkumar for his time in mentoring me on this project. It was a wonderful opportunity to work under his tutelage. I am grateful for his patience, enthusiasm and all the knowledge I gained from him during those numerous valuable discussions.

I would like to thank Alipriyo Hoory, Suvashis Maity, Sagarika Tripathy and Neel Shah for important discussions, advice and for being wonderful seniors to me.

I would also like to thank my close friends Sumant, Saurabh, Viraj, Aniket, Daksh and Sarthak for a wonderful five years at this college and for their mental support during the pandemic.

Finally, I am deeply grateful to my parents and my brother for their support not only during the pandemic and the years I spent at IIT Madras but for my whole life. Words are not enough to express my gratitude to them.

ABSTRACT

KEYWORDS Inflation; perturbations; power spectra; $f(R)$ theories of gravitation; conformal transformation; Einstein frame; Jordan frame; Starobinsky model; Higgs model; radiative corrections; Critical Higgs Inflation

Inflation is a period of accelerated expansion of the universe during its early stages which was originally proposed to overcome the drawbacks of the standard big bang model. It also provides us a mechanism to generate primordial perturbations in the early universe which left their imprints on the Cosmic Microwave Background Radiation as anisotropies. Over the last few decades, different inflationary scenarios have been proposed and studied in the framework of general relativity as well as modified theories of gravitation beyond general relativity. The goal of this thesis is to study modified theories of gravitation, specifically $f(R)$ theories and understand how inflation arises from a purely gravitational origin in these theories without the need of an inflaton field. We will also study the generation of primordial perturbations during inflation in $f(R)$ theories and their relation to the single-field inflationary models in the framework of general relativity (usually referred to as the Einstein and Jordan frames). We will study the Starobinsky's $R + \alpha R^2$ inflationary model in detail. We will also discuss the inflationary dynamics in the theory of the non-minimally coupled Higgs field to gravitation in detail. W will see that both the theories agree very well with the observational constraints from the Planck 2018 data and are potential candidates for a viable inflationary theory.

CONTENTS

LIST OF FIGURES

NOTATION

η Conformal time

λ, ξ, σ Self-coupling, non-minimal coupling and vacuum expectation value of Higgs field

$\mathcal{H}$ Conformal Hubble parameter

$\mathcal{P}_S(k)$ Power spectrum of scalar curvature perturbation

$\mathcal{P}_T(k)$ Power spectrum of tensor perturbations

$\mathcal{R}_k$ Fourier modes of scalar curvature perturbation

ϕ Scalar field

$a(t)$ Scale factor

$F(R)$ Scalaron field: $\partial f/\partial R$

G Gravitational constant, $6.674 \times 10^{-11}\mathrm{Nkg}^{-2}\mathrm{m}^2$

H Hubble parameter

h_k Fourier modes of tensor perturbations

M_{Pl} Reduced Planck mass, $2.435 \times 10^{18}\mathrm{GeV/c}^2$

N E-folds

n_S Scalar spectral index

n_T Tensor spectral index

R Ricci scalar

r Tensor-to-scalar ratio

t Cosmic time

CHAPTER 1

INTRODUCTION

Einstein's insights and proposal of special relativity that described the intertwining of space and time to a degree never imagined before was of sheer brilliance. He, then, went on to propose the general theory of relativity where he linked the curvature of the spacetime with its mass-energy content. General Relativity (GR) is the most widely accepted fundamental theory of gravitation and spacetime today. The description of the geometric properties of spacetime and the hot big bang cosmological model which is the prevailing theory describing the evolution of universe at large scales can all be understood in the framework of GR. GR has passed observational tests time and time again from precession of the perihelion of Mercury to the existence of black holes, to the detection of the gravitational waves in 2015 and the list goes on.

The general theory of relativity is a tensor theory of gravitation. Gravitation is described by the metric tensor which relates the geometric properties of spacetime to the radiation and matter content of the universe. The final results of this idea are the *Einstein's field equations*, the relativistic equivalent of the Poisson's equation in Newtonian dynamics and are described by:

$$R_{\mu\nu} - \frac{1}{2} g_{\mu\nu} R = \frac{8\pi G}{c^4} T_{\mu\nu}. \tag{1.1}$$

In this equation, $g_{\mu\nu}$ is the metric tensor, $R_{\mu\nu}$ is the Ricci tensor, R is called the Ricci scalar, c is the speed of light in vacuum, G is the Newton's gravitational constant and $T_{\mu\nu}$ is called the stress-energy tensor. This set of elegant equations is what has cemented our understanding of gravitation and the universe.

Before moving forward, its best to clarify the notations and conventions that will be followed throughout the thesis. We shall set $\hbar = c = 1$ and assume the Planck mass to

be $M_{\rm Pl} = (8\pi G)^{-1/2}$. We shall work in $(3+1)$ spacetime dimensions with the metric signature of $(-,+,+,+)$ for the FLRW metric unless explicitly mentioned otherwise. An overdot will represent the derivative with respect to the cosmic time t and an overprime will represent the derivative with respect to the conformal time $\eta = \int dt/a(t)$. We will use Greek indices to denote the spacetime coordinates and Latin indices to denote the spatial coordinates.

1.1 THE FLRW UNIVERSE

Decades of observations have pointed to the fact that we live in an expanding universe. Today, the universe is assumed to be isotropic and homogeneous on large scales and is in a phase of accelerated cosmic expansion. The Friedmann-Lemaître-Robertson-Walker (FLRW) metric which describes such a homogeneous and isotropic universe is given by:

$$ds^2 = -dt^2 + a^2(t)\left(\frac{dr^2}{1-\kappa r^2} + r^2(d\theta^2 + sin^2\theta d\phi^2)\right), \tag{1.2}$$

where the curvature constant κ takes on the values [-1, 0, 1] describing a hyperbolic (spatially open), Euclidean (spatially flat) or a spherical (spatially closed) universe, respectively. The scale factor $a(t)$ describes how the physical distances change overtime as the universe expands or contracts. Observations have shown that we live in a nearly spatially flat universe.

1.1.1 The Friedmann equations

For the FLRW metric described by Eq.(1.2) and the stress-energy tensor of the form $T^{\mu}_{\nu} = diag(-\rho, p, p, p)$, the Einstein's equations simplify to the following form:

$$\left(\frac{\dot{a}}{a}\right)^2 + \frac{\kappa}{a^2} = \frac{8\pi G}{3}\rho, \tag{1.3}$$

$$\frac{\ddot{a}}{a} = -\frac{4\pi G}{3}(\rho + 3p). \tag{1.4}$$

These are the famous *Friedmann equations* derived by Alexander Alexandrovich Friedmann in 1922. The quantities ρ and p denote the energy density and pressure of

additional fields respectively. We can see that depending on the equation of state of the energy content of the universe, we will have different solutions to the Friedmann equations. A very useful quantity called the Hubble parameter is defined as $H = \dot{a}/a$ and its present value is called the Hubble constant and is denoted by H_0.

1.1.2 Solutions to the Friedmann equations

Eq.(1.3) and Eq.(1.4) can be used to get another equation which governs the conservation of the stress-energy tensor and is given by:

$$\dot{\rho} = -3H(\rho + p). \tag{1.5}$$

This means that the conservation of the stress-energy tensor does not give an independent equation and therefore, we have a set of 2 independent equations describing the FLRW universe. For an equation of state of the form: $p = w\rho$, we can solve Eq.(1.5) which gives us the following solution:

$$\rho = \rho_0 \left(\frac{a}{a_0}\right)^{-3(1+w)}. \tag{1.6}$$

We can always take the scale factor at present times and set $a_0 = 1$. Three major components of the universe are:

- **Radiation**: The equation of state for radiation is $p = \rho/3$ and so $\rho_\gamma \propto a^{-4}$.
- **Non-relativistic matter**: The equation of state for non-relativistic matter is $p = 0$ and so $\rho_M \propto a^{-3}$.
- **Dark energy**: Also referred to as the cosmological constant, it exerts a negative pressure with the equation of state given by: $p = -\rho$ which leads to $\rho_\Lambda = constant$.

Now, the first observation is that the the energy density of the radiation decreases at a faster rate than that of the non-relativistic matter while on the other hand the energy density of the dark energy is constant with the expansion of the universe. This leads to the crucial point that the early universe was radiation dominated followed by an epoch of matter domination. Today, we believe that we are in the epoch where the cosmological constant dominates the universe and although we still don't know the nature of the dark

energy we have strong observational evidence that it is out there and is responsible for the accelerated expansion of the universe at present times.

1.2 DRAWBACKS OF THE HOT BIG BANG MODEL

The decreasing nature of the energy density of matter and radiation with the expansion of the universe coupled with the earlier conclusion that the density of radiation falls at a much faster rate than that of the matter points to the vital conclusion that the early universe was in a hot and dense phase dominated by radiation and with its expansion it cooled down, the hot plasma combined to form neutral atoms and radiation stopped interacting with matter leading to a transition to the matter dominated era. Hence, the theory is named the *hot* big bang model. The Cosmic Microwave Background (CMB) Radiation is the relic radiation that reaches us today from the last scattering surface (the epoch of matter-radiation decoupling) and is a treasure box full of information describing the state of the early universe. In fact, the discovery of CMB was one of the crucial reasons that favoured the hot big bang model as in a big bang universe, the CMB would arise naturally if the universe was initially hot and very dense. The CMB is fairly isotropic but it does have small fluctuations. While the CMB favoured the hot big bang model over others, it also showed us a major flaw in the theory.

1.2.1 The horizon problem

The CMB that we see today was emitted when the universe was about 300,000 years old. Today, the universe is about 13.6 billion years old and photons from CMB that are reaching us from sufficiently separated regions of the sky should not have interacted with each other at the time of decoupling. So, the CMB sky that we see should actually be like a collection of causally disconnected mini-universes. They could not have interacted with each other from the time of big bang till the epoch of decoupling under the hot big bang model. And yet, what we see is that the temperature of photons from these disconnected mini-universes is identical with a variation of one part in 10^5. The hot

big bang model fails to provide an explanation to this observation. This is the *horizon problem*. Figure 1.1 shows the horizon problem interpreted in terms of the past light cones.

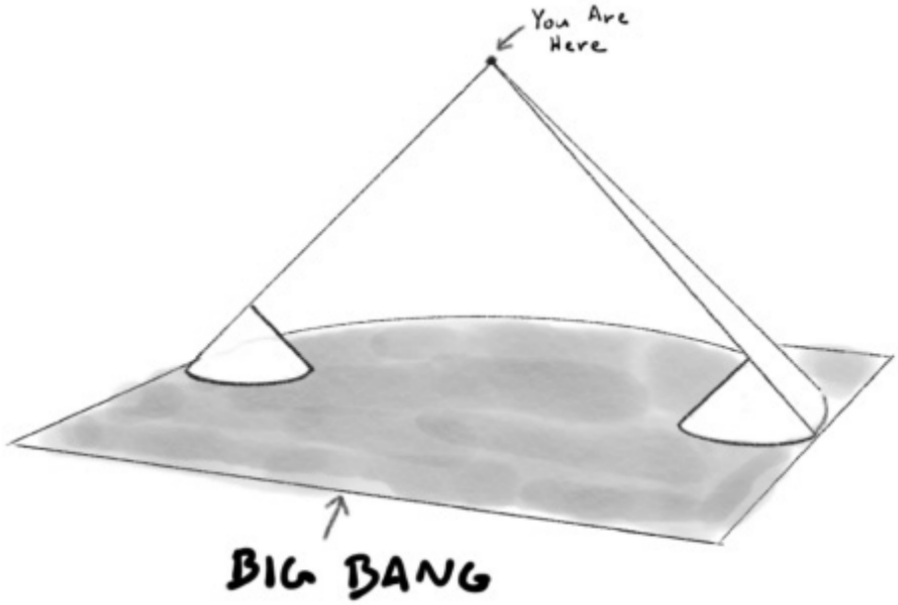

Figure 1.1: Diagram showing the horizon problem. If we look along the past light cones of two sufficiently separated points in spacetime, we find that they should not be causally connected at all in the past. Image obtained from Will Kinney [2].

We will now see a quantitative explanation of the horizon problem. The size of the observable universe also referred to as the cosmological horizon is the maximum distance light could have travelled before reaching the observer throughout the age of the universe. The horizon is therefore given by:

$$h(t) = a(t) \int_0^t \frac{d\tilde{t}}{a(\tilde{t})}. \tag{1.7}$$

Now, if we assume that the universe has been matter-dominated since the time of decoupling t_{dec} till today t_0, then the size of the backward light cone at the time of decoupling is given by:

$$l_B(t_0, t_{dec}) \simeq 3(t_{dec}^2 t_0)^{1/3}. \tag{1.8}$$

Similarly, assuming a radiation dominated universe from the big bang till the last scattering surface, the size of the forward light cone at the time of decoupling is:

$$l_F(t_{dec}, 0) = 2t_{dec}. \tag{1.9}$$

Taking $t_0 \simeq 10^{10}$ years and $t_{dec} \simeq 10^5$ years [3], the ratio of these two reduces down to:

$$\frac{l_B}{l_F} = \frac{3}{2}\left(\frac{t_0}{t_{dec}}\right)^{1/3} \simeq 70. \tag{1.10}$$

So, we see that the backward light cone is about 70 times larger than the forward light cone at the last scattering surface and hence the entire CMB sky could not have been in causal interaction. And yet, mother nature begs to differ! There are other shortcomings of the big bang model such as the flatness problem which questions how the energy density of the universe is fine-tuned to be so close to its critical value to maintain a spatially flat universe even after billions of years (See Refs.[7]-[10] for detailed discussions). So, how can we explain all this?

1.3 THE IDEA OF COSMIC INFLATION

The inflationary scenario is the most widely accepted solution to the problems with the big bang model: the horizon and the flatness problem [1]. Inflation refers to a period of exponential expansion of the universe in its very early stages. So, we say that just after the big bang (say at about $t \simeq 10^{-36}$ sec.), there was an epoch of accelerated outward expansion of the universe enough to make-up for the differences in the sizes of the forward and the backward light cones at decoupling allowing for a causal interaction of the CMB in the past and resolving the horizon problem. Figure 1.2 illustrates this discussion on how inflation resolves the horizon problem.

But that's not the only thing it offers! It also provides us with a natural mechanism for the origin and evolution of primordial perturbations which left their imprints as anisotropies in the CMB sky. Chapter 2 is primarily focused on the generation of

primordial perturbations to explain the fluctuations in the CMB.

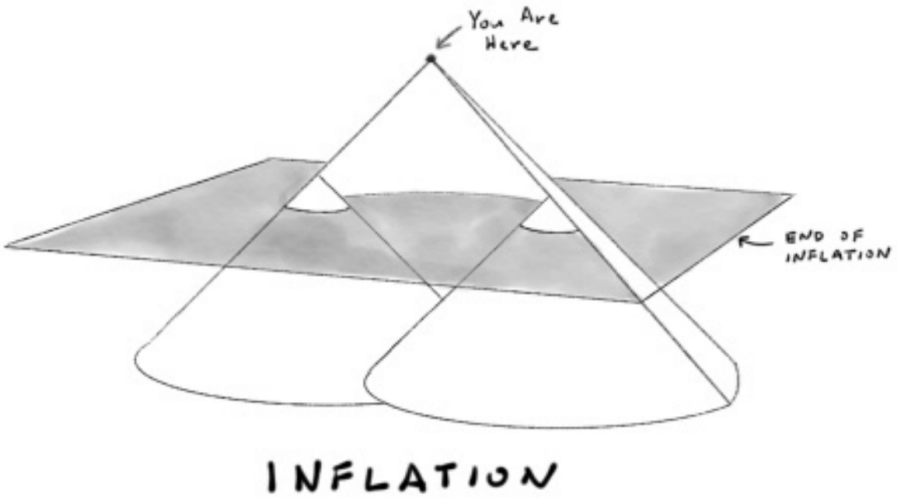

Figure 1.2: Diagram explaining how inflation resolved the horizon problem. The era of inflation allows for the light cones to overlap in the distant past allowing their causal interaction before. Image obtained from Will Kinney [2].

So, we believe that our universe underwent two stages of cosmic acceleration: one in its very early stages which also stretched the curvature of the universe to a very large scale thus flattening it out and the other is the accelerated expansion ongoing today. But now the question is, what caused inflation?

Now, the physical wavelengths (λ_P) are proportional to the scale factor $a(t)$. On the other hand, the Hubble radius $d_H = H^{-1} \propto a^{1/q}$ assuming the scale factor $a(t) \propto t^q$. For both matter as well as radiation, $q < 1$. This means that Hubble radius expands at a faster rate compared to the physical wavelengths which means that they enter the Hubble radius at certain points in time during one of the epochs. Observations have shown that the large scales associated with the CMB (1 Mpc to 10^4 Mpc) are highly isotropic with an anisotropy of about one part in 10,000. Unless we impose isotropic initial conditions on these scales, they must be in causal interaction in the past as well which means that they were once inside the Hubble radius sometime in the past. So, to avoid assuming isotropic initial conditions or invoking an acausal mechanism, there must be an epoch in the early universe when the physical wavelengths grew faster than the Hubble radius

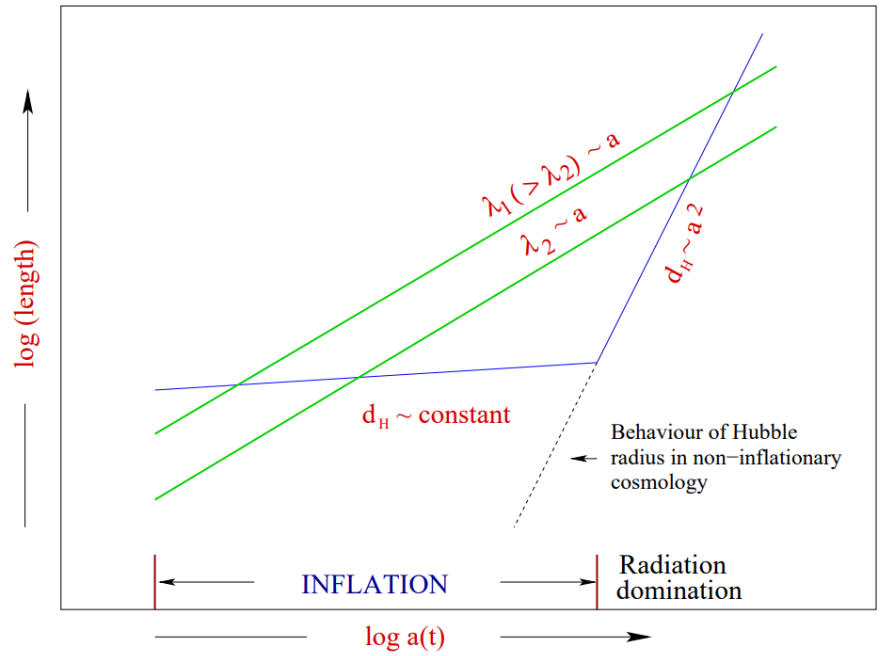

Figure 1.3: Evolution of the Hubble radius and the physical wavelengths during inflation and the radiation dominated epoch. Image obtained from L. Sriramkumar [3].

giving the condition:

$$\frac{d}{dt}\left(\frac{\lambda_P}{d_H}\right) > 0. \tag{1.11}$$

And this gives us the condition that $\ddot{a} > 0$ which implies accelerated expansion of the scale factor, that is, *a period of inflation*. Now, during inflation the Hubble radius remains almost the same and so modes leave the Hubble radius during inflation and re-enter at later times. Figure 1.3 illustrates the evolution of the physical wavelengths and the Hubble radius during inflation and the radiation dominated epoch.

1.3.1 How long must inflation last?

We take this opportunity to introduce another important variable called the e-folds N which is defined as:

$$N = \int H dt = ln\left(\frac{a}{a_i}\right). \tag{1.12}$$

Now, if we assume that the scale factor evolved as $a(t) \propto e^{Ht}$ during inflation, the size of the forward light cone assuming that inflation occurs from $t = t_i$ till $t = t_f$ and is mainly responsible for the expansion of the scale factor till the time of decoupling, then:

$$l_{\mathrm{F}}\left(t_0, t_{\mathrm{dec}}\right) = a\left(t_{\mathrm{dec}}\right) \int_{t_{\mathrm{dec}}}^{t_0} \frac{\mathrm{d}\tilde{t}}{a(\tilde{t})} \simeq \left[\frac{a\left(t_{\mathrm{dec}}\right)}{H_{\mathrm{I}}}\right] \left(\frac{t_{\mathrm{dec}}}{t_{\mathrm{f}}}\right)^{1/2} e^{N}. \tag{1.13}$$

For $H_I = 10^{13}$, the ratio of the forward and the backward light cones reduces to:

$$\frac{l_B}{l_F} = \frac{10^{26}}{e^N}, \tag{1.14}$$

and so it is often said that we need about 60 e-folds of inflation to resolve the horizon problem. Typically, we expect to achieve around 60-70 e-folds of inflation in the models we study.

1.3.2 Driving inflation with the cosmological constant

We make use of the Friedmann equation given by Eq.(1.4) and impose the condition $\ddot{a} > 0$ which implies that $\rho + 3p < 0$ or $w < -1/3$ on the equation of state which rules out matter and radiation. Usually, we assume that the early universe had an early epoch when the positive cosmological constant (Λ) dominated corresponding to $w = -1$. From hereon, we shall assume a $spatially\ flat$ Friedmann universe which is supported by various observations on the distribution of the large scale structures, data from supernovae, the CMB, etc. Using Eq.(1.3) with $\kappa = 0$, we can write:

$$\left(\frac{\dot{a}}{a}\right)^2 = \frac{\Lambda}{3}, \tag{1.15}$$

which gives us:

$$a = a_i e^{\sqrt{\frac{\Lambda}{3}}t}, \tag{1.16}$$

and corresponds to an accelerated exponential expansion of the universe i.e. inflation. But there is a serious problem with using the cosmological constant to drive inflation since it will lead to eternal inflation and we need to connect inflation to the radiation dominated epoch at some point in time. So, we need something else which has a dynamical equation

of state, which effectively has an equation of state satisfying: $w < -1/3$ during inflation but changes overtime and causes inflation to end.

1.3.3 Driving inflation with scalar fields

The idea to use scalar fields to drive inflation was not realised until after a few years since the proposal of the inflationary scenario. Now, we know that models of inflation driven by a canonical scalar field agree very well with the observations. The scalar field ϕ is minimally coupled to gravitation and the potential $V(\phi)$ is required to be smooth so that the field ϕ evolves very slowly referred to as the slow roll evolution. The energy density and pressure of the scalar field turn out to be [4]:

$$\begin{aligned} \rho &= \frac{\dot{\phi}^2}{2} + V(\phi), \\ p &= \frac{\dot{\phi}^2}{2} - V(\phi), \end{aligned} \tag{1.17}$$

which shows us that if the field rolls slowly, the potential term dominates the kinetic term which leads to $\rho \simeq -p$ similar to what we got for the cosmological constant. But now, the equation of state is dynamical which will eventually cause inflation to end. Imposing the condition $w < 1/3$ on Eq.(1.17) gives us the condition:

$$V(\phi) > \dot{\phi}^2, \tag{1.18}$$

on the scalar field ϕ to cause inflation. The action with gravitation coupled minimally to ϕ in the framework of GR is given by:

$$S = \int d^4x\sqrt{-g}\left[\frac{1}{2\kappa^2}R - \frac{1}{2}g^{\mu\nu}\partial_\mu\phi\partial_\nu\phi - V(\phi)\right]. \tag{1.19}$$

For now, we will account for the field ϕ and won't account for additional fields. These are the single-field inflationary models. The Friedmann equations then simplify to give:

$$\begin{aligned} H^2 &= \frac{1}{3M_{\rm Pl}^2}\left(\frac{\dot{\phi}^2}{2} + V(\phi)\right), \\ \dot{H} &= -\left(\frac{1}{2M_{\rm Pl}^2}\right)\dot{\phi}^2, \end{aligned} \tag{1.20}$$

and the equation of motion governing the scalar field is given by:

$$\ddot{\phi} + 3H\dot{\phi} + \frac{dV}{d\phi} = 0. \tag{1.21}$$

Integrating these equations with respect to the cosmic time t, we get:

$$\begin{aligned} \phi(t) &= \sqrt{2}M_{\rm Pl}\int \mathrm{d}t\sqrt{-\dot{H}}, \\ V(t) &= M_{\rm Pl}^2\left(3H^2 + \dot{H}\right). \end{aligned} \tag{1.22}$$

Slow-roll inflation

We can construct analytical solutions to the background dynamics under the condition that the field rolls slowly down the potential for an adequate period of time which guarantees inflation to take place. This is denoted by:

$$\begin{aligned} \dot{\phi}^2 &\ll V(\phi), \\ \ddot{\phi} &\ll 3H\dot{\phi}. \end{aligned} \tag{1.23}$$

Inflation can also be achieved with non-trivial potentials which violate the slow-roll conditions and in such cases, we need a numerical approach to solve for the dynamics which we will see later. We now define the slow-roll parameters to get a better understanding of the background dynamics and the evolution of the field:

$$\begin{aligned} \epsilon_1 &= \frac{\mathrm{d}\ln H}{\mathrm{d}N} = -\frac{\dot{H}}{H^2}, \\ \epsilon_n &= \frac{\mathrm{d}\ln\epsilon_{n-1}}{\mathrm{d}N}, \quad n > 1. \end{aligned} \tag{1.24}$$

The first slow-roll parameter ϵ_1 is of crucial importance since it's evolution tells us about the background evolution and marks the end of inflation when $\epsilon_1 > 1$. Under the slow-roll approximations, the first two slow-roll parameters can be used to determine the nature of the potential. Their relation to the potential can be expressed as [3]:

$$\begin{aligned} \epsilon_1 &\simeq \frac{M_{\rm Pl}^2}{2}\left(\frac{V_\phi}{V}\right)^2, \\ \epsilon_2 &\simeq 2M_{\rm Pl}^2\left[\left(\frac{V_\phi}{V}\right)^2 - \frac{V_{\phi\phi}}{V}\right], \end{aligned} \tag{1.25}$$

where $V_\phi = dV/d\phi$ and $V_{\phi\phi} = d^2V/d\phi^2$. We shall discuss the background dynamics for specific potentials in the next chapter. We will also see that the slow-roll parameters are very useful in the calculations of the perturbations and primordial power spectra.

1.4 ORGANIZATION OF THE THESIS

In chapter 2, we will discuss the cosmological perturbation theory to the linear order and study the evolution of perturbations in the inflationary universe. We will also discuss the analytical solutions of the power spectra in slow-roll inflation and conclude the chapter with numerical approaches to study the perturbations with examples of two specific inflationary models.

In chapter 3, we will start our discussion of modified theories of gravity. The primary focus of this thesis are the $f(R)$ models of gravity: how inflation is driven in these models, how the background and perturbations evolve in these models during inflation and the conformal transformations that relate $f(R)$ theories to a scalar-tensor theory in the Einstein frame. We shall also discuss approximate analytical solutions (similar to slow-roll) to the perturbations in $f(R)$ theories and the numerical methods to compute the evolution of perturbations.

In chapter 4, we will take on the Starobinsky's $R + \alpha R^2$ model. We will first discuss approximate solutions to the background dynamics during inflation in the Starobinsky model and then discuss the evolution of perturbations during inflation in both the Einstein and Jordan frame.

In chapter 5, we will present the non-minimally coupled Higgs inflationary model and discuss the dynamics in both the Einstein and Jordan frame. We will conclude this chapter with a comparison of the dynamics in the Higgs model with the Starobinsky model.

In chapter 6, we will talk about modifications to the Higgs model from quantum field theory to the potential. First, we will discuss radiative corrections to the Higgs potential due to one loop corrections. Second, the critical Higgs inflation (CHI) model which incorporates the running of couplings. We shall also touch upon the unitarity problem and possible modifications in the Higgs model to unitarize the theory.

CHAPTER 2

COSMOLOGICAL PERTURBATION THEORY

In the previous chapter, we discussed the background dynamics during inflation in a smooth and spatially flat FLRW universe. However, the CMB does posses small anisotropies which need to be explained. Fortunately, inflation also provides us with a mechanism to explain the origin and evolution of primordial perturbations in the early universe which left their imprints on the CMB. In this chapter, we shall discuss the cosmological perturbation theory to linear order and the evolution of primordial perturbations in single-field inflationary models driven by a canonical scalar field. The scalar field driving inflation is also referred to as the inflaton field.

2.1 METRIC PERTURBATIONS

The Einstein's equations show us that we need to consider inhomogeneous metric perturbations about the FLRW metric for an inhomogeneous matter distribution. The perturbed FLRW metric is then described as [5]:

$$ds^2 = -(1+2A)dt^2 + 2a\left(\partial_i B - S_i\right)dx^i dt + a^2\left[(1-2C)\delta_{ij} + 2\partial_{ij}E + 2\partial_{(i}F_{j)} + h_{ij}\right]dx^i dx^j. \tag{2.1}$$

The metric perturbations can be decomposed into scalar, vector and tensor perturbations depending on how they transform on spatial hypersurfaces. In Eq.(2.1) A, B, C, E represent the scalar perturbations; F_i, S_i represent the divergence-free vector perturbations and h_{ij} represents the transverse, traceless and symmetric tensor perturbations. At the linear order, they evolve independently and so we can study them separately.

2.1.1 Gauge fixing

We can see from Eq.(2.1) that the perturbed FLRW metric possesses 10 degrees of freedom: 4 describing scalar perturbations, 4 describing vector perturbations and 2 describing tensor perturbations. But that's not the end of the story because some of them are redundant degrees of freedom. Four degrees of freedom are associated with coordinate transformations which are dictated by the amplitude of the perturbations in different coordinate systems and are referred to as gauge transformations. So, what is this gauge dependence and why is it a problem?

Well, we know that the Einstein's equations put space and time on an equal footing. But to describe our universe we chose the background which has maximally symmetric spatial hypersurfaces, that is, the FLRW background. So, we picked the comoving coordinate system and this preferred space+time split in FLRW cosmology broke the symmetry of Einstein's theory at the cost of describing a maximally symmetric spatial universe as we desired. But now in an inhomogeneous universe, there is no unique choice of coordinate system because the symmetry in the matter flow is broken. So, we have an arbitrary choice of coordinate system which leads to the gauge problem: Amplitudes of perturbations are different in different gauges. Hence, we need to work in a particular gauge to get unique solutions or use gauge invariant quantities as we shall see later in this chapter [3, 4].

There are different gauges described in the literature which help simplify the calculations. We will list down a few here (refer [5] for details).

- Longitudinal or the Conformal Newtonian gauge
- Uniform density gauge
- Comoving gauge
- Spatially flat gauge

and the list goes on. So in a 3+1 dimensional spacetime, there exists six degrees of

freedom: 2 each of scalar, vector and tensor perturbations. We will now start our discussion on the scalar perturbations.

2.1.2 Scalar perturbations

In Eq.(2.1), A, B, C, E are the scalar perturbations. Generally, A is referred to as the lapse perturbation, $\partial_i B$ as the shift perturbation, C as the spatial curvature perturbation and $\partial_{ij} E$ as the off-diagonal spatial perturbation. We shall work in the longitudinal gauge which corresponds to $A = \Phi, B = 0, C = \Psi, E = 0$ and study the scalar perturbations only since we can study them separately at the linear order. The Friedmann line element is then given by:

$$\mathrm{d}s^2 = -(1+2\Phi)\mathrm{d}t^2 + a^2(t)(1-2\Psi)\mathrm{d}\boldsymbol{x}^2. \tag{2.2}$$

We shall be working with scalar sources with do not possess anisotropic stress. Under this assumption, perturbing the Einstein's equations to linear order for the above metric gives us the following set of equations [3]:

$$\begin{aligned}
&\Phi = \Psi, \\
&\delta G^0_0 = 6H(\dot{\Phi} + H\Phi) - \frac{2}{a^2}\nabla^2\Phi = -8\pi G\delta\rho, \\
&\delta G^0_i = -2\nabla_i(\dot{\Phi} + H\Phi) = -8\pi G\left(\nabla_i\delta\sigma\right), \\
&\delta G^i_j = 2\left[\ddot{\Phi} + 4H\dot{\Phi} + \left(2\dot{H} + 3H^2\right)\Phi\right]\delta^i_j = 8\pi G\delta p\delta^i_j.
\end{aligned} \tag{2.3}$$

We make use of the second and the fourth relations in the above set of equations to get the evolution of the scalar perturbation Φ (also known as the Bardeen potential) [3]:

$$\Phi'' + 3\mathcal{H}\left(1 + c_{\mathrm{A}}^2\right)\Phi' - c_{\mathrm{A}}^2\nabla^2\Phi + \left[2\mathcal{H}' + \left(1 + 3c_{\mathrm{A}}^2\right)\mathcal{H}^2\right]\Phi = \left(4\pi G a^2\right)\delta p^{\mathrm{NA}}, \tag{2.4}$$

where $\mathcal{H} = a'/a$ is referred to as the conformal Hubble parameter, c_A is the adiabatic speed of perturbations and δp^{NA} is the non-adiabatic component of the pressure perturbation defined as:

$$\begin{aligned}
c_A &= \sqrt{p'/\rho'}, \\
\delta p^{NA} &= \delta p - c_A^2\delta\rho.
\end{aligned} \tag{2.5}$$

A very useful gauge invariant quantity

We shall now define a very useful quantity which remains conserved at super-Hubble scales. This is the scalar curvature perturbation which is defined in terms of the Bardeen potential as follows [3]:

$$\mathcal{R} = \Phi + \left(\frac{2\rho}{3\mathcal{H}}\right)\left(\frac{\Phi' + \mathcal{H}\Phi}{\rho + p}\right). \tag{2.6}$$

We now move to the Fourier space to study the evolution of different modes of the curvature perturbations. Using Eq.(2.6), (2.4) and the background equations, we get:

$$\mathcal{R}_k' = \left(\frac{\mathcal{H}}{\mathcal{H}^2 - \mathcal{H}'}\right)[(4\pi G a^2)\delta p_k^{NA} - c_A^2 k^2 \Phi_k], \tag{2.7}$$

where the subscript k denotes the Fourier modes of perturbations. If we consider perturbations at super Hubble scales which corresponds to $k/aH \ll 1$, then we can neglect the second term. Under the assumption that the non-adiabatic component of the pressure perturbations vanishes, we get that $\mathcal{R}_k' \simeq 0$ and hence the curvature perturbation remains conserved at super-Hubble scales.

2.1.3 Vector perturbations

F_i and S_i are the two divergence-free vector perturbations. If we consider only the vector perturbations, perturbing the Einstein's equations yields the following [6]:

$$\begin{aligned} \nabla^2(F_i' + S_i) &= 16\pi G a^2 [V_i^v - S_i][\rho + p], \\ F_i'' + S_i' + 6\mathcal{H}[F_i' + S_i] &= 16\pi G a^2 \Pi_i^v, \end{aligned} \tag{2.8}$$

where V_i^v represents the transverse part of the matter velocity and Π_i^v represents the vector sources. The first relation in the above pair of equations is the momentum constraint and the second equation is the dynamical equation for the vector perturbations. In the absence of any anisotropic stress, we get:

$$F_i' + S_i \propto a^{-6}, \tag{2.9}$$

which shows that the transverse vector perturbations decay rapidly in the absence of any vector sources. This is why we will not observe them in the early universe because scalar

sources like the inflaton field do not have any vorticity and so we don't see any signatures of the vector perturbations in the CMB either.

2.1.4 Tensor perturbations

The tensor perturbations have two degrees of freedom which correspond to the two polarization states of the gravitational waves. The Friedmann line element is then given by:

$$\mathrm{d}s^2 = -\mathrm{d}t^2 + a^2(t)(\delta_{ij} + h_{ij})\mathrm{d}x^i\mathrm{d}x^j. \tag{2.10}$$

Perturbing the Einstein's equations and imposing the transverse and traceless conditions on h_{ij} gives us:

$$\ddot{h}_{ij} + 3H\dot{h}_{ij} - \nabla^2 h_{ij} = (8\pi G)\Pi^t, \tag{2.11}$$

where Π^t represents the tensor sources. It is interesting to note that even in the absence of any tensor sources, we get non-trivial solutions to the above equation i.e. freely propagating gravitational waves exist and we will study their evolution during inflation driven by the inflaton field.

2.2 GENERATING PRIMORDIAL PERTURBATIONS DURING INFLATION

How does inflation provide a mechanism for generating primordial perturbations? It is the quantum fluctuations of the inflaton field that got stretched to the classical regime during inflation and left their imprints as inhomogeneities on the CMB. We will now derive the equations of motion for scalar and tensor curvature perturbations when the universe was dominated by the inflaton field.

Given the inflaton field ϕ, we will denote the perturbations in the field as $\delta\phi$. We can then calculate the perturbed stress-energy tensor which is given by the following equations

[3]:

$$\begin{aligned}
\delta T^0_0 &= \left(\dot{\phi}\dot{\delta\phi} - \dot{\phi}^2\Phi + V_\phi\delta\phi\right) = \delta\rho, \\
\delta T^0_i &= \nabla_i(\dot{\phi}\delta\phi) = \nabla_i(\delta\sigma), \\
\delta T^j_i &= -\left(\dot{\phi}\dot{\delta\phi} - \dot{\phi}^2\Phi - V_\phi\delta\phi\right)\delta^j_i = -\delta p\delta^j_i.
\end{aligned} \tag{2.12}$$

Substituting the above equations in Eq.(2.3) and comparing the result to Eq.(2.4) shows that the non-adiabatic pressure perturbation associated with the inflaton field turns out to be:

$$\delta p^{NA} = \left(\frac{1 - c_A^2}{4\pi G a^2}\right)\nabla^2\Phi, \tag{2.13}$$

and Eq.(2.7) reduces to:

$$\mathcal{R}' = \left(\frac{\mathcal{H}}{\mathcal{H}^2 - \mathcal{H}'}\right)\nabla^2\Phi. \tag{2.14}$$

From Eq.(2.13), we see that the inflaton field has a non-zero non-adiabatic pressure perturbation. Writing Eq.(2.14) in terms of Fourier modes, at super-Hubble scales we get $\mathcal{R}'_k \simeq 0$. The modes freeze after they leave the Hubble radius and so we only need to concern ourselves with the evolution of the modes during inflation when they are inside the Hubble radius. Differentiating the above equation and using Eq.(2.4), Eq.(2.13) and the Friedmann equations, we arrive at the equation of motion describing the evolution of the scalar curvature perturbation:

$$\mathcal{R}'' + 2\left(\frac{z'}{z}\right)\mathcal{R}' - \nabla^2\mathcal{R} = 0, \tag{2.15}$$

where z = $\frac{a\dot{\phi}}{H} = \frac{a\phi'}{\mathcal{H}}$.

2.2.1 Quantization of primordial perturbations

We now quantize the primordial perturbations $\mathcal{R}$ and h_{ij} since they originate from the quantum fluctuations stretched to large scales during inflation. On quantizing the perturbations, we can write $\mathcal{R}$ and h_{ij} in terms of their Fourier modes due to the homogeneity of the Friedmann universe. This gives us the equations of motion for the evolution of the Fourier modes of the scalar and tensor curvature perturbations (both polarizations) as the following:

$$\mathcal{R}_k'' + 2\left(\frac{z'}{z}\right)\mathcal{R}_k' + k^2\mathcal{R}_k = 0, \tag{2.16}$$

$$h_k'' + 2\mathcal{H}h_k' + k^2 h_k = 0. \tag{2.17}$$

We will be using the above equations for the exact numerical computation of the evolution of the perturbations later. It is worthwhile to note that the above pair of equations can also be derived from the action governing these perturbations at the quadratic order given by:

$$\begin{aligned}\mathcal{S}_2[\mathcal{R}] &= \frac{1}{2}\int \mathrm{d}\eta \int \mathrm{d}^3\boldsymbol{x} z^2 \left[(\mathcal{R}')^2 - (\partial\mathcal{R})^2\right], \\ \mathcal{S}_2\left[h_{ij}\right] &= \frac{M_{\rm Pl}^2}{8}\int \mathrm{d}\eta \int \mathrm{d}^3\boldsymbol{x} a^2 \left[(h_{ij}')^2 - \left(\partial h_{ij}\right)^2\right].\end{aligned} \tag{2.18}$$

These actions are derived by making use of the ADM formalism of general relativity which is especially used to derive the three-point correlation functions of the primordial perturbations. We have discussed the derivation of the above actions from the ADM formalism in Appendix A.

The Mukhanov-Sasaki variable

We now introduce the Mukhanov-Sasaki variable which is defined as $v = \mathcal{R}z$. Substituting this in terms of the Fourier modes of the variable v back in Eq.(2.16) simplifies to the following:

$$v_k'' + \left(k^2 - \frac{z''}{z}\right)v_k = 0. \tag{2.19}$$

Similarly, we can substitute $u = ha/\sqrt{16\pi G}$ in Eq.(2.17) which gives us:

$$u_k'' + \left(k^2 - \frac{a''}{a}\right)u_k = 0. \tag{2.20}$$

These two equations will come in handy to impose initial conditions on the Fourier modes of the perturbations. Now, the initial conditions on the perturbations are imposed when they are deep within the Hubble radius i.e. at sub-Hubble scales which corresponds to $k/aH \gg 1$. Under this condition, we can see from Eq.(2.19) that the modes will not be affected by the spacetime curvature when the modes satisfy $k \gg \sqrt{z''/z}$ and $k \gg \sqrt{a''/a}$

respectively, which reduces the above equations to that of a simple harmonic oscillator. The vacuum state associated with the modes in this limit is known as the Bunch-Davies vacuum and the normalised initial conditions imposed on the modes have the asymptotic form [8]:

$$\lim_{k/aH\to\infty} u_k, v_k \to \frac{1}{\sqrt{2k}} e^{-ik\eta}. \tag{2.21}$$

The primordial power spectra

The scalar and tensor power spectra are defined in terms of the two-point correlation functions of $\mathcal{R}_k$ and h_k respectively through the following relations:

$$\begin{aligned} \left\langle \hat{\mathcal{R}}_{\boldsymbol{k}}\left(\eta_{\rm e}\right) \hat{\mathcal{R}}_{\boldsymbol{k}'}\left(\eta_{\rm e}\right)\right\rangle &= \frac{2\pi^2}{k^3}\mathcal{P}_{\rm S}(k)\delta^{(3)}\left(\boldsymbol{k}+\boldsymbol{k}'\right), \\ \left\langle \hat{h}^{\boldsymbol{k}}_{ij}\left(\eta_{\rm e}\right) \hat{h}^{ij}_{\boldsymbol{k}'}\left(\eta_{\rm e}\right)\right\rangle &= \frac{2\pi^2}{k^3}\mathcal{P}_{\rm T}(k)\delta^{(3)}\left(\boldsymbol{k}+\boldsymbol{k}'\right). \end{aligned} \tag{2.22}$$

Simplifying and using the Mukhanov-Sasaki variables in the above equations leads to:

$$\begin{aligned} \mathcal{P}_{\rm S}(k) &= \frac{k^3}{2\pi^2}\left(\frac{|v_k|^2}{z^2}\right), \\ \mathcal{P}_{\rm T}(k) &= \frac{4k^3}{M_{\rm Pl}^2\pi^2}\left(\frac{|u_k|^2}{a^2}\right). \end{aligned} \tag{2.23}$$

We can also define the scalar and tensor spectral indices and the tensor-to-scalar ratio in the following way:

$$\begin{aligned} n_{\rm S} &= 1 + \frac{{\rm dln}\mathcal{P}_{\rm S}}{{\rm dln}k}, \\ n_{\rm T} &= \frac{{\rm dln}\mathcal{P}_{\rm T}}{{\rm dln}k}, \\ r &= \frac{\mathcal{P}_{\rm T}}{\mathcal{P}_{\rm S}}. \end{aligned} \tag{2.24}$$

Now that we have derived all the equations governing the evolution of the background and the perturbations during inflation, we shall now discuss solutions to these equations.

2.3 SLOW-ROLL SOLUTIONS TO THE PRIMORDIAL POWER SPECTRA

We cannot obtain exact analytical solutions to the evolution of the perturbations as well as the background. So, generally we employ numerical means. However, we can obtain

analytical solutions in the slow-roll approximation. In slow-roll inflation, we can express the quantities z''/z and a''/a in terms of the slow-roll parameters using the following equations:

$$\begin{aligned} z &= M_{\rm Pl}\sqrt{2\epsilon_1}a, \\ \mathcal{H} &\simeq -\frac{1}{(1-\epsilon_1)\eta}. \end{aligned} \tag{2.25}$$

Using these equations, we express the quantities z''/z and a''/a to the leading order in ϵ_1 and ϵ_2 as follows:

$$\begin{aligned} \frac{z''}{z} &\simeq \left(2+3\epsilon_1+\frac{3\epsilon_2}{2}\right)\frac{1}{\eta^2}, \\ \frac{a''}{a} &\simeq (2+3\epsilon_1)\,\frac{1}{\eta^2}. \end{aligned} \tag{2.26}$$

Treating the slow-roll parameters as constant, we can rewrite Eq.(2.19) and Eq.(2.20) as Bessel differential equations whose solutions to the Mukhanov-Sasaki variables are the Hankel functions of the first kind. We can then obtain an analytical expression for the scalar and tensor power spectra in the slow-roll regime given by the following [3]:

$$\begin{aligned} \mathcal{P}_S(k) &\simeq \left(\frac{H^2}{2\pi\dot{\phi}}\right)^2\left((1-\epsilon_1)\frac{\Gamma(\nu_S)}{\Gamma(3/2)}\right)^2\left(\frac{|k\eta|}{2}\right)^{3-2\nu_S}, \\ \mathcal{P}_T(k) &\simeq 8\left(\frac{H}{2\pi M_{\rm Pl}}\right)^2\left((1-\epsilon_1)\frac{\Gamma(\nu_T)}{\Gamma(3/2)}\right)^2\left(\frac{|k\eta|}{2}\right)^{3-2\nu_T}, \end{aligned} \tag{2.27}$$

where $\nu_S \simeq \frac{3}{2}+\epsilon_1+\frac{\epsilon_2}{2}$, $\nu_T \simeq \frac{3}{2}+\epsilon_1$ and $\Gamma(\nu)$ denotes the Gamma function. We can also express the spectral indices and the tensor-to-scalar ratio in terms of the slow-roll parameters as follows:

$$\begin{aligned} n_S &\simeq 1-2\epsilon_1-\epsilon_2, \\ n_t &\simeq -2\epsilon_1, \\ r &\simeq 16\epsilon_1. \end{aligned} \tag{2.28}$$

We will compare these expressions to the approximate analytical solutions of the power spectra and the indices in the $f(R)$ theories in chapter 3 and specifically for the Starobinsky model in chapter 4.

2.4 NUMERICAL APPROACH TO THE POWER SPECTRA

We will now discuss the numerical approach to compute and study the exact background dynamics and the primordial power spectra. For numerical computations, we express all derivatives with respect to the e-foldings N and use the fourth-order Runge-Kutta method [11]. The equation of motion for the inflaton field is then:

$$\phi_{NN} + \left(3 - \frac{\phi_N^2}{2M_{\rm Pl}^2}\right)\left(\phi_N + \frac{V_\phi}{V}M_{\rm Pl}^2\right) = 0, \tag{2.29}$$

where the subscript N denotes derivative with respect to e-foldings N. Similarly, we can describe the Hubble parameter, the slow-roll parameters and the scale factor as:

$$\begin{aligned} H^2(N) &= \frac{V(\phi(N))}{M_{\rm Pl}^2[3-\epsilon_1(N)]}, \\ \epsilon_1(N) &= -\frac{\dot{H}}{H^2} = \frac{\phi_N^2}{2M_{\rm Pl}^2}, \\ \epsilon_2(N) &= \frac{{\rm d}\ln\epsilon_1}{{\rm d}N} = 2\frac{\phi_{NN}}{\phi_N}, \\ a(N) &= a_i e^N. \end{aligned} \tag{2.30}$$

So, with suitable initial conditions on the scalar field, we can solve Eq.(2.29) and hence obtain all the other quantities. To obtain the value of scale factor at the beginning of inflation, we fix when the pivot scale which corresponds to $k = 0.05{\rm Mpc}^{-1}$ leaves the Hubble radius and use the following equation:

$$a_i = \frac{k_{pivot}}{exp[N_{end} - N_{pivot}]H(N_{end} - N_{pivot})}, \tag{2.31}$$

where N_{end} is the duration of inflation in terms of e-folds and N_{pivot} denotes the e-folding at which the pivot scale exits the Hubble radius counted backwards from the end of inflation.

Now that we have the tools to evaluate the background dynamics, we talk about the evolution of perturbations. Rewriting Eq.(2.16), Eq.(2.17) in terms of derivatives of N

gives:

$$\begin{aligned}
&\frac{d^2\mathcal{R}_k}{dN^2} + \frac{d\mathcal{R}_k}{dN}\left(1 - \frac{1}{2M_{\rm Pl}^2}\left(\frac{d\phi}{dN}\right)^2 + \frac{2}{z}\frac{dz}{dN}\right) + \frac{k^2}{a^2H^2}\mathcal{R}_k = 0, \\
&\frac{d^2h_k}{dN^2} + \frac{dh_k}{dN}\left(3 - \frac{1}{2M_{\rm Pl}^2}\left(\frac{d\phi}{dN}\right)^2\right) + \frac{k^2}{a^2H^2}h_k = 0,
\end{aligned} \tag{2.32}$$

with the initial conditions imposed on the modes of curvature perturbation as follows:

$$\begin{aligned}
&\mathcal{R}_k\left(N_0\right) = \frac{1}{z\left(N_0\right)}\frac{1}{\sqrt{2k}}, \\
&\frac{d\mathcal{R}_k}{dN}\left(N_0\right) = -\mathcal{R}_k\left(N_0\right)\left\{1 + \frac{\phi_{NN}\left(N_0\right)}{\phi_N\left(N_0\right)}\right\} + i\sqrt{\frac{k}{2}}\frac{1}{z\left(N_0\right)a\left(N_0\right)H\left(N_0\right)},
\end{aligned} \tag{2.33}$$

where N_0 is some e-folding at which we impose the initial conditions. Similarly, we can derive the form of the initial conditions for the tensor perturbations and hence calculate the primordial power spectra. Now, we take a look at the evolution of background and perturbations for two specific potentials.

2.4.1 The quadratic potential

The first inflationary model we consider is the quadratic potential described by:

$$V(\phi) = \frac{1}{2}m^2\phi^2. \tag{2.34}$$

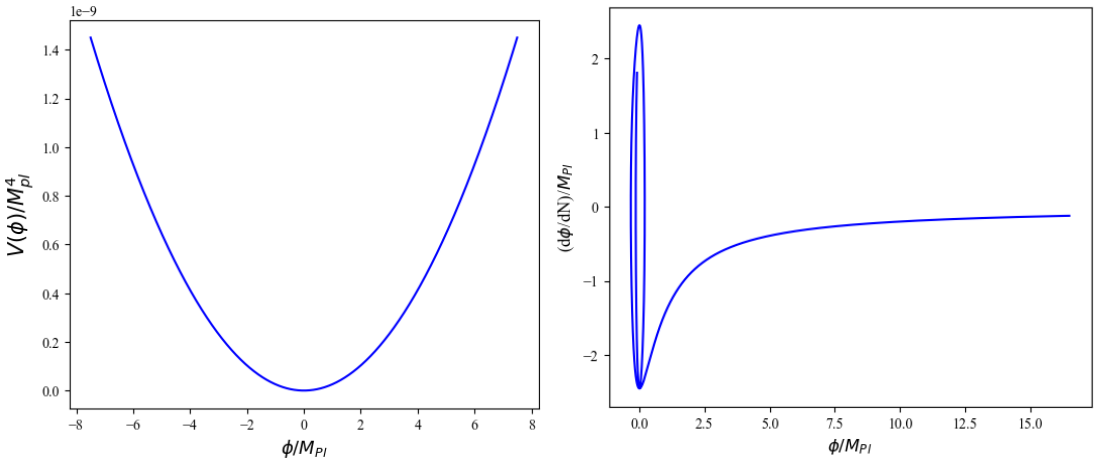

Figure 2.1: The quadratic potential plotted against ϕ and the phase-space plot during inflation for the quadratic potential.

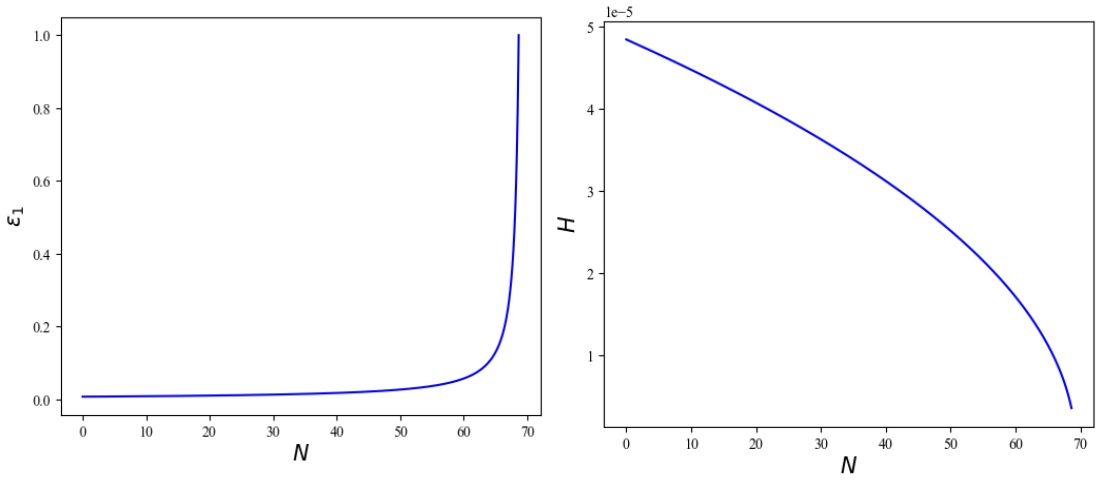

Figure 2.2: Evolution of the first slow-roll parameter and the Hubble parameter during inflation for the quadratic potential.

We set $m = 7.18 \times 10^{-6} M_{\rm Pl}$ and set the initial conditions on the scalar field and ϵ_1 as $\phi_i = 16.5 M_{\rm Pl}$ and $\epsilon_{1i} = 7.346 \times 10^{-3}$. For this choice of initial conditions we see that inflation lasts for about 68.63 e-folds. The evolution of background quantities is plotted in Fig.2.1 and Fig.2.2.

We shall set $N_{pivot} = 50$ i.e. the pivot scale leaves the horizon about 50 e-folds before inflation ends. WMAP renormalisation fixes N_{pivot} to 50-60 e-folds. The evolution of the absolute values of the real and imaginary part of the curvature perturbation for $k = 0.05 \text{Mpc}^{-1}$ is plotted in Fig.2.3. We can see that after around 18-19 e-folds of inflation, the mode does not evolve which means it has escaped the horizon. This seems about right since we set $N_{pivot} = 50$ e-folds which is about 18.6 e-folds since the beginning of inflation. Figure 2.4 shows the primordial scalar and tensor power spectra plotted for the quadratic potential. For numerical evaluation, we have imposed the Bunch-Davies initial conditions when $k/aH = 100$. We observe that both the spectra are nearly scale invariant. The tensor power spectrum is suppressed compared to the scalar power spectrum. The value of the scalar spectral index $n_S \simeq 0.96$ at $k = 0.05 \text{Mpc}^{-1}$ and the tensor-to-scalar ratio $r = 0.158$ at $k = 0.002 \text{Mpc}^{-1}$. The Planck 2018 results constrain the two parameters at $n_S = 0.9649 \pm 0.0042$ and $r_{0.002} < 0.064$ [12]. We can

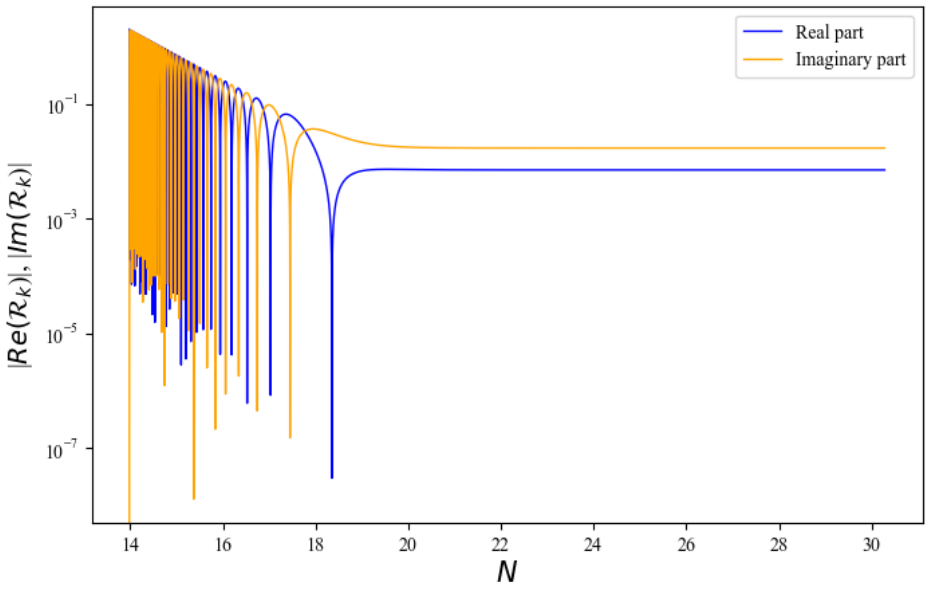

Figure 2.3: Evolution of the absolute values of the real and imaginary parts of the mode of the curvature perturbation corresponding to the pivot scale. The mode freezes after it exits the horizon.

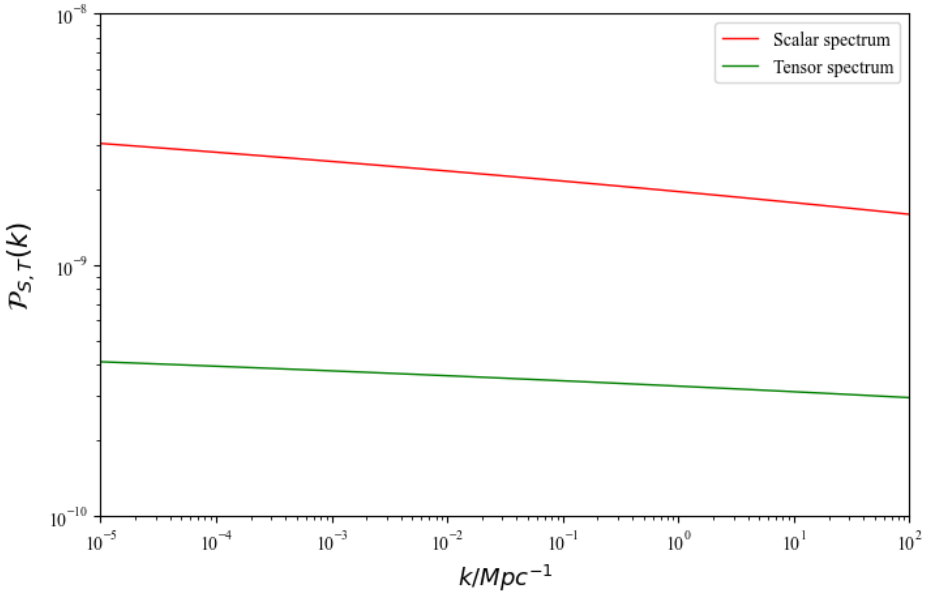

Figure 2.4: Scalar and tensor power spectra for the quadratic potential. We observe that the spectra is nearly scale invariant.

see that the tensor-to-scalar ratio is too high for the quadratic potential model and so this model has been disfavoured by the Planck data.

2.4.2 The axion monodromy model

The second model we shall consider is the axion monodromy model described by the potential [13, 14]:

$$V(\phi) = u\left(\phi + bcos\left(\frac{\phi}{f}\right)\right). \tag{2.35}$$

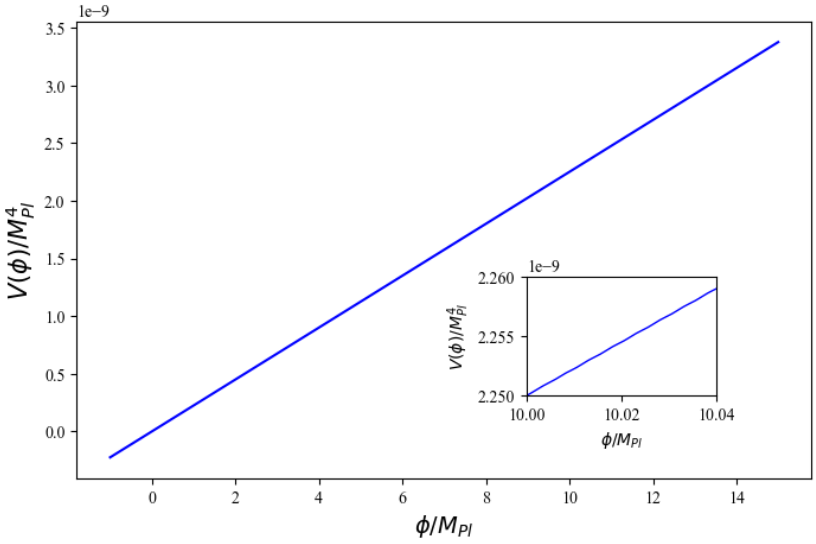

Figure 2.5: The axion monodromy potential.

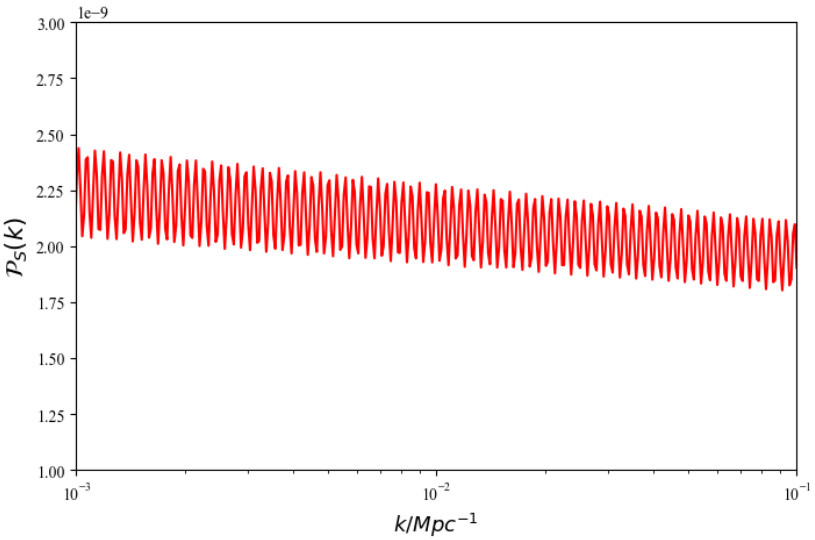

Figure 2.6: Scalar power spectrum for the axion monodromy model. The oscillating features in the spectrum have been shown to better fit the Planck data.

We have set $u = 2.25 \times 10^{-10} M_{\rm Pl}^3$, $b = 10^{-4} M_{\rm Pl}$ and $f = 8 \times 10^{-4} M_{\rm Pl}$ [14]. b quantifies the relative strength of the sinusoidal oscillations with respect to the ϕ term. We have set $\phi_i = 12 M_{\rm Pl}$ which leads to about 72.86 e-folds of inflation. We have also set $N_{pivot} = 50$ e-folds. The scalar power spectrum for this model has been plotted in figure 2.5. The chosen parameters also satisfy the constraint the scalar power spectrum at pivot scale i.e. $\mathcal{P}_S(k) = 2.1 \times 10^{-9}$ at $k = 0.05 \text{Mpc}^{-1}$. The cosine term in the potential leads to oscillating features in the scalar power spectrum which has received considerable interest recently as they seem to better fit the observational constraints from the Planck 2018 data.

CHAPTER 3

$f(R)$ THEORIES

In chapter 1, we saw that the standard big bang model has its own drawbacks. So, there are two ways to introduce changes in the theory. If we look at the Einstein's field equations, we will realize that one way is to introduce new fields like the inflationary models driven by scalar fields and the cosmological constant as we discussed in the previous chapters. These modify the stress-energy tensor on the RHS of Einstein's equations. Another way is to modify the LHS i.e. the gravitational sector and go beyond general relativity. Weinberg and Deser stated before that *Einstein's general relativity is the unique low energy theory of a Lorentz invariant massless particle of helicity-2*. So, modifications to GR can primarily be done in the following ways:

- Giving mass to graviton
- Introducing new degrees of freedom through Lorentz scalars
- Breaking Lorentz invariance.

The aim of these modifications is to turn some of the constraint equations into dynamical equations to achieve greater freedom in the gravitational sector. However, they may also introduce higher derivative terms which may cause ghost-like instabilities in the theory (Ostrogradsky instabilities). Figure 3.1 shows the theoretical landscape of the gravitational sector since the proposal of general relativity.

3.0.1 Lovelock gravity

Lovelock stated a theorem in 1971 which goes as follows: *The only possible second-order, Euler-Lagrangian equations obtainable in a 4-dimensional spacetime from an action solely containing the metric and its derivatives are the Einstein's equations* [15]. So, general relativity is the simplest theory of gravitation which provides us with

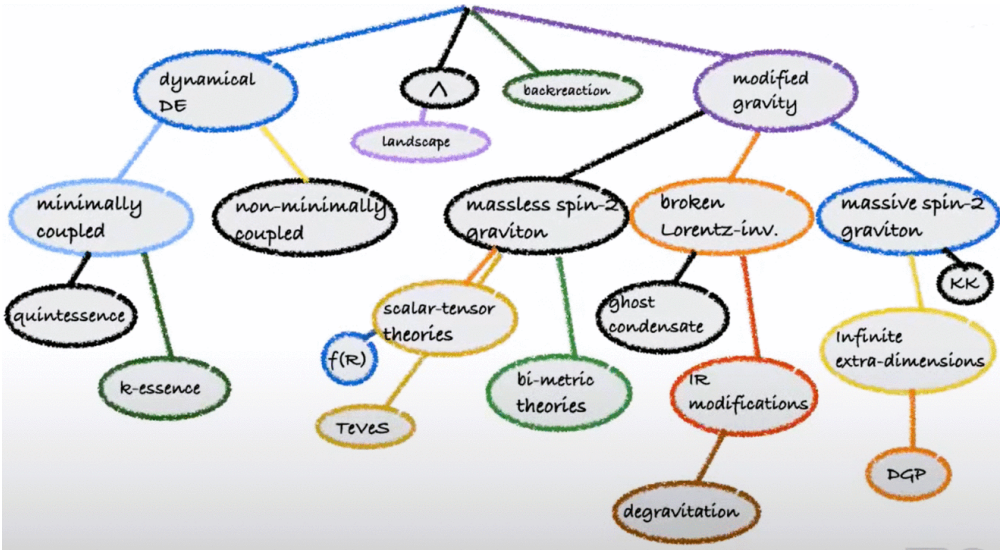

Figure 3.1: Theoretical landscape of the gravitational sector since the proposal of general relativity has been shown here. Image obtained from Alessandra Silvestri [16].

the Einstein's equations and that's what makes it special! Now, to avoid instabilities due to the higher-order derivative terms, we introduce the *Lovelock scalars* [15]. The Lovelock scalars are a combination of Riemann tensors and the metric which may contain higher-order derivative terms in the Lagrangian but they only introduce second-order derivative terms to the equations of motion. Example of one such class of Lagrangian densities is as follows [16]:

$$\mathcal{L} = \sqrt{-g}(A_1 f(R) + A_2 f(\mathcal{G})), \tag{3.1}$$

where $\mathcal{G} = R^2 + R_{\alpha\beta\gamma\delta}R^{\alpha\beta\gamma\delta} - 4R_{\alpha\beta}R^{\alpha\beta}$ is the Gauss-Bonnet term. For generalised functions $f(R) \neq R$ and $f(\mathcal{G}) \neq \mathcal{G}$, the theory possesses two additional scalar degrees of freedom. Any additional degrees of freedom introduced because of the Lovelock scalars will not be tensor-like. So, we can use the Lovelock scalars to write down the most generalised theory of gravitation that leads to second-order equations of motion. This is what Horndeski, a student of Lovelock, did in 1974. We shall not go deeper into the Horndeski theory. From hereon, we shall discuss $f(R)$ modified theories of gravity.

3.1 $f(R)$ GRAVITY

We shall now consider $f(R)$ theories which is the primary topic of this thesis. The $f(R)$ models are one of the simplest modifications to general relativity where we just replace R, the Ricci scalar in the Einstein-Hilbert action with an arbitrary function $f(R)$:

$$S = \frac{1}{2\kappa^2}\int d^4x\sqrt{-g}f(R) + \int d^4x\sqrt{-g}\mathcal{L}_M, \tag{3.2}$$

where $\kappa = 1/M_{\rm Pl} = (8\pi G)^{1/2}$ and $\mathcal{L}_M$ represents the Lagrangian density for additional fields. To derive the field equations for an $f(R)$ theory, there are two ways [17]:

- **Palatini formalism**: In Palatini formalism, we treat the affine connections $\Gamma^{\alpha}_{\beta\gamma}$ and the metric $g_{\mu\nu}$ as independent quantities. Varying the action with respect to the metric and the connection gives us the complete set of equations of motion.
- **Metric formalism**: In metric formalism, the affine connections are defined in terms of the metric and varying the action with respect to the metric alone yields us the equations of motion.

In general relativity, both formalisms lead to Einstein's field equations but this is not true for $f(R)$ theories.

3.1.1 Field equations in Palatini formalism

The Ricci tensor can be expressed explicitly in terms of the affine connections, $\Gamma^{\alpha}_{\beta\gamma}$, and it is necessary to note that $R_{\mu\nu}(\Gamma)$ is different than $R_{\mu\nu}(g)$. Varying the $f(R)$ action with respect to the affine connection yields us:

$$F(R)R_{\mu\nu}(\Gamma) - \frac{1}{2}f(R)g_{\mu\nu} = \kappa^2 T_{\mu\nu}, \tag{3.3}$$

and varying the action with respect to the metric connection gives the following equations of motion [17]:

$$\begin{aligned} R_{\mu\nu}(g) - \frac{1}{2}g_{\mu\nu}R(g) =& \frac{\kappa^2 T_{\mu\nu}}{F} - \frac{FR(T) - f}{2F}g_{\mu\nu} + \frac{1}{F}\left(\nabla_\mu\nabla_\nu F - g_{\mu\nu}\Box F\right) \\ & - \frac{3}{2F^2}\left[\partial_\mu F\partial_\nu F - \frac{1}{2}g_{\mu\nu}(\nabla F)^2\right]. \end{aligned} \tag{3.4}$$

Eq.(3.3) and Eq.(3.4) together form the set of equations of motion for describing

gravitation in $f(R)$ theories. The trace form of Eq.(3.3) turns out to be:

$$RF(R) - 2f(R) = \kappa^2 T, \tag{3.5}$$

which means that R, the Ricci scalar, is directly determined by the stress-energy tensor in the Palatini formalism of $f(R)$ gravity similar to general relativity.

3.1.2 Field equations in metric formalism

Varying the action given by Eq.(3.2) with respect to metric gives the following equations of motion:

$$F(R)R_{\mu\nu} - \frac{1}{2}f(R)g_{\mu\nu} + (g_{\mu\nu}\Box - \nabla_\mu\nabla_\nu)F(R) = \kappa^2 T_{\mu\nu}, \tag{3.6}$$

where $F(R) = \partial f/\partial R$. Substituting $f(R) = R$ gives us the Einstein's equations. Note that the equations of motion have fourth-order derivative terms which may lead to instabilities. So, we need to set some conditions on the theory to check for its viability. We will be working in the metric formalism from now on.

3.1.3 Viability conditions

To obtain a viable theory free of any instabilities, the theory must pass the following conditions [16, 18]:

- All the alternative theories must resemble general relativity on certain scales and pass the local gravity tests.

$$f(R) \to R \text{ as } R \to 0. \tag{3.7}$$

- $$f(R) > 0 \quad \text{and} \quad F(R) > 0. \tag{3.8}$$

  This condition has to do with the rescaling of the gravitational constant (needs to be always positive) and other length scales in modified theories of gravity as well as to avoid anti-gravity scenarios.

- High-curvature regime should be stable otherwise it may lead to a tachyonic instability. Therefore,

$$\partial^2 f/\partial R^2 > 0. \tag{3.9}$$

- Avoid matter instabilities i.e. curvature perturbations should be stable and large

curvature perturbations should not be easily realizable to avoid singularities.

- The theory should have a quasi-stable de Sitter solution which will correspond to inflation in the early universe. It should also have a stable de Sitter solution to describe the late-time evolution of the universe.

and the list goes on.

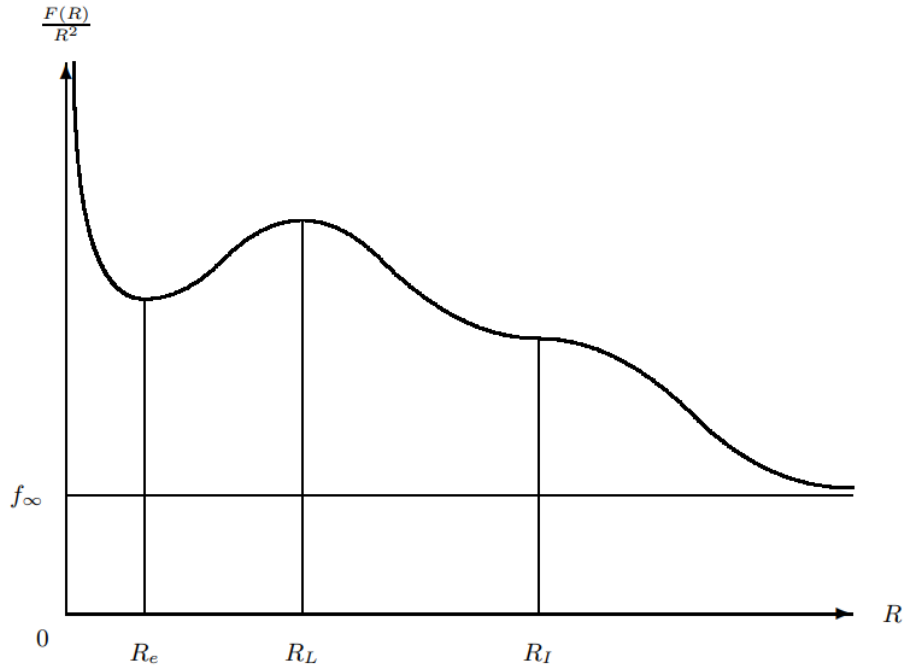

Figure 3.2: Behaviour of a viable $f(R)$ theory. R_I corresponds to a large curvature (10^{16} – 10^{19}GeV) corresponding to inflation in the early universe. R_L corresponds to a small curvature (10^{-33}eV) corresponding to the late-time acceleration of the universe (a stable de Sitter solution). R_e corresponds to an unstable de Sitter solution that must be present due to certain viability conditions. f_∞ corresponds to the asymptotic value for avoiding a singularity as $R \to \infty$ and finally $f(R) \to R$ as $R \to 0$. (Note: $F(R)$ on the y-axis does not correspond to the scalaron but corresponds to the function in the action. Only in this plot, $F(R)$ is used instead of $f(R)$.) Image obtained from Nojiri et al. [18].

3.1.4 The scalaron field

We can view the higher-order derivative terms in Eq.(3.6) as second-order derivatives of the scalar quantity $F(R)$. If we take the trace of Eq.(3.6), we get:

$$3\Box F(R) + F(R)R - 2f(R) = \kappa^2 T, \tag{3.10}$$

where T denotes the trace of the stress-energy tensor and $\Box$ denotes the d'Alambertian operator in 4-D spacetime. Remember that in general relativity $R = -\kappa^2 T$ which means that the Ricci scalar can be directly determined from the stress-energy tensor. However, Eq.(3.10) is a dynamical equation and shows that an $f(R)$ theory can have non-trivial solutions for R even in the absence of any source. This shows that the $f(R)$ theory possesses an additional *propagating scalar degree of freedom* in the quantity $F(R)$ which is also referred to as the *scalaron* in literature. Now, compare the above trace equation with the one in Palatini formalism given by Eq.(3.5). The $\Box F$ term is absent in the one in Palatini formalism and hence there is no propagating degree of freedom like the scalaron in the Palatini formalism. Note that we can use Eq.(3.10) to find a de Sitter solution even in a vacuum universe by taking R as constant which causes the $\Box F$ term to vanish.

3.1.5 Generalised Friedmann equations

For a spatially flat FLRW background described by the metric:

$$\mathrm{d}s^2 = -\mathrm{d}t^2 + a^2(t)\mathrm{d}\mathbf{x}^2, \tag{3.11}$$

the Friedmann equations in a spatially flat $f(R)$ FLRW universe are described by the following:

$$\begin{aligned} 3FH^2 &= \frac{1}{2}(FR - f) - 3H\dot{F} + \kappa^2\rho, \\ -2F\dot{H} &= \ddot{F} - H\dot{F} + \kappa^2(\rho + P). \end{aligned} \tag{3.12}$$

Using the above equations, we can also derive the equation corresponding to the conservation of the stress-energy tensor:

$$\dot{\rho} = -3H(\rho + p), \tag{3.13}$$

which is the same as Eq.(1.5). We shall make use of these Friedmann equations in an $f(R)$ FLRW universe to study the inflationary dynamics.

3.2 INFLATION IN $f(R)$ THEORIES

In general relativity, we had to introduce a scalar field to drive inflation. What sets the $f(R)$ theories apart is that inflation occurs naturally in these theories and has a purely gravitational origin. Moreover, these theories also predict a nearly scale-invariant power spectra which agrees very well with the CMB constraints. The first such $f(R)$ theory was proposed by Starobinsky in 1980 when he considered quantum corrections to the Einstein's equations [19].

For now, we shall ignore any additional fields and shall study the background dynamics during inflation for models of the form:

$$f(R) = R + \alpha R^n. \tag{3.14}$$

Simplifying the field equations for this class of models gives us the following:

$$3\left(1 + n\alpha R^{n-1}\right) H^2 = \frac{1}{2}(n-1)\alpha R^n - 3n(n-1)\alpha H R^{n-2}\dot{R}. \tag{3.15}$$

In the regime $F = 1 + n\alpha R^{n-1} \gg 1$, we can approximate the above equation to the following [17]:

$$H^2 \simeq \frac{n-1}{6n}\left(R - 6nH\frac{\dot{R}}{R}\right). \tag{3.16}$$

Since the Hubble parameter evolves very slowly during inflation, we can assume $|\dot{H}| \ll |H^2|$ and $|\ddot{H}| \ll |H\dot{H}|$ which simplifies the above equation:

$$\frac{\dot{H}}{H^2} \simeq -\epsilon_1 \text{ where } \epsilon_1 = \frac{2-n}{(2n-1)(n-1)}. \tag{3.17}$$

This equation can be easily integrated which gives us the following form of the scale factor:

$$a(t) \propto t^{1/\epsilon_1}. \tag{3.18}$$

Now, lets take a look at the value of ϵ_1 here. ϵ_1 has to be smaller than 1 for inflation to occur which is equivalent to $n > (\sqrt{3}+1)/2$. If $n > 2$, then $\dot{H} > 0$ which is referred to as super inflation. So, for the inflationary dynamics with decreasing $\dot{H}$, we need

$(\sqrt{3}+1)/2 < n < 2$. So, we see that for a certain range of values for n, inflation occurs without any need for an additional field for these class of models. Note that in the single-field inflationary models in the framework of GR that we discussed in chapter 2, we could only have standard inflation and not super inflation (see Eq.(1.20)).

3.3 CONFORMAL TRANSFORMATION AND THE EINSTEIN FRAME

The extra scalar degree of freedom in the theory can be seen more clearly when we rewrite the $f(R)$ theory into a scalar-tensor theory using conformal transformations. For this we first introduce an auxiliary field, say A, and rewrite the action as [18]:

$$S = \frac{1}{2\kappa^2}\int d^4x\sqrt{-g}[F(A)(R-A)+f(A)] + \int d^4x\sqrt{-g}\mathcal{L}_M. \tag{3.19}$$

We can see that for $R = A$, we recover the $f(R)$ action. Using a conformal transformation of the form:

$$\tilde{g}_{\mu\nu} = \Omega^2 g_{\mu\nu} = F g_{\mu\nu}, \tag{3.20}$$

we can rewrite the action given in Eq.(3.19) in the following manner:

$$S = \frac{M_{\rm Pl}^2}{2}\int d^4\tilde{x}\sqrt{-\tilde{g}}\left(\tilde{R} - \frac{3}{2}\partial_\mu(\ln F)\partial^\mu(\ln F) - \frac{AF(A)-f(A)}{F^2(A)}\right) + \int d^4x\sqrt{-\tilde{g}}\tilde{\mathcal{L}}_M(F^{-1}\tilde{g}_{\mu\nu},\psi), \tag{3.21}$$

where ψ is some field describing the Lagrangian density $\tilde{\mathcal{L}}_M = \mathcal{L}_M/F^2$. We, now define a scalar field ϕ and its potential $V(\phi)$ in the following manner:

$$\begin{aligned} \phi &\equiv M_{\rm Pl}\sqrt{\frac{3}{2}}\ln F, \\ V(\phi) &= \frac{M_{\rm Pl^2}}{2}\left(\frac{AF(A)-f(A)}{F^2(A)}\right). \end{aligned} \tag{3.22}$$

With this definition, we arrive at the final form of the action that we wanted:

$$S = \int d^4\tilde{x}\sqrt{-\tilde{g}}\left[\frac{M_{\rm Pl}^2\tilde{R}}{2} - \frac{1}{2}\partial_\mu(\phi)\partial^\mu(\phi) - V(\phi)\right] + \int d^4\tilde{x}\sqrt{-\tilde{g}}\tilde{\mathcal{L}}_M(F^{-1}\tilde{g}_{\mu\nu},\psi), \tag{3.23}$$

where the symbol $\sim$ denotes the quantities in the new frame. The action written in Eq.(3.23) describes a scalar field ϕ minimally coupled to gravitation in general relativity! With the new definition in Eq.(3.22) relating ϕ and F, we can now see that the extra scalar degree of freedom in $f(R)$ theories now manifests itself as a canonical scalar field with a potential defined in Eq.(3.22). Generally, we call this the *Einstein frame* and the other one describing the $f(R)$ theory as the *Jordan frame*. So, we conclude that an $f(R)$ theory is conformally equivalent to a theory of general relativity minimally coupled with a canonical scalar field. This is why we studied single-field inflationary models in general relativity in chapter 2 of this thesis. Both the frames have their own uses in studying $f(R)$ theories: the gravitational sector is easy to study in the Einstein frame while the non-gravitational sector is easy to study in the Jordan frame since gravity is now non-minimally coupled to the additional fields in the Einstein frame (take a look at the action in Eq.(3.23)!). However, the big question now is: *Do the Einstein and Jordan frames describe physically equivalent universes?*

Conformal transformation of $f(R) = R + \alpha R^n$

The most essential quantity that we need to study inflationary dynamics in a single-field inflationary model in general relativity is the potential $V(\phi)$. We shall now construct the potential in the Einstein frame for $f(R) = R + \alpha R^n$. Using the relation between ϕ and F described by Eq.(3.22), we can write:

$$A \equiv \left(\frac{exp\left(\sqrt{\frac{2}{3}}\frac{\phi}{M_{\rm Pl}}\right) - 1}{n\alpha} \right)^{1/(n-1)} . \tag{3.24}$$

Using the above relation for this class of $f(R)$ models, we can rewrite the potential defined in (3.22) as:

$$V(\phi) = \frac{M_{\rm Pl}^2}{2} \frac{n-1}{(n^n\alpha)^{1/(n-1)}} \left[exp\left(\sqrt{\frac{2}{3}}\left(\frac{2-n}{n}\right)\frac{\phi}{M_{\rm Pl}}\right) - exp\left(-2\sqrt{\frac{2}{3}}\left(\frac{n-1}{n}\right)\frac{\phi}{M_{\rm Pl}}\right)\right]^{n/(n-1)} . \tag{3.25}$$

So, using this potential, we can now study the gravitational sector in the Einstein frame for the class of $f(R)$ theories discussed above.

3.3.1 Relating background quantities in the Einstein and Jordan frames

From the conformal transformation, $\tilde{g}_{\mu\nu} = F g_{\mu\nu}$, the relation between the stress-energy tensor for additional fields in the Einstein and Jordan frames is expressed as [17]:

$$\tilde{T}^{\mu}_{\nu} = \frac{T^{\mu}_{\nu}}{F^2}. \tag{3.26}$$

Relating the FLRW line-element in the Einstein and Jordan frames:

$$\begin{aligned} \mathrm{d}\tilde{s}^2 &= F^2 \mathrm{d}s^2, \\ -\mathrm{d}\tilde{t}^2 + \tilde{a}^2(\tilde{t}) d\mathbf{x}^2 &= F^2(-\mathrm{d}t^2 + a^2(t)\mathrm{d}\mathbf{x}^2), \end{aligned} \tag{3.27}$$

which gives us the following relations for the time element and the scale factor:

$$\begin{aligned} \mathrm{d}\tilde{t} &= \sqrt{F}\mathrm{d}t, \\ \tilde{a} &= \sqrt{F}a, \end{aligned} \tag{3.28}$$

with $F > 0$. Using these relations, we can also obtain a relation between the Hubble parameter in the two frames which is given by the following:

$$\tilde{H} = \left(H + \frac{\dot{F}}{2F}\right)\frac{1}{\sqrt{F}}. \tag{3.29}$$

We can also relate the number of e-foldings in the two frames using the above relations:

$$\begin{aligned} \tilde{N} &= \int_{\tilde{t}_i}^{\tilde{t}} \tilde{H} d\tilde{t} \\ &= \int_{t_i}^{t} H dt + \int_{t_i}^{t} dt \frac{\dot{F}}{2F} \\ &= N + \frac{1}{2}[\ln(F(t)) - \ln(F_i)]. \end{aligned} \tag{3.30}$$

where t_i denotes the cosmic time when inflation starts in the Jordan frame and F_i denotes the corresponding value of the function $F(R)$. Similarly, we can derive relations for other background quantities such as the Ricci scalar, Hubble radius,etc. in the Einstein and Jordan frames.

3.4 PRIMORDIAL PERTURBATIONS IN $f(R)$ THEORIES

We will now discuss perturbation theory in $f(R)$ models. We will first discuss perturbations in an $f(R)$ theory coupled minimally to a scalar field since this can help us derive results for general relativity coupled with a scalar field as well as $f(R)$ theories with no coupling to a field (the Einstein and Jordan frames for $f(R)$ theories). For this, we consider the following action:

$$S = \int d^4x\sqrt{-g}\left[\frac{1}{2\kappa^2}f(R) - \frac{1}{2}\omega(\phi)g^{\mu\nu}\partial_\mu\phi\partial_\nu\phi - V(\phi)\right]. \tag{3.31}$$

The Friedmann equations for such a theory are then given by:

$$\begin{aligned} 3FH^2 &= \frac{1}{2}(RF - f) - 3H\dot{F} + \kappa^2\left[\frac{1}{2}\omega\dot{\phi}^2 + V(\phi)\right], \\ -2F\dot{H} &= \ddot{F} - H\dot{F} + \kappa^2\omega\dot{\phi}^2, \\ \ddot{\phi} &+ 3H\dot{\phi} + \frac{1}{2\omega}\left(\omega_\phi\dot{\phi}^2 + 2V_\phi\right) = 0. \end{aligned} \tag{3.32}$$

Now, we consider the perturbed FLRW metric of the following form:

$$ds^2 = -(1+2A)dt^2 + 2a\left(\partial_i B - S_i\right)dx^i dt + a^2\left[(1+2C)\delta_{ij} + 2\partial_{ij}E + 2\partial_{(i}F_{j)} + h_{ij}\right]dx^i dx^j. \tag{3.33}$$

Since vector perturbations decay very rapidly, we will focus our analysis on scalar and tensor perturbations only during inflation. The decomposition theorem again applies in the context of $f(R)$ theories and we see that the scalar, vector and tensor perturbations decouple and evolve independently. We shall look at scalar perturbations first.

3.4.1 Scalar perturbations in $f(R)$ theories

Perturbing the field equations to linear order and accounting only for the scalar perturbations in a smooth FLRW background gives us the following set of equations [17]:

$$\begin{aligned} \frac{\Delta}{a^2}C + H\alpha = -\frac{1}{2F}\Bigg[&\left(3H^2 + 3\dot{H} + \frac{\Delta}{a^2}\right)\delta F - 3H\delta\dot{F} + \frac{1}{2}\left(\kappa^2\omega_\phi\dot{\phi}^2 + 2\kappa^2V_\phi\right)\delta\phi \\ &+\kappa^2\omega\dot{\phi}\dot{\delta\phi} + \left(3H\dot{F} - \kappa^2\omega\dot{\phi}^2\right)A + \dot{F}\alpha\Bigg], \end{aligned} \tag{3.34}$$

$$HA - \dot{C} = \frac{1}{2F}\left[\kappa^2\omega\dot{\phi}\delta\phi + \delta\dot{F} - H\delta F - \dot{F}A\right], \tag{3.35}$$

$$\dot{\chi} + H\chi - A - C = \frac{1}{F}(\delta F - \dot{F}\chi), \tag{3.36}$$

$$\begin{aligned}\dot{\alpha} + 2H\alpha + \left(3H + \frac{\Delta}{a^2}\right)A = \frac{1}{2F}\Bigg[&3\delta\ddot{F} + 3H\delta\dot{F} - \left(6H^2 + \frac{\Delta}{a^2}\right)\delta F + 4\kappa^2\omega\dot{\phi}\dot{\delta\phi} \\ &+ \left(2\kappa^2\omega_\phi\dot{\phi}^2 - 2\kappa^2 V_\phi\right)\delta\phi - 3\dot{F}\dot{A} - \dot{F}\alpha \\ &- \left(4\kappa^2\omega\dot{\phi}^2 + 3H\dot{F} + 6\ddot{F}\right)A\Bigg],\end{aligned} \tag{3.37}$$

$$\begin{aligned}&\ddot{\delta F} + 3H\dot{\delta F} - \left(\frac{\Delta}{a^2} + \frac{R}{3}\right)\delta F + \frac{2}{3}\kappa^2\dot{\phi}\dot{\delta\phi} + \frac{1}{3}\left(\kappa^2\omega_\phi\dot{\phi}^2 - 4\kappa^2 V_\phi\right)\delta\phi \\ &= \dot{F}(\alpha + \dot{A}) + \left(2\ddot{F} + 3H\dot{F} + \frac{2}{3}\kappa^2\omega\dot{\phi}^2\right)A - \frac{1}{3}F\delta R,\end{aligned} \tag{3.38}$$

$$\begin{aligned}&\delta\ddot{\phi} + \left(3H + \frac{\omega_\phi}{\omega}\dot{\phi}\right)\delta\dot{\phi} + \left[-\frac{\Delta}{a^2} + \left(\frac{\omega_\phi}{\omega}\right)_\phi\frac{\dot{\phi}^2}{2} + \left(\frac{2V_\phi}{2\omega}\right)_\phi\right]\delta\phi \\ &= \dot{\phi}\dot{A} + \left(2\ddot{\phi} + 3H\dot{\phi} + \frac{\omega_\phi}{\omega}\dot{\phi}^2\right)A + \dot{\phi}\alpha,\end{aligned} \tag{3.39}$$

where some quantities have been defined as:

$$\begin{aligned}&\chi \equiv -a(B + a\dot{E}), \\ &\alpha \equiv 3(HA - \dot{C}) - \frac{\Delta}{a^2}\chi, \\ &\delta R = -2\left(\dot{\alpha} + 4H\alpha + \left(\frac{\Delta}{a^2} + 3\dot{H}\right)A + 2\frac{\Delta}{a^2}C\right).\end{aligned} \tag{3.40}$$

where Δ denotes the d'Alambertian in 3-D space. Eq.((3.34)-(3.39)) with Eq.(3.40) describe the evolution of scalar perturbations in an $f(R)$ + scalar field universe in a spatially flat FLRW background. Before further analysis of these equations, it is better to talk about gauge fixing and gauge-invariant quantities.

Gauge fixing and defining curvature perturbation

We already know that 2 degrees of freedom of the scalar perturbations are redundant and so we need to work in a particular gauge. We will work in the longitudinal gauge which corresponds to $A = \Phi, B = 0, C = \Psi, E = 0$. However, for an $f(R)$ + scalar field theory, there are two more scalar degrees of freedom: one associated with the field ϕ and the

other associated with the scalaron F. To make the derivations of the equations of motion easier, we now work in another particular gauge which corresponds to $\delta\phi = 0, \delta F = 0$. We can see that if we put $f(R) = R$ and recover general relativity, the gauge corresponds to $\delta\phi = 0$, which is referred to as the uniform field gauge. For a purely $f(R)$ theory with no additional scalar field, the gauge we work in corresponds only to $\delta F = 0$ which is analogous to the uniform field gauge and so we are effectively applying only one of the two conditions.

Now, we shall take a look at the gauge invariant quantities related to the scalar perturbations. Some gauge-invariant quantities related to the curvature perturbation are follows [17]:

$$\begin{aligned} \mathcal{R} &= \Psi + \frac{H}{\rho + p}\delta q, \\ \mathcal{R}_{\delta\phi} &= \Psi - \frac{H}{\dot{\phi}}\delta\phi, \\ \mathcal{R}_{\delta F} &= \Psi - \frac{H}{\dot{F}}\delta F. \end{aligned} \tag{3.41}$$

Since we are working in the $\delta\phi = 0, \delta F = 0$ gauge, we have $\mathcal{R} = \mathcal{R}_{\delta\phi} = \mathcal{R}_{\delta F}$. In general, $\mathcal{R} = \mathcal{R}_{\delta\phi}$ for a single-field inflationary model.

Evolution of the scalar curvature perturbation

Now, using the definition of curvature perturbation expressed in Eq.(3.41), we can now derive the equation of motion governing the evolution of $\mathcal{R}$. Using the perturbed field equations Eq.(3.34), Eq.(3.35), Eq.(3.37) and the Friedmann equations (3.32), we can write the equation of motion describing the evolution of the Fourier modes of $\mathcal{R}$ in terms of derivatives with respect to the conformal time as:

$$\mathcal{R}_k'' + 2\left(\frac{z_s'}{z_s}\right)\mathcal{R}_k' + k^2\mathcal{R}_k = 0, \tag{3.42}$$

where

$$z_s = a\left(\frac{\omega\dot{\phi}^2 + 3\dot{F}^2/(2\kappa^2 F)}{(H + \dot{F}/2F)^2}\right)^{1/2}. \tag{3.43}$$

Take a look at Eq.(3.42) and compare it to Eq.(2.16). They are the same equations with the quantity z_s defined in a more general manner! Also, we see that for a single-field inflationary model in GR and for a purely $f(R)$ theory respectively, z_s reduces to:

$$\begin{aligned} z_s^{GR} &= a\frac{\dot{\phi}}{H}, \\ z_s^{f(R)} &= a\left(\frac{3\dot{F}^2/(2\kappa^2 F)}{(H+\dot{F}/2F)^2}\right)^{1/2}, \end{aligned} \tag{3.44}$$

which is exactly how we described z for the curvature perturbations in the previous chapter. That's not surprising since we are working on a more general theory.

3.4.2 Tensor perturbations in $f(R)$ theories

Since the scalar field does not affect the tensor perturbations, we get freely propagating gravitational waves. So, for the transverse, traceless tensor perturbations in $f(R)$ gravity, the equation of motion governing their evolution is given by:

$$h_k'' + \left(2 + \frac{F'}{\mathcal{H}F}\right)\mathcal{H}h_k'' + k^2 h_k = 0. \tag{3.45}$$

Notice that there is an additional frictional term in this equation compared to the result in general relativity (2.17). The origin of this additional term has to do with the rescaling of the gravitational constant in modified theories and has consequences like affecting the luminosity distance of gravitational waves [16]. We can also reduce this equation to the form we got in GR in the previous chapter:

$$h_k'' + 2\left(\frac{z_t'}{z_t}\right)h_k' + k^2 h_k = 0, \tag{3.46}$$

where $z_t = a\sqrt{F}$. Both the polarization states of the freely propagating gravitational waves are governed by this equation.

The Mukhanov-Sasaki variable and initial conditions on modes

Since the form of the equations of motion for scalar and tensor perturbations in the $f(R)$ + scalar field theory is the same as in GR + scalar field, we can also introduce the Mukhanov-Sasaki variable here and talk about initial conditions on the modes.

Substituting $v = \mathcal{R} z_s$ and $u = h z_t / \sqrt{16\pi G}$ in Eq.(3.42) and Eq.(3.46) respectively, we get:

$$\begin{aligned} v_k'' + \left(k^2 - \frac{z_s''}{z_s}\right) v_k &= 0, \\ u_k'' + \left(k^2 - \frac{z_t''}{z_t}\right) u_k &= 0. \end{aligned} \tag{3.47}$$

So we can see that in the sub-Hubble limit i.e. $k \gg \sqrt{z_s''/z_s}$ and $k \gg \sqrt{z_t''/z_t}$ respectively, the modes are not affected by the spacetime curvature and we can use the Bunch-Davies vacuum conditions described by Eq.(2.21) to impose initial conditions on the modes when they are deep inside the Hubble radius. The scalar and tensor power spectra is defined in Eq.(2.23). With this, we have all the tools to study primordial perturbations during inflation in linear perturbation theory in $f(R)$ models.

3.5 APPROXIMATE SOLUTIONS TO THE POWER SPECTRA DURING INFLATION IN $f(R)$ THEORIES

To derive the approximate analytical solutions for the evolution of perturbations during inflation, we adopt the same procedure that we used in the slow-roll inflation in the chapter 2. We, first introduce the slow-roll type parameters in this general $f(R)$ + scalar field theory which are expressed as follows [20]:

$$\begin{aligned} \epsilon_1 &= -\frac{\dot{H}}{H^2}, \\ \epsilon_2 &= \frac{\ddot{\phi}}{H\dot{\phi}}, \\ \epsilon_3 &= \frac{\dot{F}}{2HF}, \\ \epsilon_4 &= \frac{\dot{E}}{2HE}. \end{aligned} \tag{3.48}$$

where $E \equiv F[\omega + 3\dot{F}/(2\kappa^2\dot{\phi}^2 F)]$. Now, we shall take a look at the solutions on super-Hubble scales and then use the above parameters to get approximate analytical solutions for the power spectra during inflation.

At super-Hubble scales i.e. $\sqrt{z_s''/z_s} \gg k^2$ and $\sqrt{z_t''/z_t} \gg k^2$, we can neglect the k^2 term

in Eq.(3.47). This reduces the equation of motion for curvature perturbations given by Eq.(3.42) to:

$$\mathcal{R}_k'' + 2\left(\frac{z_s'}{z_s}\right)\mathcal{R}_k' = 0, \tag{3.49}$$

which can now be integrated very easily to get the following solution:

$$\mathcal{R}_k = c_1 + c_2 \int dt \frac{1}{a z_s}. \tag{3.50}$$

The second term in the above solution decays very rapidly during inflation (it is proportional to a^{-3}) and so we can approximate that the modes freeze once they leave the horizon.

Now, we move onto the more general solutions for the perturbations during inflation. Using the parameters defined in Eq.(3.48) and assuming that the parameters $\dot{\epsilon_1} = \dot{\epsilon_2} = \dot{\epsilon_3} = \dot{\epsilon_4} = 0$ during inflation (this is a good approximation unless the $f(R)$ theory has some abrupt features), we can approximate the Hubble parameter as [17]:

$$H \simeq -\frac{1}{a(1-\epsilon_1)\eta}, \tag{3.51}$$

and

$$\frac{z_s''}{z_s} = \frac{\nu_s^2 - 1/4}{\eta^2}, \quad \text{with} \quad \nu_s^2 = \frac{1}{4} + \frac{(1+\epsilon_1+\epsilon_2-\epsilon_3+\epsilon_4)\,(2+\epsilon_2-\epsilon_3+\epsilon_4)}{(1-\epsilon_1)^2}. \tag{3.52}$$

Substituting this in the equation of motion for the Mukhanov-Sasaki variable (3.47) for the scalar curvature perturbation and substituting $U_k = \eta v_k$ simplifies it to:

$$(k\eta)^2 \frac{d^2 U_k}{d(k\eta)^2} + 2(k\eta)\frac{dU_k}{d(k\eta)} + \left(k^2\eta^2 - \left(\nu_s - \frac{1}{2}\right)\left(\nu_s + \frac{1}{2}\right)\right) U_k = 0, \tag{3.53}$$

which is the spherical Bessel differential equation. For the Bunch-Davies initial conditions, we use the Hankel functions of the first kind to solve this equation. The final form of the scalar power spectrum defined in Eq.(2.23) in this approximation during inflation is then

given by:

$$\begin{aligned}\mathcal{P}_S(k) &\simeq \frac{1}{Q}\left(\frac{H}{2\pi}\right)^2\left((1-\epsilon_1)\frac{\Gamma(\nu_s)}{\Gamma(3/2)}\right)^2\left(\frac{|k\eta|}{2}\right)^{3-2\nu_s}, \\ Q &= \left(\frac{z_s}{a}\right)^2 = \left(\frac{\omega\dot{\phi}^2 + 3\dot{F}^2/(2\kappa^2 F)}{(H+\dot{F}/2F)^2}\right).\end{aligned} \tag{3.54}$$

We evaluate this expression for the modes at horizon crossing, that is, when $k = aH$. Note that for the single-field inflationary model in GR, $Q = (\dot{\phi}/H)^2$ and we get back the slow-roll solution for the scalar power spectrum given in Eq.(2.27). Similarly, the approximate analytical solution for the tensor perturbations during inflation turns out to be:

$$\begin{aligned}\mathcal{P}_T(k) &\simeq \frac{8}{F}\left(\frac{H}{2\pi M_{\rm Pl}}\right)^2\left((1-\epsilon_1)\frac{\Gamma(\nu_t)}{\Gamma(3/2)}\right)^2\left(\frac{|k\eta|}{2}\right)^{3-2\nu_t}, \\ \nu_t^2 &= \frac{1}{4} + \frac{(1+\epsilon_3)\,(2-\epsilon_1+\epsilon_3)}{(1-\epsilon_1)^2}.\end{aligned} \tag{3.55}$$

Again, in GR, $F = 1$ and we retrieve the formula in Eq.(2.27).

Perturbations and spectral indices in a purely $f(R)$ theory

For a purely $f(R)$ theory, we just put $\omega = 0, V = 0$ in Eq.(3.54). For spectral indices, we first take a look at the parameters ϵ_2 and ϵ_4. Since the scalar field is absent, we get $\epsilon_2 = 0$ and redefine the other one as $\epsilon_4 = \ddot{F}/(H\dot{F})$. The calculations remain the same and so we can now write down the scalar and tensor spectral indices as:

$$\begin{aligned}n_S &\simeq 1 - 4\epsilon_1 + 2\epsilon_3 - 2\epsilon_4, \\ n_T &\simeq -2\epsilon_1 - 2\epsilon_3.\end{aligned} \tag{3.56}$$

Also, the tensor-to-scalar ratio is then obtained to be:

$$r \simeq 48\epsilon_1^2. \tag{3.57}$$

We shall see in the next chapter that the indices turn out to be same for both the frames. Now, that we are equipped with the tools to study primordial perturbations during inflation in an $f(R)$ theory, we shall study them in specific inflationary models.

CHAPTER 4

THE STAROBINSKY MODEL

In chapter 3, we discussed the background dynamics and evolution of perturbations in $f(R)$ theories. We shall now take a look at a very specific $f(R)$ theory: the Starobinsky model [19]. In 1970s, Alexei Starobinsky started to consider different models to avoid the singularity in the past. With the great advances in quantum field theory, he started considering quantum corrections to the Einstein's field equations. He started working on quantum corrections to the stress-energy tensor i.e. the right-hand side of the Einstein's field equations. These quantum corrections corresponded to the one-loop corrections arising from the interaction of the quantum matter fields with gravitation. It was noted later that these corrections could be reproduced by considering an $f(R)$ theory which is described by [22]:

$$S = \frac{M_{\rm Pl}^2}{2}\int d^4x\sqrt{-g}\left[R + \alpha R^2 + \beta R^2 ln\left(\frac{R}{C}\right)\right], \tag{4.1}$$

with $\alpha \gg \beta$ and C being some constant. Within this approximation, we generally neglect the last term in the action given above. This is the theory of gravity that Starobinsky proposed in 1980 and is considered a prime candidate for theories explaining inflation and our universe today. The Starobinsky model that we shall be studying in this chapter is:

$$f(R) = R + \frac{R^2}{6M^2}, \tag{4.2}$$

where M is some constant with the dimensions of mass and we have neglected the last term in Eq.(4.1). We are primarily interested in the universe described by this $f(R)$ theory during the inflationary epoch. Unlike general relativity, inflation has a purely gravitational origin in this theory with no need for a scalar field or the cosmological constant to drive inflation. The R^2 term causes inflation and as the Ricci scalar decreases,

the linear term dominates that ends inflation.

4.1 FRIEDMANN EQUATIONS IN STAROBINSKY MODEL

We shall use the metric formalism to study the dynamics as we did in chapter 3. Substituting Eq.(4.2) in Eq.(3.12), gives us the following the set of equations in the absence of any additional fields:

$$\begin{aligned} &\ddot{H} - \frac{\dot{H}^2}{2H} + 3H\dot{H} + \frac{1}{2}M^2 H = 0, \\ &\ddot{R} + 3H\dot{R} + M^2 R = 0. \end{aligned} \tag{4.3}$$

The above equations show that the evolution of the Ricci scalar is governed by a second-order dynamical differential equation and can have non-trivial solutions in a vacuum FLRW universe in the Starobinsky model. The second equation in Eq.(4.3) is the expanded version of the trace equation (3.10) for the Starobinsky model.

4.2 CONFORMAL TRANSFORMATION AND THE EINSTEIN FRAME

To move to the Einstein frame in the Starobinsky model, we use the conformal transformation relations (3.22) that defines the scalar field as:

$$\phi \equiv \sqrt{\frac{3}{2}} M_{\rm Pl} ln\left(1 + \frac{R}{3M^2}\right), \tag{4.4}$$

and using the form of the potential derived earlier, given by Eq.(3.25) for $n = 2$ and $\alpha = 1/(6M^2)$, we get:

$$V(\phi) = \frac{3}{4}M^2 M_{\rm Pl}^2 \left(1 - exp\left[-\sqrt{\frac{2}{3}}\frac{\phi}{M_{\rm Pl}}\right]\right)^2. \tag{4.5}$$

This is also referred to as the Starobinsky potential. So, the $f(R)$ Starobinsky model in the Jordan frame has a conformally equivalent partner in the Einstein frame which is a theory of general relativity coupled minimally to a canonical scalar field described by the potential (4.5). We can see that when $\phi/M_{\rm Pl} \gg 1$, the potential is almost constant which leads to slow-roll inflation. Figure 4.1 shows the qualitative behaviour of the two

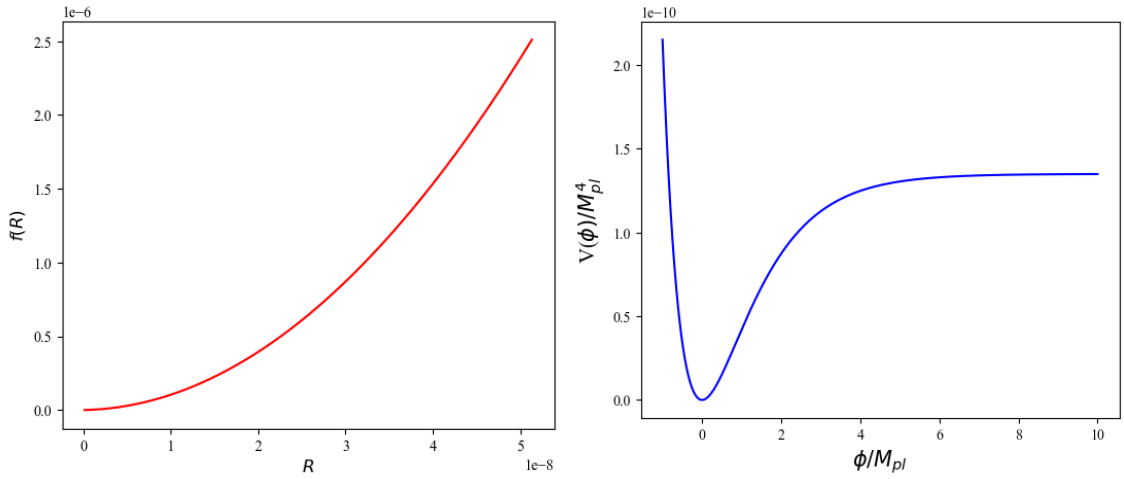

Figure 4.1: Qualitative behaviour of $f(R)$ that describes the Starobinsky model in the Jordan frame and the Starobinsky potential that governs the dynamics in the Einstein frame.

quantities $f(R)$ and $V(\phi)$ that govern the dynamics in the Starobinsky model in the Einstein and the Jordan frames.

4.3 APPROXIMATE SOLUTIONS TO THE BACKGROUND DURING INFLATION

We shall now look for approximate analytical solutions to the background quantities during inflation in the Starobinsky model. The approximate solutions during inflation can also be used to constrain the value of M in this model as we will see later.

4.3.1 Background dynamics in the Jordan frame

Since the Hubble parameter varies very slowly during inflation, we can neglect the first two terms in the equation of motion governing the evolution of H in (4.3). This leads to $\dot{H} \simeq -M^2/6$ which on integrating gives us the approximate solution for the Hubble parameter during inflation as:

$$H \simeq H_i - \frac{M^2}{6}(t - t_i), \tag{4.6}$$

which shows that the Hubble parameter decreases with time during inflation. We can use the above solution to derive the following solution for the evolution of the scale factor $a(t)$ during inflation:

$$a \simeq a_i exp\left[H_i(t-t_i) - \frac{M^2}{12}(t-t_i)^2\right], \tag{4.7}$$

where t_i denotes the cosmic time when inflation starts and H_i, a_i denote the values of the Hubble parameter and the scale factor at the beginning of inflation. Note that the scale factor shows an exponentially expanding universe during this period in the Jordan frame. We can also approximate the evolution of the Ricci scalar R from the above relations of H as:

$$R \simeq 12H^2 - M^2 \simeq 12\left[H_i - \frac{M^2}{6}(t-t_i)\right]^2 - M^2. \tag{4.8}$$

Since the Hubble parameter decreases with time during inflation, we can see from the above equation that during inflation, the scalar curvature decreases as well. The first-slow roll parameter can then be written as:

$$\epsilon_1 = -\frac{\dot{H}}{H^2} \simeq \frac{M^2}{6H^2}. \tag{4.9}$$

Since inflation will end when $\epsilon_1 = 1$, we can say that at the end of inflation, $H \simeq M/\sqrt{6}$ which corresponds to $R \simeq M^2$. Therefore, we can find the time at which inflation ends:

$$\begin{aligned} \frac{M}{\sqrt{6}} &= H_i - \frac{M^2}{6}(t_f - t_i) \\ \implies t_f &\simeq t_i + \frac{6}{M^2}\left(H_i - M/\sqrt{6}\right) \simeq t_i + \frac{6}{M^2}H_i, \end{aligned} \tag{4.10}$$

where we have approximated $H_i \gg M/\sqrt{6}$. We can also find the duration of inflation in this approximation which turns out to be:

$$N = \int_{t_i}^{t_f} H dt \simeq H_i(t_f - t_i) - \frac{M^2}{12}(t_f - t_i)^2 \simeq \frac{3H_i^2}{M^2} = \frac{1}{2\epsilon_1(t_i)}. \tag{4.11}$$

4.3.2 Background dynamics in the Einstein frame

First, we relate the time coordinate in the two frames [17]:

$$\begin{aligned}\tilde{t} &= \int_{t_i}^{t} \sqrt{F}dt \simeq \int_{t_i}^{t} \sqrt{\frac{R}{3M^2}}dt \simeq \int_{t_i}^{t} \frac{2H}{M}dt \\ &= \frac{2}{M}\left[H_i(t-t_i) - \frac{M^2}{12}(t-t_i)^2\right],\end{aligned} \tag{4.12}$$

where $t = t_i$ corresponds to $\tilde{t} = 0$. Using this and the relation between the scale factors in the two frames, we can then write:

$$\tilde{a}(\tilde{t}) \simeq \frac{2a_iH_i}{M}\left(1 - \frac{M^2}{12H_i^2}M\tilde{t}\right)e^{M\tilde{t}/2}. \tag{4.13}$$

We can also relate the Hubble parameters using Eq.(3.29) which gives us the following:

$$\tilde{H}(\tilde{t}) \simeq \frac{M}{2}\left[1 - \frac{M^2}{6H_i^2}\left(1 - \frac{M^2}{12H_i^2}M\tilde{t}\right)^{-2}\right]. \tag{4.14}$$

The above equation shows that even in the Einstein frame, the Hubble parameter decreases i.e. the Hubble radius increases and the scalar curvature decreases during inflation in the two frames. The scale factor in Eq.(4.13) corresponds to a quasi-exponentially expanding universe. So, both the Einstein and Jordan frames explain an epoch of inflation in the early universe in the Starobinsky model. Also,

$$\tilde{N} = N + \frac{1}{2}\ln\left(\frac{F}{F_i}\right) \simeq N + \frac{1}{2}\ln\left(\frac{R}{R_i}\right) \simeq N + \ln\left(\frac{H}{H_i}\right). \tag{4.15}$$

Therefore, in slow-roll type inflation where the Hubble parameter varies very slowly, $\tilde{N}$ is almost identical to N. In the Einstein frame, under the slow-roll conditions, we can write:

$$\tilde{N} = \int_{\tilde{t}_i}^{\tilde{t}} \tilde{H}d\tilde{t} \simeq \frac{1}{M_{\rm Pl}^2}\int_{\phi}^{\phi_i} \frac{V}{V_\phi}d\phi \simeq \frac{3}{4}exp\left(\sqrt{\frac{2}{3}}\frac{\phi_i}{M_{\rm Pl}}\right). \tag{4.16}$$

Using the above relations, the first two slow-roll parameters defined in Eq.(3.48) reduce to the leading order in $\tilde{N}$ as:

$$\begin{aligned}\tilde{\epsilon_1} &= -\frac{\dot{\tilde{H}}}{\tilde{H}^2} \simeq \frac{M_{\rm Pl}^2}{2}\left(\frac{V_\phi}{V}\right)^2 \simeq \frac{3}{4\tilde{N}^2},\\ \tilde{\epsilon_2} &= \frac{\ddot{\phi}}{\tilde{H}\dot{\phi}} \simeq \frac{1}{\tilde{N}}.\end{aligned} \tag{4.17}$$

We will use this form of the slow-roll parameters under the slow-roll approximations during the discussion on solutions to the power spectra and especially the spectral indices in the next section.

4.4 APPROXIMATE SOLUTIONS TO THE POWER SPECTRA DURING INFLATION

4.4.1 Primordial power spectra in the Jordan frame

Let us take a look back at our discussion on approximate analytical solutions to the power spectra for an $f(R)$ theory coupled with scalar field in the previous chapter. We use Eq. (3.54) and Eq.(3.55) where $\omega = 0$ and $F \simeq R^2/(3M^2) \simeq 4H^2/M^2$ for the Starobinsky model in the Jordan frame. This gives us another relation, that is, $\epsilon_1 = -\epsilon_3 \simeq -\epsilon_4$ and so at the leading order, we can write the scalar and tensor power spectra as:

$$\begin{aligned}\mathcal{P}_S &\simeq \frac{M^2}{96\pi^2 M_{\rm Pl}^2}\frac{1}{\epsilon_1^2},\\ \mathcal{P}_T &\simeq \frac{M^2}{2\pi^2 M_{\rm Pl}^2},\end{aligned} \tag{4.18}$$

where we evaluate the spectra at the time when the modes leave the Hubble radius i.e. $k = aH$. We see that at the leading order the tensor power spectrum is scale-invariant. If we assume that the modes we have constrained from observations ($k = 0.05\text{Mpc}^{-1}$) leave the horizon very early during inflation, then using Eq.(4.10) and Eq.(4.11), we can write $\epsilon_1(t_i) \simeq \epsilon_1(t_k) \simeq 1/(2N_k)$ where t_k denotes the time when the mode leaves the horizon and N_k denotes the e-foldings when the mode leaves the Hubble radius counted backwards from the end of inflation. Using this and Eq.(4.18), we can then approximate

the tensor-to-scalar ratio as:

$$r(k) \simeq 48\epsilon_1^2 \simeq \frac{12}{N_k^2}. \tag{4.19}$$

For $N_k = 55$(the WMAP renormalisation constrains N_k to about 50-60 e-foldings), we get $r \simeq 3.967 \times 10^{-3}$ which agrees very well with the constraints from observations. We can also approximate the scalar spectral index as:

$$n_S(k) = 1 - 4\epsilon_1 + 2\epsilon_3 - 2\epsilon_4 \simeq 1 - 4\epsilon_1 \simeq 1 - \frac{2}{N_k}, \tag{4.20}$$

which gives us $n_S \simeq 0.9636$ for $N_k = 55$. This value is also within the constraints from the Planck 2018 data. Also, we can constrain the value of M by using the scalar spectrum constraint at $k = 0.05\text{Mpc}^{-1}$ i.e. $\mathcal{P}_S = 2.1 \times 10^{-9}$, which gives us $M \simeq 2.56 \times 10^{-5} M_{\text{Pl}}$.

4.4.2 Primordial power spectra in the Einstein frame

In the Einstein frame, we can approximate the scalar spectral index as:

$$\begin{aligned} \tilde{n}_S(k) &\simeq 1 - 4\tilde{\epsilon}_1 - 2\tilde{\epsilon}_2 \\ &\simeq 1 - \frac{3}{\tilde{N}_k^2} - \frac{2}{\tilde{N}_k} \\ &\simeq 1 - \frac{2}{\tilde{N}_k}, \end{aligned} \tag{4.21}$$

to the leading order in $\tilde{N}_k$. Since we argued from Eq.(4.15) that under the slow-roll approximation, $N_k \simeq \tilde{N}_k$, we conclude that $n_S \simeq \tilde{n}_S$. Again using Eq.(3.54) and Eq.(3.55) with $\omega = 1$ and $F = 1$, we can write:

$$\begin{aligned} \tilde{\mathcal{P}}_S(k) &\simeq \left(\frac{\tilde{H}^2}{2\pi\dot{\phi}}\right)^2_{k=\tilde{a}\tilde{H}} = -\frac{1}{8\pi^2 M_{\text{Pl}}^2}\left(\frac{\tilde{H}^4}{\dot{\tilde{H}}}\right)_{k=\tilde{a}\tilde{H}}, \\ \tilde{\mathcal{P}}_T(k) &\simeq \frac{8}{M_{\text{Pl}}^2}\left(\frac{\tilde{H}}{2\pi}\right)^2_{k=\tilde{a}\tilde{H}}, \end{aligned} \tag{4.22}$$

to the leading order. Using these approximated forms, the tensor-to-scalar ratio turns out to be:

$$\tilde{r}(k) \simeq 16\tilde{\epsilon}_1 \simeq \frac{12}{\tilde{N}_k^2}, \tag{4.23}$$

where we have used Eq.(4.17) for the last relation. So, we again conclude that $r \simeq \tilde{r}$. So, we have showed that the primordial power spectra is equivalent in the Einstein and Jordan frames under the slow-roll approximation for the Starobinsky model. Such an equivalence also holds for non-minimally coupled models of gravitation which will be discussed in chapter 5.

4.5 NUMERICAL APPROACH

In the previous section, we studied the dynamics in the Starobinsky model under the slow-roll approximation. However, that is not enough and so we shall employ numerical methods to compute the evolution of background and perturbations in the two frames in this model. We discussed the numerical approach for the dynamics in the Einstein frame i.e. single-field model coupled minimally to gravitation in section 2.4. Now, we shall discuss the numerical approach in Jordan frame.

4.5.1 Numerical approach to the background dynamics in Jordan frame

The first task is to rewrite the equations in terms of derivatives with respect to the e-foldings N. Therefore, rewriting the Friedmann equations for the Starobinsky model given by Eq.(4.3) gives us :

$$\begin{aligned} H_{NN} + \frac{H_N^2}{2H} + 3H_N + \frac{M^2}{2H} &= 0, \\ R_{NN} + \left(3 + \frac{H_N}{H}\right) R_N + \frac{M^2}{H^2} R &= 0. \end{aligned} \tag{4.24}$$

Since the initial conditions are easier to set in the Einstein frame, what we do is we set initial conditions on the inflaton field ϕ in the Einstein frame and use the conformal transformation relations to set conformally equivalent initial conditions on H in the Jordan frame. With this, we can derive all the background quantities in the Jordan frame like the slow-roll parameters and the Ricci scalar.

For numerical analysis, we have set the parameter $M = 1.336 \times 10^{-5} M_{\rm Pl}$. We have chosen the initial conditions on the field $\phi_i = 5.6 M_{\rm Pl}$ in the Einstein frame [23] which

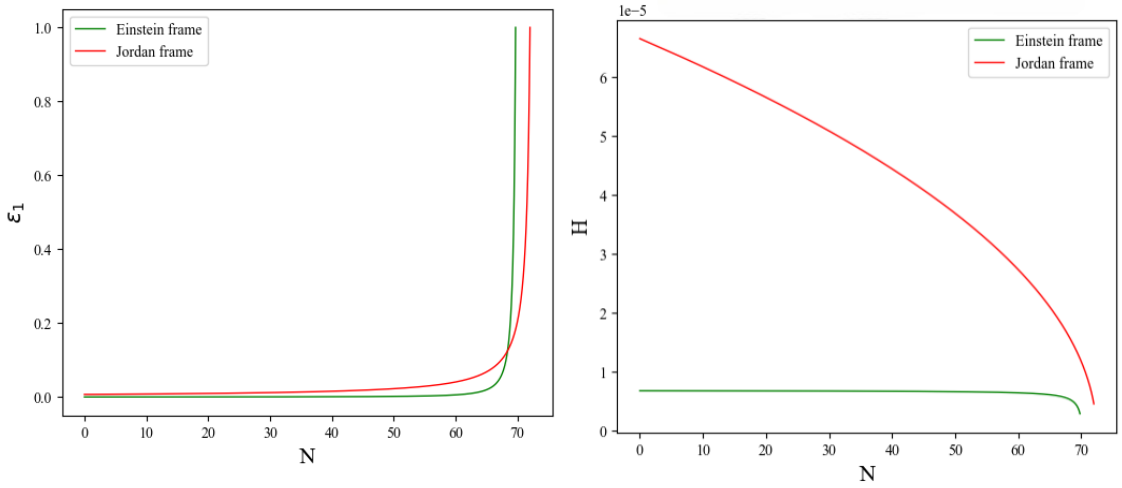

Figure 4.2: Evolution of the first slow-roll parameter ϵ_1 and the Hubble parameter during inflation in the Einstein and Jordan frames. We observe that inflation lasts longer in the Jordan frame. The Hubble parameter varies more slowly during inflation in the Einstein frame.

corresponds to $H_i \simeq 6.552 \times 10^{-5}$ in the Jordan frame. For these values of parameters and the initial conditions, we find that inflation lasts for about 69.675 e-folds in the Einstein frame and about 72.009 e-folds in the Jordan frame. Figure 4.2 shows the evolution of the first-slow parameter and the Hubble parameter during inflation in the Einstein and Jordan frames. It is important to note that the first slow-roll parameter ϵ_1 is not invariant under the conformal transformation in this case and so *the duration of inflation is different in the Einstein and Jordan frames*. The plot for the Ricci scalar in the two frames has a similar nature to that of the Hubble parameter.

4.5.2 Numerical approach to the evolution of perturbations in Jordan frame

Now, we come to the primordial perturbations. The first task is to determine the value of the scale factor at the beginning of inflation. To maintain the conformal equivalence of the two frames, we set the initial value of scale factor in the Einstein frame and use the

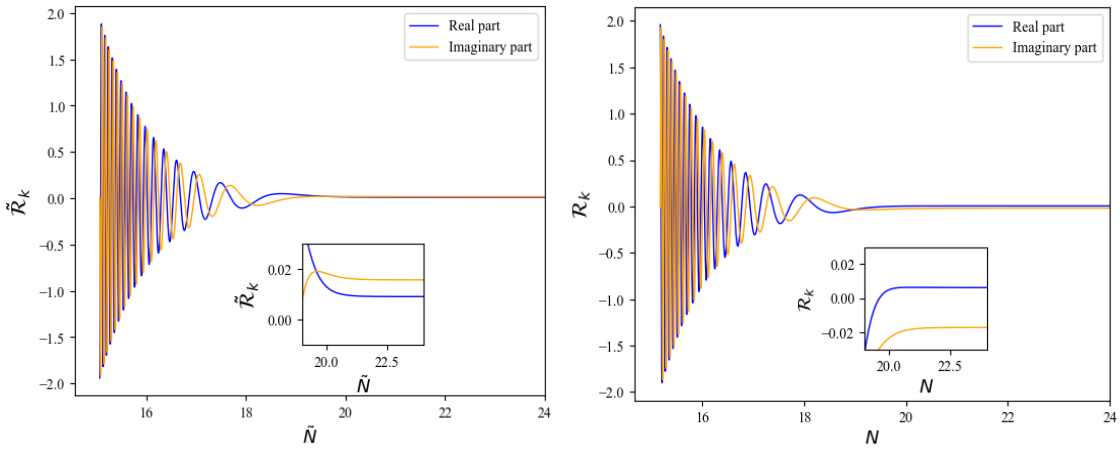

Figure 4.3: Evolution of the mode of the scalar curvature perturbation corresponding to the pivot scale as a function of e-folds in the Einstein frame (left) and Jordan frame (right).

following expression to compute the initial value of scale factor in the Jordan frame.

$$\begin{aligned} \tilde{a}_i &= a_i\sqrt{F}, \\ \implies a_i &= \frac{\tilde{a}_i}{\sqrt{F}} = \tilde{a}_i exp\left(-\sqrt{\frac{1}{6}}\frac{\phi_i}{M_{\rm Pl}}\right). \end{aligned} \tag{4.25}$$

We can calculate $\tilde{a}_i$ from Eq.(2.31). For numerical analysis, we have assumed that the mode corresponding to the pivot scale ($k = 0.05\text{Mpc}^{-1}$) crosses the horizon about 50 e-folds before the end of inflation in the Einstein frame. Using the above relation to calculate a_i in the Jordan frame and from Eq.(2.31), we find that the mode corresponding to the pivot scale then crosses the horizon about 52.174 e-folds before the end of inflation in the Jordan frame. Now, we rewrite the equations of motion for the Fourier modes of scalar curvature perturbation and the tensor perturbations in terms of derivatives with respect to N. We derive these equations for a general $f(R)$ model. So, rewriting Eq.(3.42) gives us:

$$\frac{d^2\mathcal{R}_k}{dN^2} + \left(3 + \frac{1}{H}\frac{dH}{dN} + \frac{1}{Q}\frac{dQ}{dN}\right)\frac{d\mathcal{R}_k}{dN} + \frac{k^2}{a^2H^2}\mathcal{R}_k = 0, \tag{4.26}$$

where

$$\frac{1}{Q}\frac{dQ}{dN} = \frac{\left(2\frac{F_{NN}}{F_N} + \frac{1}{2}\frac{F_N^2}{F^2} - \frac{F_N}{F}\right)}{\left(1 + \frac{F_N}{2F}\right)}, \tag{4.27}$$

where $F_N = dF/dN$ and $F_{NN} = d^2F/dN^2$. Similarly, the equation of motion for the Fourier modes of tensor perturbations can be rewritten as:

$$\frac{d^2h_k}{dN^2} + \left(3 + \frac{1}{H}\frac{dH}{dN} + \frac{1}{F}\frac{dF}{dN}\right)\frac{dh_k}{dN} + \frac{k^2}{a^2H^2}h_k = 0. \tag{4.28}$$

The initial conditions imposed on the Fourier modes of the scalar curvature perturbation then correspond to:

$$\begin{aligned}
\mathcal{R}_k(N_0) &= \frac{1}{\sqrt{2k}}\frac{1}{a(N_0)\sqrt{Q(N_0)}}, \\
\frac{d\mathcal{R}_k}{dN}(N_0) &= -\mathcal{R}_k\left(1 + \frac{1}{2Q(N_0)}\frac{dQ}{dN}(N_0)\right) + i\sqrt{\frac{k}{2}}\left(\frac{1}{a^2(N_0)H(N_0)\sqrt{Q(N_0)}}\right),
\end{aligned} \tag{4.29}$$

where N_0 is some e-folding at which we impose the initial conditions and Q is given by the following expression:

$$Q = \frac{3}{2\kappa^2}\frac{F_N^2/F}{(1 + F_N/(2F))^2}. \tag{4.30}$$

Similarly for the initial conditions on the Fourier modes for the tensor perturbations, Q is replaced by F in the above pair of equations. Figure 4.3 shows the evolution of the mode corresponding to $K = 0.05\text{Mpc}^{-1}$ of the scalar curvature perturbation in the Einstein and Jordan frames. We see that they approach a constant value at about 20 e-folds which is what we expected.

Figure 4.4 shows the comparison of the scalar and tensor power spectra in the Einstein and Jordan frames for the Starobinsky model. The value of scalar power spectra at the pivot scale ($k = 0.05\text{Mpc}^{-1}$): $\mathcal{P}_S \simeq 2.1089 \times 10^{-9}$ in the Einstein frame and $\mathcal{P}_S \simeq 2.1093 \times 10^{-9}$ in the Jordan frame which shows a difference of about 0.018% in the two values. Not only they agree very well with each other but also with the observational data which constrains the spectra to $\mathcal{P}_S = 2.1 \times 10^{-9}$. Figure 4.5 shows the comparison of the scalar spectral index and the tensor-to-scalar ratio in the two frames. We observe that

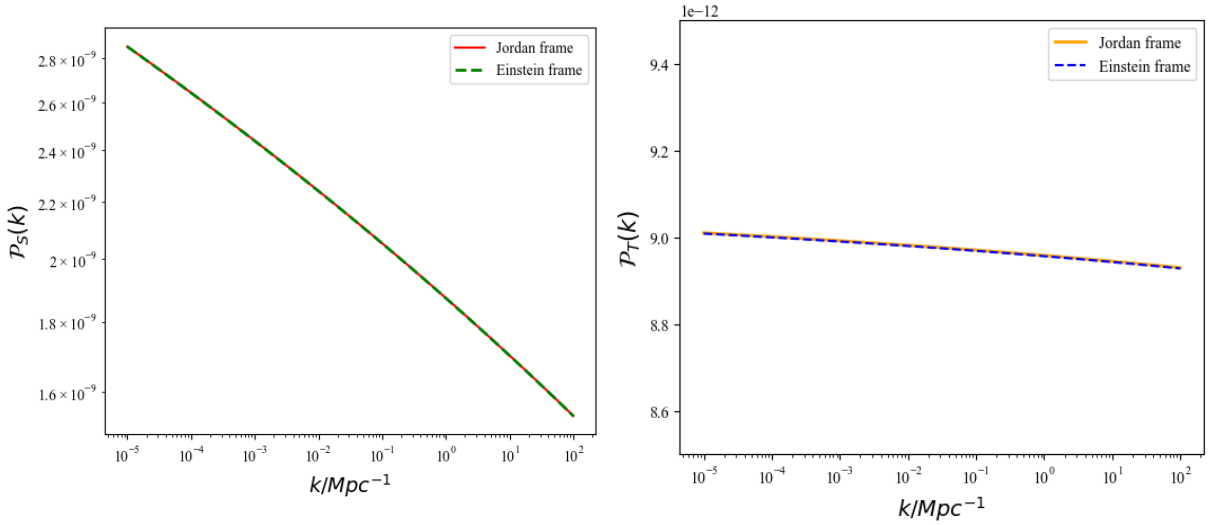

Figure 4.4: The left plot shows the comparison of the scalar power spectrum and the right plot shows the comparison of the tensor power spectrum in the Einstein and Jordan frames for the Starobinsky model. We can see that they match to a very high accuracy which means that the curvature perturbations are equivalent in the two frames.

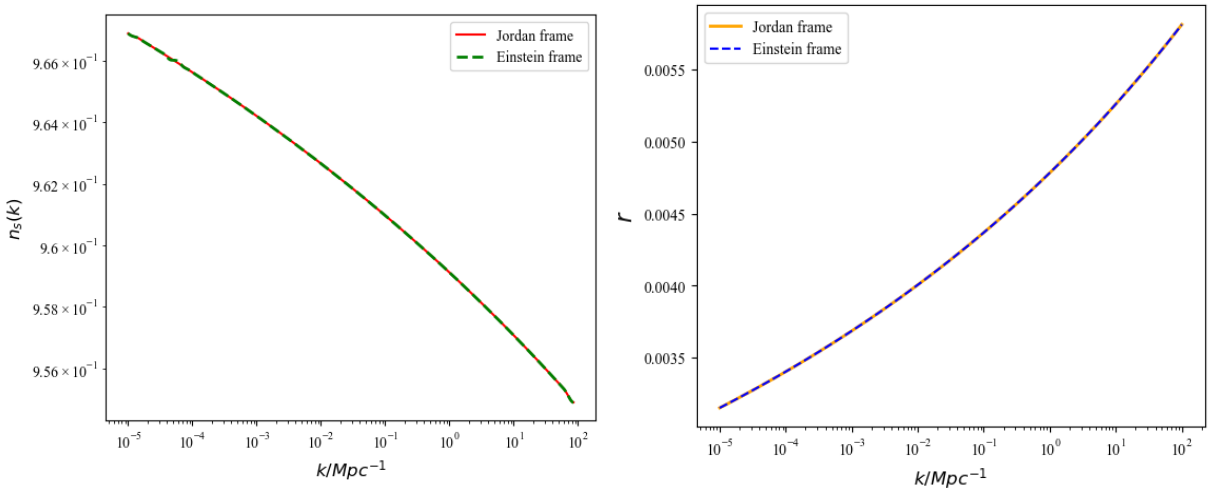

Figure 4.5: The left plot shows comparison of the scalar spectral index and the right plot shows the comparison of the tensor-to-scalar ratio in the Einstein and Jordan frames for the Starobinsky model.

$n_S \simeq 0.9612$ in the Einstein frame and $n_S \simeq 0.9614$ in the Jordan frame at the pivot scale which agrees very well with the observational constraint of $n_S = 0.9649 \pm 0.0042$ from the Planck 2018 data. Similarly, the tensor-to-scalar ratio at $k = 0.002\text{Mpc}^{-1}$ is observed

to be $r_{0.002} \simeq 3.779 \times 10^{-3}$ in both the frames which is well within the observational constraint $r_{0.002} < 0.064$ from the Planck data [12].

Proof for $\mathcal{R} = \tilde{\mathcal{R}}$

The above result was expected since we can analytically show that the curvature perturbations remain invariant in the two frames. Under conformal transformation, the scalar perturbations Φ, Ψ transform as [17]:

$$\tilde{\Phi} = \Phi + \frac{\delta F}{2F}, \qquad \tilde{\Psi} = \Psi + \frac{\delta F}{2F}. \tag{4.31}$$

We start with the definition of $\mathcal{R}_{\delta F}$ in the Jordan frame and relate it to $\tilde{\mathcal{R}}_{\delta\phi}$ in the Einstein frame. These two quantities have been defined in Eq.(3.41). Using Eq.(3.22) and Eq.(3.29) and the above transformation of Ψ, we can then write:

$$\begin{aligned}
\tilde{\mathcal{R}}_{\delta\phi} &= \tilde{\Psi} - \frac{\tilde{H}\delta\phi}{\dot{\phi}} \\
&= \Psi + \frac{\delta F}{2F} - \left(H + \frac{\dot{F}}{2F}\right)\frac{1}{\sqrt{F}}\frac{\delta F}{(\dot{F}/\sqrt{F})} \\
&= \Psi - H\frac{\delta F}{\dot{F}} \\
&= \mathcal{R}_{\delta F},
\end{aligned} \tag{4.32}$$

which shows that the scalar curvature perturbations is equivalent in the Einstein ad Jordan frames. The vector and tensor perturbations are not affected by the conformal transformation and hence they are also equivalent in the two frames.

Therefore, we see that the power spectra are equivalent in the two frames for an $f(R)$ theory and we also showed this by computing them explicitly for the Starobinsky model. The Starobinsky model also agrees very well with the observational constraints and so is a potential candidate for a viable inflationary theory.

CHAPTER 5

HIGGS INFLATION

The Higgs field is so far the only scalar field in the Standard Model and the last piece of the puzzle which completed the SM after its detection at ATLAS and CMS simultaneously in 2012. Being the only scalar field in the framework of SM, it has gained a lot of attention as the potential candidate for the inflaton field. The Higgs field as described in the Standard Model is described by the potential [24]:

$$V(\phi) = -\frac{1}{2}\mu^2\phi^2 + \frac{1}{4}\lambda\phi^4. \tag{5.1}$$

Since the energy scale at which inflation is believed to occur is very large, we generally neglect the quadratic term and approximate the Higgs potential to a quartic potential to study inflationary dynamics. However, recent observations from the CMB have strongly disfavoured quadratic and quartic potentials because they predict large values of the tensor-to-scalar ratio r and hence a very large effective cosmological constant. The self-coupling constant λ of the Higgs field from electroweak observations is too large to fit the data. Hence, a theory where Higgs is minimally coupled to gravitation is not viable.

However, different methods to source inflation with the Higgs field have been proposed [25, 26, 27]. One of the methods is to consider a non-canonical kinetic term with the SM Higgs potential which was shown to be consistent with the observations from the CMB. The other method is to non-minimally couple the Higgs field to gravitation which has also been shown to agree with the observational constraints. We are going to discuss the second approach i.e. a theory of Higgs field non-minimally coupled to gravitation.

5.1 ACTION FOR THE NON-MINIMALLY COUPLED HIGGS MODEL

The action describing the Higgs field ϕ coupled non-minimally to the Ricci scalar R is given by [26, 28]:

$$S = \int d^4x\sqrt{-g}\left(\frac{M_{\rm Pl}^2}{2}Rf(\phi) - \frac{1}{2}\partial_\mu\phi\partial^\mu\phi - V(\phi)\right) + \int d^4x\sqrt{-g}\mathcal{L}_M, \tag{5.2}$$

where $\mathcal{L}_M$ denotes the Lagrangian density accounting for additional matter fields. The function $f(\phi)$ describes the coupling of the field to the Ricci scalar R. For minimal coupling $f(\phi) = 1$ and we introduce terms dependent on ϕ to consider non-minimal coupling. The Higgs potential $V(\phi)$ is described by [28]:

$$V(\phi) = \frac{\lambda}{4}\left(\phi^2 - \sigma^2\right)^2, \tag{5.3}$$

where λ denotes the self-coupling strength of the Higgs and σ is the vacuum expectation value (vev) of the Higgs field. From the electroweak observations, we have $\lambda = 0.1$ and $\sigma = 246\text{GeV} = 1.1 \times 10^{-16}M_{\rm Pl}$. This value of the vev of the Higgs is very small compared to the Planckian scale and so we neglect the σ^2 term in the potential when studying inflationary dynamics. The function $f(\phi)$ we have considered in the Higgs model is described as:

$$f(\phi) = \frac{m^2 + \xi\phi^2}{M_{\rm Pl}^2}, \tag{5.4}$$

where ξ denotes the non-minimal coupling strength of the Higgs with R and m is a mass parameter satisfying $m^2 = M_{\rm Pl}^2 - \xi\sigma^2$. For the values of σ and $\xi = 1.3658 \times 10^4$ that we shall work with, we can approximate $m \simeq M_{\rm Pl}$. We will show that this value of the non-minimal coupling constant agrees well with the observations. This is the Jordan frame representation in which the theory was initially proposed.

5.2 FIELD EQUATIONS AND FRIEDMANN EQUATIONS

Varying the action (5.2) with respect to the metric gives us the following field equations:

$$(R_{\mu\nu} - \frac{1}{2}g_{\mu\nu}R)f(\phi) + (g_{\mu\nu}\Box - \nabla_\mu\nabla_\nu)f(\phi) = \kappa^2 T_{\mu\nu}, \tag{5.5}$$

where $T^{\mu}_{\nu} = diag(-\rho, p, p, p)$ considering only the scalar field ϕ given by Eq.(1.17). The equation of motion governing the field ϕ is given by:

$$\Box\phi - V_{\phi} + \frac{1}{2\kappa^2} R f_{\phi} = 0, \tag{5.6}$$

where $f_{\phi} = df/d\phi$. Note that there is an extra last term in this equation due to the non-minimal coupling. From hereon, we won't take any additional fields into account. For a spatially flat FLRW universe, the Friedmann equations in this theory are then given by:

$$\begin{aligned} 3Hf(\dot{\phi}) + 3H^2 f(\phi) &= \kappa^2 \left(\frac{\dot{\phi}^2}{2} + V(\phi) \right), \\ f(\ddot{\phi}) - Hf + 2\dot{H}f &= -\kappa^2 \dot{\phi}^2. \end{aligned} \tag{5.7}$$

Note that these equations are very similar to the Friedmann equations derived for the $f(R)$ theory with only $F(R)$ replaced by $f(\phi)$. In fact, we shall see that the derivations and the final equations of motion for this theory have exactly the same form with just $F(R)$ replaced by $f(\phi)$. Eq.(5.6) and Eq.(5.7) govern the background dynamics in the Higgs model in a smooth and homogeneous FLRW background.

5.3 REDEFINING THE FIELD IN THE EINSTEIN FRAME

We shall now use conformal transformation to rewrite the non-minimally coupled Higgs theory in the framework of general relativity where the field is minimally coupled to R and see how the potential turns out. W use the conformal transformation of the form:

$$\tilde{g}_{\mu\nu} = \Omega^2 g_{\mu\nu} = f(\phi) g_{\mu\nu}. \tag{5.8}$$

The method is rather straightforward after this. We redefine the field in the Einstein frame to make the kinetic term canonical which gives us:

$$S = \int d^4x \sqrt{-\tilde{g}} \left(\frac{\tilde{R}}{2\kappa^2} - \frac{1}{2}\partial_{\mu}\chi\partial^{\mu}\chi - U(\chi) \right) - \int d^4x \sqrt{-\tilde{g}} \tilde{\mathcal{L}}_M (f(\phi(\chi))^{-1} \tilde{g}_{\mu\nu}, \psi_M), \tag{5.9}$$

in the Einstein frame. The redefined field χ and the potential $U(\chi)$ are related to ϕ and $V(\phi)$ through the following relation [27]:

$$\frac{d\chi}{d\phi} = \frac{1}{f(\phi)}\sqrt{f(\phi) + 6\kappa^2\xi^2\phi^2}, \tag{5.10}$$

$$U(\chi) = \frac{V(\phi(\chi))}{\Omega^4} = \frac{V(\phi(\chi))}{f^2(\phi(\chi))}. \tag{5.11}$$

Once again, we see that this theory in the Einstein frame is a theory of the redefined Higgs field coupled minimally to gravitation but at the same time it is coupled non-minimally to the additional fields. The two frames again have their own convenience, studying the gravitational sector is easier in the Einstein frame because of the simplified Einstein's equations. However, studying the non-gravitational sector has to be done in the Jordan frame. Because of this, the Jordan frame is the *physical frame* as far as the non-gravitational sector is concerned because this is where we have the SM description of the Higgs and other fields. Nevertheless, we shall study the evolution of background and the dynamics during inflation in both the frames for the Higgs model.

5.3.1 Approximate analytical form of the Higgs potential in the Einstein frame

Using Eq.(5.10) and Eq.(5.11), we can approximate the the potential $U(\chi)$ in different limiting cases [27].

1. For the limit, $\phi \ll \frac{M_{\rm Pl}}{\sqrt{6}\xi}$ we get:

$$\phi = \pm\chi \implies U(\chi) \simeq \frac{\lambda}{4}\chi^4, \quad |\chi| \ll \frac{M_{\rm Pl}}{\sqrt{6}\xi}. \tag{5.12}$$

2. For the limit, $\frac{M_{\rm Pl}}{\sqrt{6}\xi} \ll \phi \ll \frac{M_{\rm Pl}}{\sqrt{\xi}}$ we get:

$$\chi = \pm\sqrt{\frac{3}{2}}\frac{\xi}{M_{\rm Pl}}\phi^2 \implies U(\chi) \simeq \frac{\lambda M_{\rm Pl}^2}{6\xi^2}\chi^2, \quad \frac{M_{\rm Pl}}{2\sqrt{6}\xi} \ll |\chi| \ll \sqrt{\frac{3}{2}}M_{\rm Pl}. \tag{5.13}$$

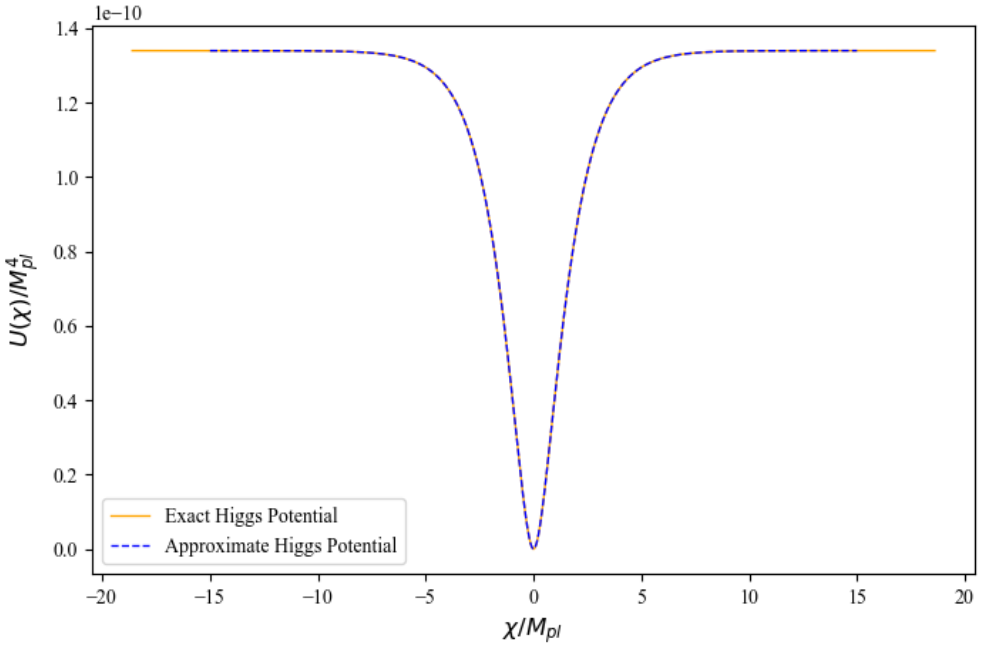

Figure 5.1: Higgs inflation potential in the Einstein frame. The (solid) orange line shows the numerically calculated exact form of the potential and the (dashed) blue line shows approximate potential described in Eq.(5.15).

3. For the limit, $\phi \gg \frac{M_{\rm Pl}}{\sqrt{\xi}}$,

$$\chi = \pm\sqrt{\frac{3}{2}} M_{\rm Pl} ln\left(\frac{\xi}{M_{\rm Pl}^2}\phi^2\right) \implies U(\chi) \simeq \frac{\lambda M_{\rm Pl}^4}{4\xi^2}\left(1 + e^{-\sqrt{\frac{2}{3}}\frac{|\chi|}{M_{\rm Pl}}}\right)^{-2}, \tag{5.14}$$

where the modulus of χ in (5.14) maintains the limiting condition on ϕ.

Since inflation occurs in the regime $\phi \gg \frac{M_{\rm Pl}}{\sqrt{6\xi}}$, we are interested in only this limit. It can be checked that in this regime, the potential $U(\chi)$ can be approximated to the following form:

$$U(\chi) \simeq \frac{\lambda M_{\rm Pl}^4}{4\xi^2}\left(1 - e^{-\sqrt{\frac{2}{3}}\frac{|\chi|}{M_{\rm Pl}}}\right)^2. \tag{5.15}$$

Figure 5.1 shows the comparison of the exact Higgs potential in the Einstein frame constructed numerically using Eq.(5.10) and Eq.(5.11) for the quartic Higgs potential and the approximate form of $U(\chi)$ given by Eq.(5.15). We can see that they match to a very precision and so this approximate form of the potential can be used to study inflationary dynamics in the Einstein frame. Now this is the interesting part! This form

of the potential for the regime $\chi > 0$ where inflation occurs is exactly the same as the Starobinsky potential we obtained in the previous chapter in the Einstein frame given by Eq.(4.5)! This means that *if the parameters M, ξ and λ satisfy the relation*:

$$\frac{M^2}{M_{\rm Pl}^2} = \frac{\lambda}{3\xi^2}, \tag{5.16}$$

the dynamics in the Einstein frame for both the Higgs and the Starobinsky model during inflation will be the same. This makes it interesting to compare the dynamics of the universe in the Higgs and Starobinsky model in the Jordan frame. We shall do this in the last section of this chapter.

5.4 PRIMORDIAL PERTURBATIONS DURING INFLATION IN THE JORDAN FRAME

The derivation of the equations of motion for the scalar curvature perturbation and the tensor perturbations in the non-minimally coupled model is the same as that of the $f(R)$ theories. Those equations are also valid for an action of the form $f(\phi)R$ and not just $f(R)$ theories. We shall not derive them again and use the results from chapter 3. However, there is a crucial difference between the two theories. Unlike in the $f(R)$ theory, the non-minimal coupling to gravitation does not introduce any additional scalar degree of freedom. This is important in gauge fixing. In the theory of non-minimal coupling, we shall be working only in the longitudinal gauge to study the scalar perturbations. So, the equation of motion governing the evolution of the Fourier modes of the scalar curvature perturbations is given by:

$$\mathcal{R}_k'' + 2\left(\frac{z_s'}{z_s}\right)\mathcal{R}_k' + k^2\mathcal{R}_k = 0, \tag{5.17}$$

where

$$z_s = a\left(\frac{\dot{\phi}^2 + 3\dot{f}^2/(2\kappa^2 f)}{(H + \dot{f}/2f)^2}\right)^{1/2}. \tag{5.18}$$

Similarly, for the tensor perturbations we can write:

$$h_k'' + 2\left(\frac{z_t'}{z_t}\right) h_k' + k^2 h_k = 0, \tag{5.19}$$

where $z_t = a\sqrt{f(\phi)}$ and we can use the Bunch-Davies vacuum conditions given by Eq.(2.21) to impose initial conditions on the Mukhanov-Sasaki variables defined as $v = \mathcal{R} z_s$ and $u = h z_t/\sqrt{16\pi G}$ when the modes are well inside the Hubble radius. The approximate solutions to the primordial power spectra defined in Eq.(2.23) takes up the same form as Eq.(3.54) and Eq.(3.55) for the non-minimally coupled Higgs model in the Jordan frame. We simply replace $F(R)$ by $f(\phi)$ in these expressions. We shall focus more on the numerical approach to compute and study the exact dynamics in the Jordan frame.

5.5 NUMERICAL APPROACH TO THE DYNAMICS IN THE JORDAN FRAME

Since, in the Einstein frame, the theory is effectively general relativity coupled minimally to the redefined Higgs field, the numerical approach for this during inflation has been discussed in section 2.4. We shall focus on the Jordan frame here.

5.5.1 Background dynamics during inflation

For numerical computations, we again express all the quantities in terms of the e-folds N. Using the Friedmann equations, the slow-roll parameters can then be expressed as:

$$\begin{aligned} \epsilon_1 &= -\frac{\dot{H}}{H^2} = \frac{\left(f_{NN} - f_N + \kappa^2 \phi_N^2\right)}{(2f + f_N)}, \\ \epsilon_n &= \frac{1}{\epsilon_{n-1}} \frac{d\epsilon_{n-1}}{dN}, \quad n > 1, \end{aligned} \tag{5.20}$$

where the subscript N denotes derivative with respect to the e-folds N. We see that for $f = 1$, we get back the equations derived in section 2.4. Similarly, the Hubble parameter is then expressed as:

$$H(N) = \left(\frac{\kappa^2 V(N)}{\left(3f + 3f_N - \kappa^2 \phi_N^2/2\right)}\right)^{1/2}. \tag{5.21}$$

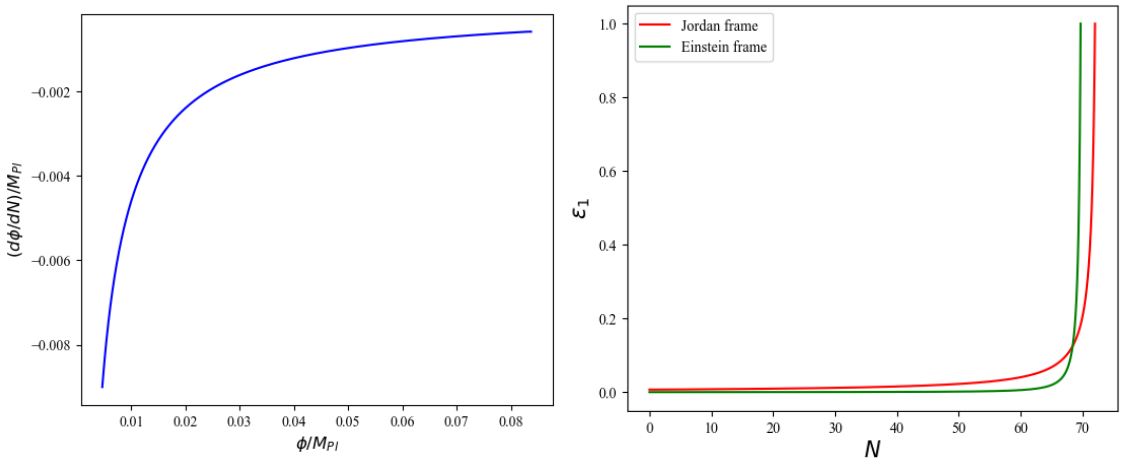

Figure 5.2: Left plot: Phase-space diagram for Higgs inflation in the Jordan frame. Right plot: Evolution of ϵ_1 vs N for Higgs inflation in Einstein and Jordan frames.

The equation of motion governing the evolution of the Higgs field ϕ is very tricky because of the extra term present in Eq.(5.6). Rewriting Eq.(5.6) gives us the following expression:

$$\begin{aligned}\phi_{NN} &+ \frac{\kappa^2\phi_N}{(2\kappa^2 f + 3f_\phi^2)}\left(6f + 4f_\phi\phi_N - f_{\phi\phi}\phi_N^2 - \kappa^2\phi_N^2\right) \\ &+ \frac{V_\phi}{2V(2\kappa^2 f + 3f_\phi^2)}\left(6f + 2f_\phi\phi_N - \kappa^2\phi_N^2\right)\left(2f + f_\phi\phi_N\right) \\ &+ \frac{3f_\phi}{(2\kappa^2 f + 3f_\phi^2)}\left(-4f - 3f_\phi\phi_N + f_{\phi\phi}\phi_N^2 + \kappa^2\phi_N^2\right) = 0,\end{aligned} \tag{5.22}$$

where $f_{\phi\phi} = d^2 f/d\phi^2$ and $\phi_{NN} = d^2\phi/dN^2$. Note that for $f = 1$, we get back Eq.(2.29). With this, we can numerically compute all the background quantities during inflation in the Jordan frame. Figure 5.2 shows the phase-space plot during inflation in the Jordan frame and the evolution of the first slow-roll parameters in the two frames. Again, it is clear that duration of inflation is different in the two frames. For $\chi_i = 5.6M_{\rm Pl}$ in the Einstein frame which corresponds to $\phi_i = 8.37 \times 10^{-2} M_{\rm Pl}$ in the Jordan frame, inflation lasts for about 69.675 e-folds and 72.0008 e-folds in the Einstein and Jordan frames respectively.

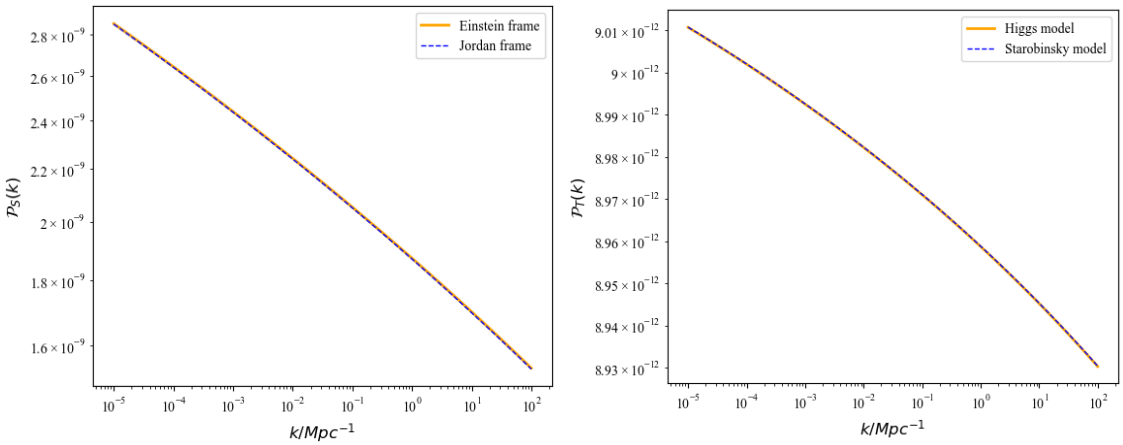

Figure 5.3: Scalar and tensor power spectra in the Einstein and Jordan frames for Higgs inflation.

5.5.2 Primordial perturbations and power spectra during inflation

First, we derive initial conditions for the scale factor. Again, we compute scale factor at the beginning of inflation in the Einstein frame using Eq.(2.31) and then use the following relation to calculate a_i in the Jordan frame:

$$\begin{aligned} \tilde{a}_i &= a_i\sqrt{f(\phi_i)} \\ \implies a_i &= \frac{\tilde{a}_i}{\sqrt{f(\phi_i)}} \simeq \tilde{a}_i exp\left(-\sqrt{\frac{1}{6}}\frac{\chi_i}{M_{\rm Pl}}\right). \end{aligned} \tag{5.23}$$

Here, we have assumed that the mode corresponding to pivot scale leaves the horizon about 50 e-folds before the end of inflation in the Einstein frame which corresponds to the mode leaving the horizon about 52.17 e-folds before the end of inflation in the Jordan frame. Now comes the evolution of curvature and tensor perturbations. The equations of motion governing the evolution of the Fourier modes of the scalar curvature perturbations and the tensor perturbations respectively have exactly the same form as we derived in subsection (4.5.2) i.e. Eq.(4.26) and Eq.(4.28) respectively with:

$$Q = \frac{\phi_N^2 + \frac{3f_N^2}{2\kappa^2 f}}{(1 + f_N/2f)^2}, \tag{5.24}$$

and F replaced with $f(\phi)$. The initial conditions imposed on $\mathcal{R}_k$ are given by Eq.(4.29) with Q given by Eq.(5.24). Similar initial conditions are obtained for the modes of tensor perturbations. Figure 5.3 shows the scalar and tensor power spectrum in the Einstein and Jordan frames for the Higgs inflation model. We again see that they match to a very precision. For the chosen parameters, we get $n_S \simeq 0.9612$ and $n_S \simeq 0.9614$ at the pivot scale in the Einstein and Jordan frames respectively. Also, $r_{0.002} \simeq 3.78 \times 10^{-3}$ in both the frames. We can see that they are in agreement with the observational constraints.

So, we see that the theory of non-minimal coupling of Higgs field to gravitation is still favoured by the observations and is a potential candidate to explain inflation which is interesting since we will be able to explain the epoch of inflation within the context of the Standard Model of particle physics itself. We will come back to the Higgs model in the next chapter but there is one more thing to see before this chapter closes!

5.6 $R + \alpha R^2 \equiv R + \xi\phi^2 R + V(\phi)$...?

Take a look at the plots below, that is, figures (5.4), (5.5) and (5.6).

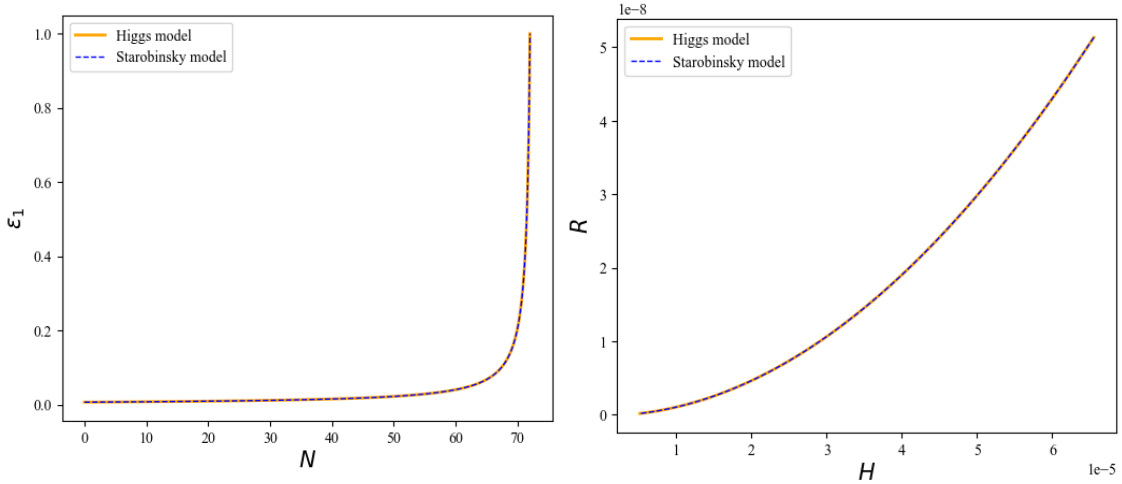

Figure 5.4: Evolution of the first slow-roll parameter ϵ_1 (on the left) and Ricci scalar R vs Hubble parameter H (on the right) during inflation in the Higgs and Starobinsky models in Jordan frame.

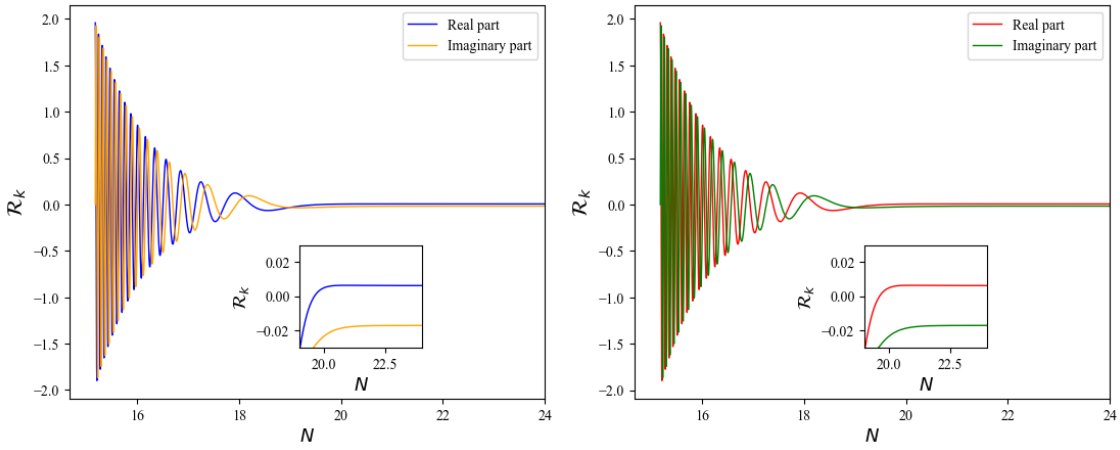

Figure 5.5: Evolution of scalar curvature perturbation corresponding to the mode $k = 0.05\text{Mpc}^{-1}$ during inflation in the Starobinsky (on the left) and Higgs (on the right) models in the Jordan frame.

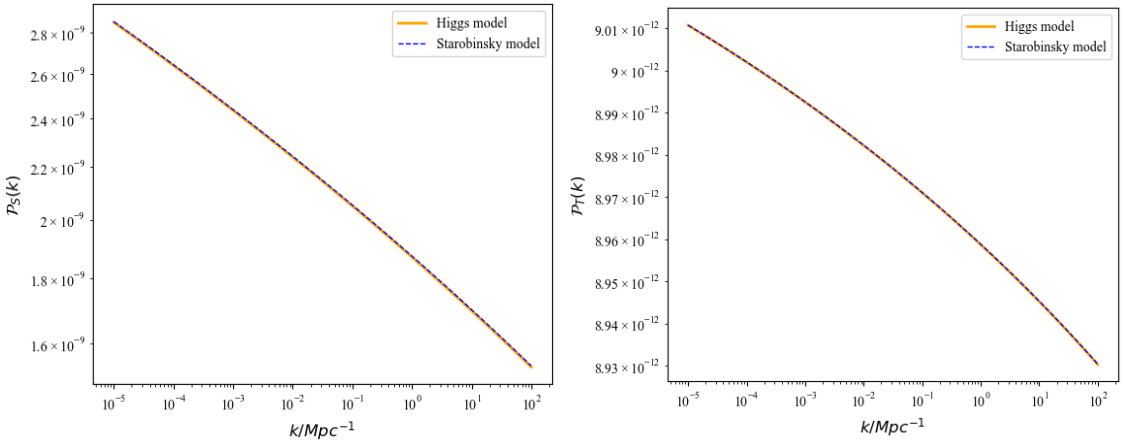

Figure 5.6: Comparison of the scalar and tensor power spectra in the Higgs and Starobinsky models in Jordan frame.

These plots compare the dynamics during inflation of two models. These are the Starobinsky's $R + \alpha R^2$ theory and the theory of Higgs non-minimally coupled to R in the Jordan frame. What do these plots show us? We already saw that the evolution of perturbations and the primordial power spectra is equivalent in the Einstein and Jordan frames which we studied separately for these two models. But what about the background dynamics? That was different (see figures (4.2) and (5.2)). But take a look at the plots in figure (5.4). The background dynamics in these models is also equivalent in the Jordan

frame in which they were originally formulated!

To put it simply:

The Starobinsky's $R + \alpha R^2$ theory is equivalent to the theory of Higgs field coupled non-minimally to gravitation!

This means that instead of using the Higgs field to drive inflation with another complexity in the theory i.e. the non-minimal coupling to satisfy the observational constraints, we can reproduce the same theory by just adding an R^2 term to the Einstein-Hilbert action! without any inflaton field! This would mean that we will not know which of the two theories is what we are looking for from just the CMB observations. Well, so much for that. Of course, there is a lot more to it. The theory of Higgs inflation that we discussed here is not complete. This is the primary focus of our last discussion in this thesis.

CHAPTER 6

MODIFICATIONS TO THE HIGGS MODEL

In chapter 5, we discussed how the non-minimal coupling of Higgs field to gravitation not only drives inflation but also satisfies the observational constraints from the CMB. This is very interesting since we are able to explain inflation in the context of the Standard Model itself. However, there is a serious problem with the pure Higgs inflation and that is the value of the non-minimal coupling constant ξ. To agree with the observational constraints from the CMB, we have to assume ξ to be of the order of 10^4. This value of ξ has been shown to lead to the loss of quantum unitarity at energy scales of about $\Lambda = M_{\rm Pl}/\xi$ which is far below the inflationary regime, that is, $h > M_{\rm Pl}/\sqrt{\xi}$ [29]. The unitarity problem and ways to resolve it will be discussed later towards the end of this chapter. Nevertheless, we need to make sure that the value of ξ remains small.

However, there is another issue with Higgs inflation. The feasibility of the Higgs inflation is dependent on the assumption that the standard Model (SM) description of Higgs is still valid at the energy scales at which inflation is believed to occur. However, it was seen that at renormalization scales of about $\mu > 10^{10}$ GeV, the quartic self coupling of Higgs λ and its beta function take up negative values leading to instability in the theory and so it puts the the theory of Higgs inflation at risk [34]. This may not be a problem if the lifetime of the electroweak vacuum is greater than the age of the universe [35]. Also, the value of λ predicted from the top quark mass measurements and the uncertainties in the Monte-Carlo simulations are large [36].

In this chapter, we shall assume absolute stability of Higgs in this regard and study two ways of tackling the first issue, that is, to somehow reduce the value of ξ and still meet the constraints by modifying the pure Higgs inflation theory.

6.1 RADIATIVE CORRECTIONS TO THE HIGGS POTENTIAL

There have been numerous proposals for the extensions of the Standard Model (SM) to explain physical processes like the existence of dark matter as well as the acoustic oscillations of solar neutrinos. This includes the introduction of sterile fermions like the axion which is considered as a potential dark matter candidate. The introduction of new particles means more Yukawa couplings which would lead to radiative corrections to the inflaton potential as well which would change the inflationary predictions of the theory. These new particles and the associated Yukawa couplings could also explain the small neutrino masses. This is why there has been an interest in connections between neutrino physics and the inflaton. These corrections to the couplings can be studied using the renormalised group equations (RGE). Here, we shall consider the one-loop corrections to the Higgs tree potential proposed by Weinberg and Coleman.

6.1.1 Coleman-Weinberg approximation

In 1973, Coleman and Weinberg showed that for massless scalar fields, radiative corrections to the tree potential can lead to spontaneous symmetry breaking (SSB) [30]. Because of SSB, the scalar field would acquire a vacuum expectation value and due to the Higgs mechanism the scalar fields would acquire a mass. This is also true for a scalar field theory with imaginary mass (negative $\mu^2\phi^2$ term in the Lagrangian density). Specifically, for a quartic potential, the one-loop radiative corrections to the tree potential will lead to an effective potential given by [30]:

$$V(\phi) = \frac{\lambda_{eff}(\phi)}{4}\phi^4 \approx \frac{\lambda}{4}\phi^4 + a\phi^4 ln\left(\frac{\phi}{M}\right), \tag{6.1}$$

where M is the renormalization scale and a quantifies the strength of the radiative correction to one-loop order. Since, we approximated the Higgs potential to ϕ^4 in the Jordan frame in the inflationary regime, we shall introduce these radiative corrections in the Jordan frame and carry out our analysis in the Einstein frame because of the equivalence of perturbations and the power spectra in the two frames.

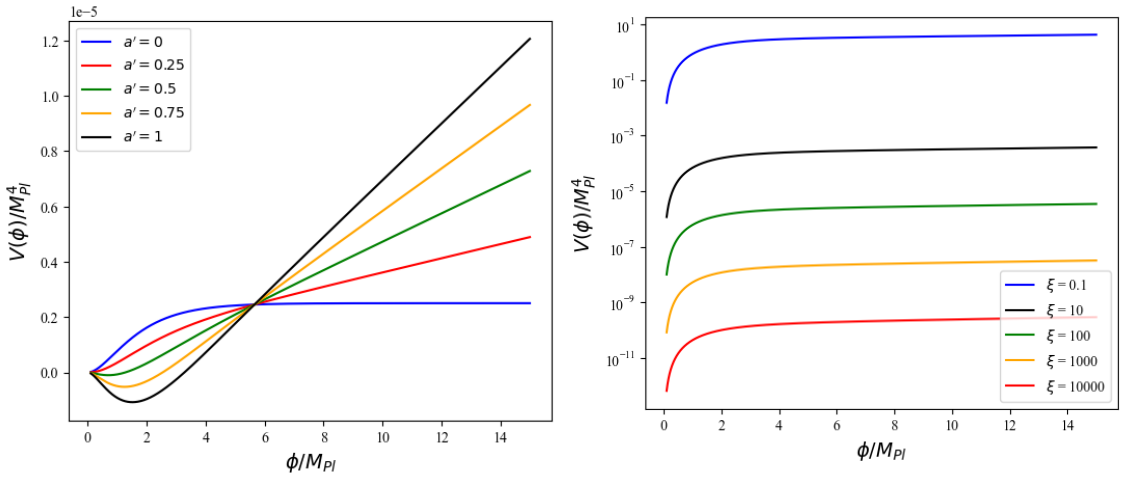

Figure 6.1: Higgs inflation potential in the Einstein frame accounting for the one-loop radiative corrections given by Eq.(6.2). The plot on the left shows how the potential changes for different values of a' for $\xi = 100$ and the plot on the right shows how it changes as ξ changes for $a' = 0.1$.

6.1.2 Radiative corrections to the Higgs potential in the Einstein frame

Using conformal transformation similar to how we did for the Higgs inflation in chapter 5, we redefine the Higgs field in the Einstein frame using Eq.(5.10) and using Eq.(5.11) we rewrite the potential in Eq.(6.1) which turns out to be [32]:

$$V(\chi) \simeq \frac{\lambda M_{\rm Pl}^4}{4\xi^2}\left(1 - e^{-\sqrt{\frac{2}{3}}\frac{\chi}{M_{\rm Pl}}}\right)^2 \times \left[1 + \frac{a'}{2} ln\left(\frac{1}{\xi}e^{\sqrt{\frac{2}{3}}\frac{\chi}{M_{\rm Pl}}} - \frac{1}{\xi}\right)\right], \tag{6.2}$$

in the Einstein frame. Here, $a' = 4a/\lambda$ and we have approximated $M \simeq M_{\rm Pl}$. The inflationary dynamics depends on four parameters from hereon: λ, ξ, a' and N_k, that is the number of e-folds before the end of inflation at which the pivot mode leaves the horizon. Since we already have constraints on N_k, we shall be studying two cases:

- First, we fix ξ, and vary two parameters N_k and a'. For different values of these two parameters, we use the slow-roll approximation of the scalar power spectrum at the pivot mode, that is,

$$P_S(k) = \frac{1}{12\pi^2 M_{\rm Pl}^6}\left(\frac{V^3}{V_\phi^2}\right)_{k=aH}, \tag{6.3}$$

  to fix the value of λ. We are mainly interested in how n_S and r values change as these two parameters change.

- Then, we fix N_k and vary ξ and a' to observe the change in λ, n_S and r.

Figure 6.1 shows the modified Higgs potential in the Einstein frame given by Eq.(6.2) as a' and ξ are varied. We can see that the potential remains smooth so the slow-roll approximation still holds and we expect a nearly scale invariant power spectrum. Since we are working in the Einstein frame, the slow-roll analysis and the numerical approach has already been discussed in detail in chapter 2. We shall move to the plots and further analysis.

6.1.3 Case-1: Effect of variation of a' and N_k on the dynamics

We shall fix $\xi = 100$ and vary a' over the range [-0.1, 1.0] for three different cases, $N_k = 50, 55, 60$. Figures 6.2 and 6.3 show our results on how n_S, r, λ and $H(N_k)$ change as we vary the above two parameters.

- The first observation is that n_s and r are sensitive to the values of N_k and a'. However, this sensitivity is only in the range of $-0.1 < a' < 0.5$ as evident from the n_S vs a' plot in figure 6.2.

- As the value of a' increases and the radiative corrections term dominates the tree potential, we see that the n_S, r and the Hubble parameter do not change which means the product $\lambda a'$ gets fixed because of the pivot mode constraint on the scalar spectrum.

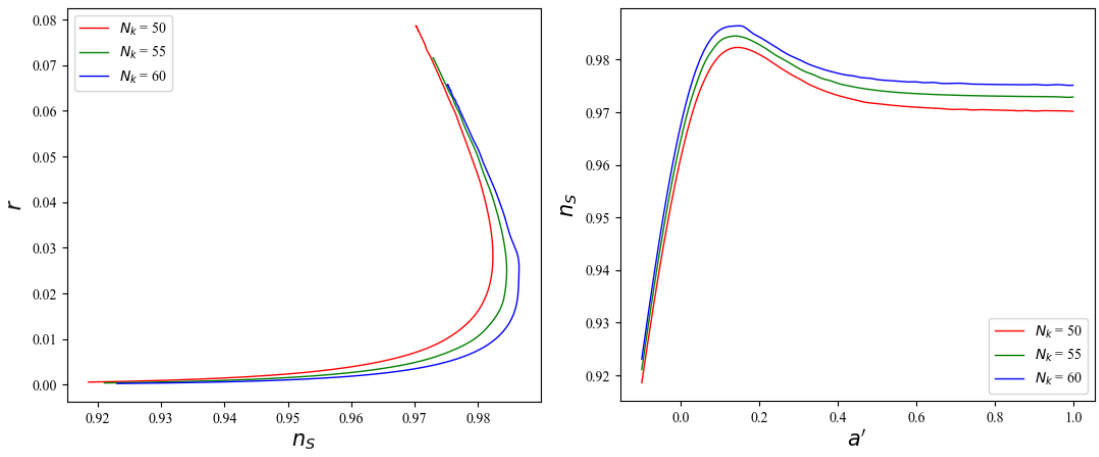

Figure 6.2: Variation in n_S and r as a' changes for $N_k = 50, 55, 60$. The $n_S - r$ plot starts with $a' = -0.1$ in the bottom-left corner and ends at $a' = 1.0$ in the top-right corner of the plot.

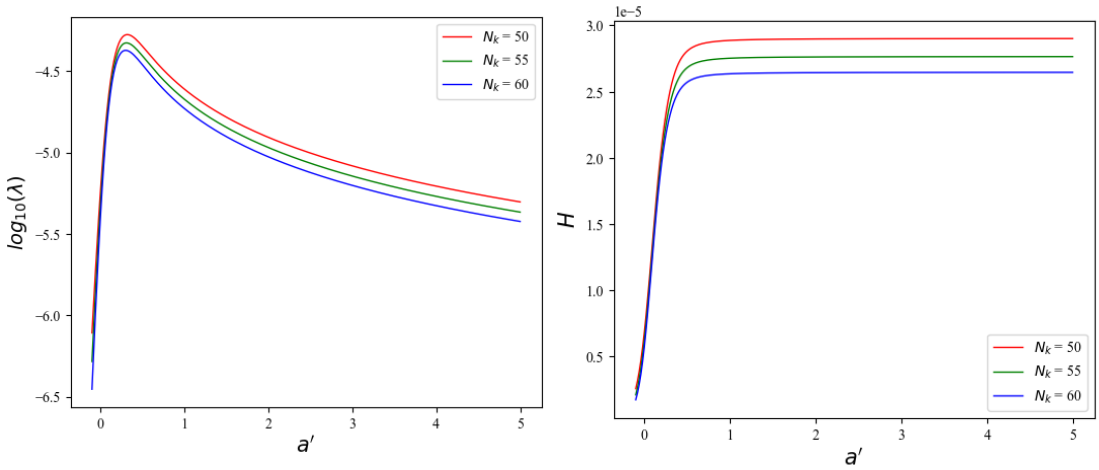

Figure 6.3: The plot on the left shows how λ changes as we vary a' in order to satisfy the constraint on the scalar power spectrum at pivot scale. The plot on the right shows the change in Hubble parameter with a' at the time when the pivot mode crosses horizon.

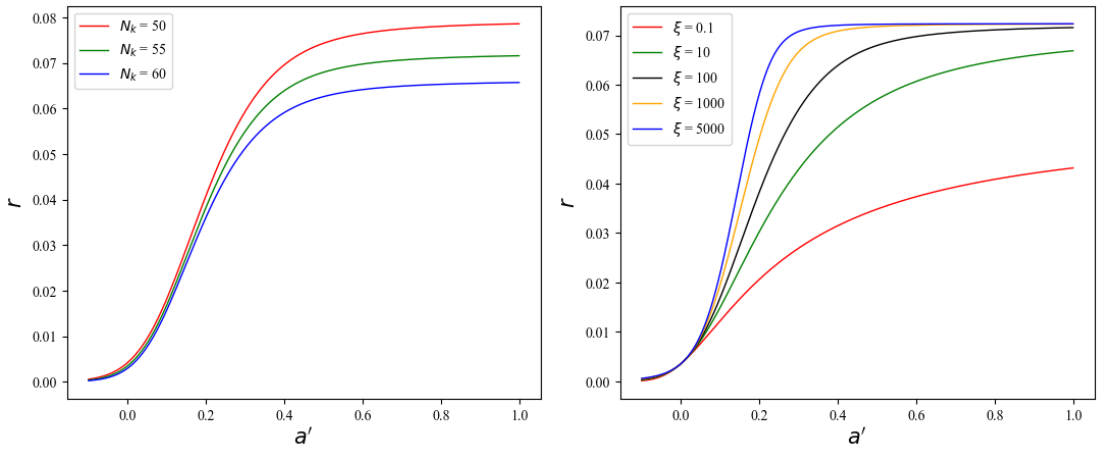

Figure 6.4: r vs a' as we vary the parameters N_k (plot on the left) and the coupling constant ξ (plot on the right). We see that the tensor-to-scalar ratio decreases as ξ decreases which works to our advantage of having a weaker coupling.

We can use the $n_S - r$ plot in figure 6.2 to constrain the parameter a' which requires computing the constraints from CosmoMC runs on the observational data which is beyond our discussion here.

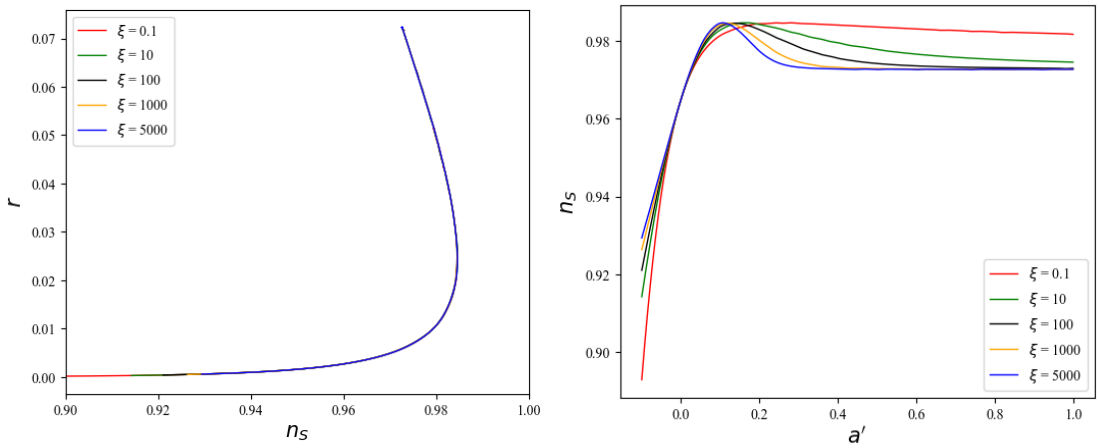

Figure 6.5: Variation in n_S and r as a' changes for five different values of ξ. The $n_S - r$ plot starts with $a' = -0.1$ in the bottom-left corner and ends at $a' = 1.0$ in the top-right corner of the plot. We observe that the $n_S - r$ plot is insensitive to the value of the non-minimal coupling constant.

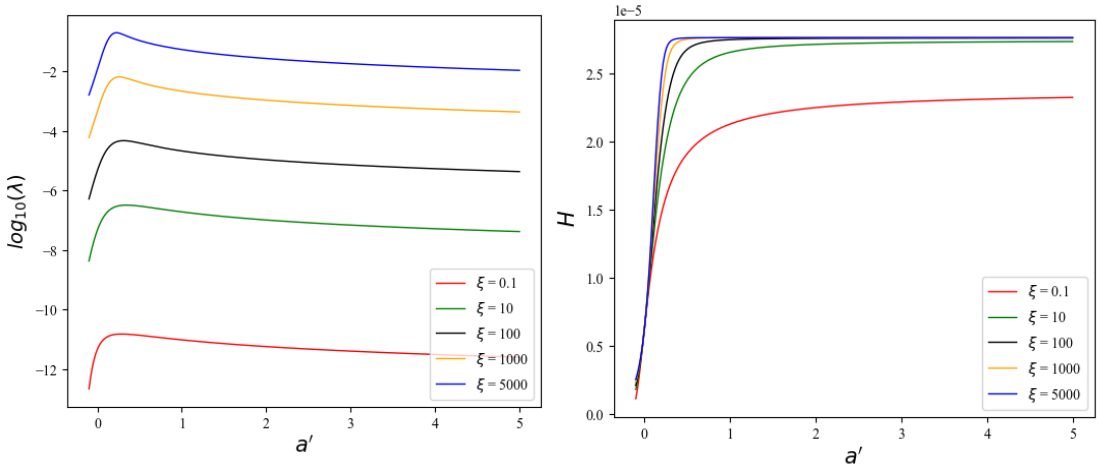

Figure 6.6: The plot on the left shows how λ changes as we vary a' in order to satisfy the constraint on the scalar power spectrum at pivot scale. We see that λ is greater for greater ξ as expected. The plot on the right shows the change in Hubble parameter with a' at the time when the pivot mode crosses horizon.

6.1.4 Case-2: Effect of variation of ξ and a' on the dynamics

Now, we examine the weak and strong coupling regimes of the Higgs to the Ricci scalar using different cases of ξ and a'. We shall fix $N_k = 55$ e-folds. Figures 6.5 and 6.6 show our results. Some observations are:

- The first observation is that the $n_S - r$ plot is insensitive to the value of the

non-minimal coupling ξ. The value of n_S is sensitive to a' only in the range $-0.1 < a' < 0.3$ especially in the strong coupling regime $\xi >= 100$.

- The n_S and r parameters are more sensitive to a' in the weak coupling regime, that is, $\xi < 100$. The smallest range of values of r is obtained for $\xi = 0.1$ as shown in the plot on the right in figure 6.4 and is well within the observational constraints on r. It comes at the cost of a very small value of the quartic coupling λ as shown in figure 6.6.

So, we have seen how the spectral indices and tensor-to-scalar ratio change for different values of the non-minimal coupling constant ξ and the strength of the one-loop correction term quantified by a'. With the observational constraints from cosmology, we can constrain a' and λ and cross-check whether they agree with the constraints from the electroweak observations of the mass of the top quark (see ref. [31, 32, 33] for full discussion).

6.2 RUNNING OF COUPLINGS AND CRITICAL HIGGS INFLATION

So far, we saw the one-loop radiative corrections to the quartic Higgs coupling λ. However, we must consider the running of the couplings λ as well as ξ described by the renormalised group equations. The running of these couplings will have consequences in Higgs inflation. For realistic values of the SM parameters, we observe that the Higgs self-coupling λ attains a minimum value at some energy scale μ. Expanding the running of the coupling λ near this minimum gives us the following [37]:

$$\lambda(\phi) = \lambda_0 + \beta_\lambda ln^2\left(\frac{\phi}{\mu}\right), \tag{6.4}$$

where λ_0 denotes the minimum value of the self-coupling at the energy scale $\mu \simeq 10^{17} - 10^{18}$ GeV [35]. This energy scale is very close to the inflationary regime and has important consequences on the inflationary dynamics. We can similarly expand the non-minimal coupling parameter ξ around this scale [37]:

$$\xi(\phi) = \xi_0 + \beta_\xi ln\left(\frac{\phi}{\mu}\right). \tag{6.5}$$

Note that the running for ξ has a linear order leading energy dependence since it does not attain a minimum value around this energy scale like $\lambda(\phi)$ which has a quadratic order leading dependence on μ. So, the theory of Higgs inflation must include the running of couplings given by Eq.(6.4) and Eq.(6.5).

Therefore, the theory of non-minimal coupling of Higgs to gravitation is described by the action (5.2), the potential (5.3) and the non-minimal coupling function $f(\phi)$ given by (5.5) but with $\lambda \to \lambda(\phi)$ and $\xi \to \xi(\phi)$ given by (6.4) and (6.5) in the Jordan frame. Using conformal transformation of the form $\tilde{g}_{\mu\nu} = f(\phi)g_{\mu\nu}$, we move to the Einstein frame. In the Einstein frame, we again redefine the Higgs field as we did in chapter 5, but the transformation is now different:

$$\frac{d\chi}{d\phi} = \frac{1}{f(\phi)}\sqrt{f(\phi) + \frac{3}{2\kappa^2}\left(\frac{df}{d\phi}\right)^2}. \tag{6.6}$$

Using this transformation, we get following action:

$$S = \int d^4x\sqrt{-\tilde{g}}\left(\frac{\tilde{R}}{2\kappa^2} - \frac{1}{2}\partial_\mu\chi\partial^\mu\chi - V(\chi)\right) - \int d^4x\sqrt{-\tilde{g}}\tilde{\mathcal{L}}_M(f(\phi(\chi))^{-1}\tilde{g}_{\mu\nu}, \psi_M), \tag{6.7}$$

with the potential $V(\chi)$ expressed as:

$$V(x) = \frac{V_0(1 + a\ln^2 x)x^4}{[1 + c(1 + b\ln x)x^2]^2}, \tag{6.8}$$

where the quantities

$$x = \frac{\chi}{\mu}, \quad a = \frac{\beta_\lambda}{\lambda_0}, \quad b = \frac{\beta_\xi}{\xi_0}, \quad c = \xi_0 \quad \text{and} \quad V_0 = \frac{\lambda_0\mu^4}{4}. \tag{6.9}$$

For our analysis, we shall set $\mu = M_{\rm Pl}$. Take a look at the potential in Eq.(6.8). We can see that as $x \to \infty$, the potential is almost constant and we get a plateau like region in the potential which corresponds to slow-roll. However, for suitable values of the quantities a, b and c, the potential has an inflection point.

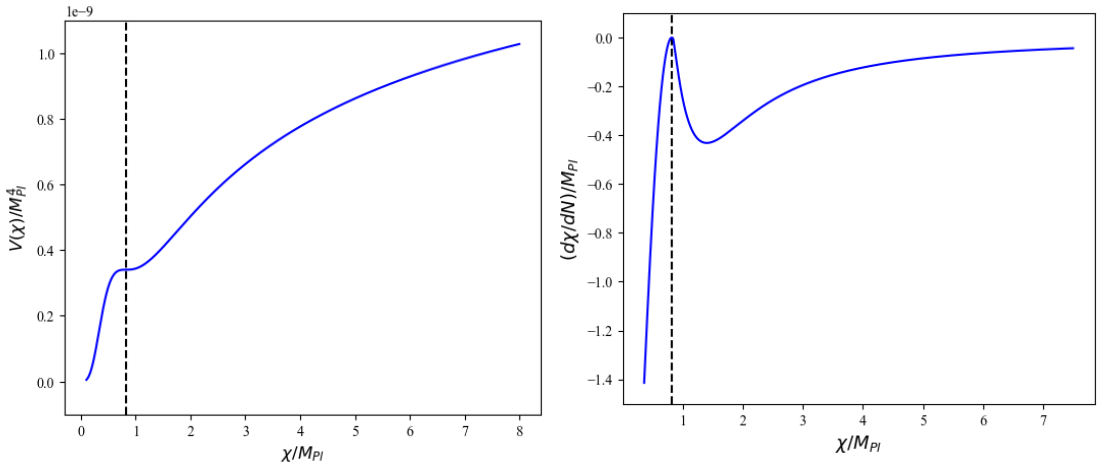

Figure 6.7: Left plot: Potential for the Critical Higgs Inflation (CHI) model. We see that the potential is smooth for $\chi/M_{\rm Pl} \gg 1$ but has an inflection point at $\chi = 0.82 M_{\rm Pl}$. Right plot: Phase-space plot for the CHI model during inflation. The vertical black (dashed) line shows the inflection point in the potential.

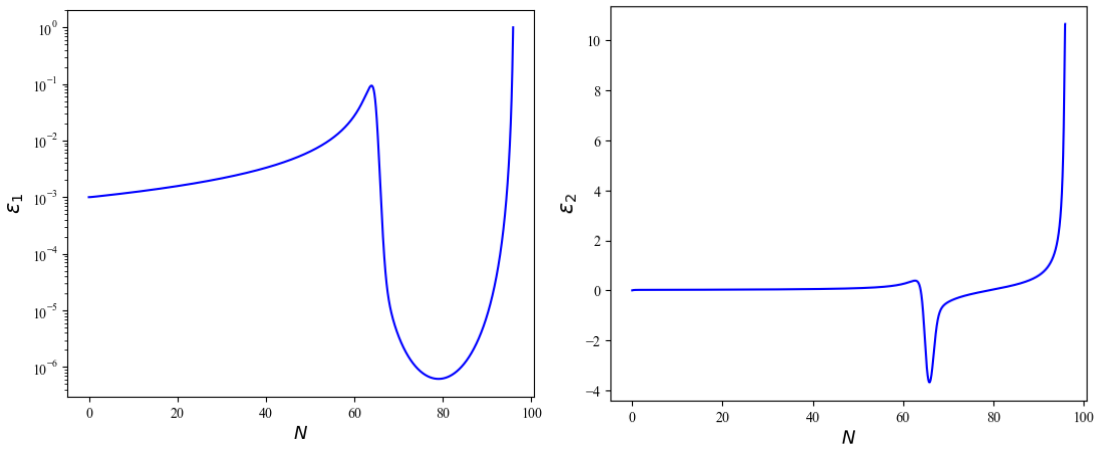

Figure 6.8: Evolution of the slow-roll parameters ϵ_1 and ϵ_2 vs N during inflation in the CHI model. We see that as the field crosses the inflection point in the potential shown in figure 6.7, the value of ϵ_1 takes a significant dip.

6.2.1 Inflationary dynamics in the CHI model

We shall choose the parameters to be: $a = 1.694$, $b = 0.601$, $c = 2.85$ and $V_0 = 5.1 \times 10^{-9} M_{\rm Pl}^4$ [39]. For these values of the potential, the inflection point occurs at $\chi = 0.82 M_{\rm Pl}$. We shall set $\chi_i = 7.5 M_{\rm Pl}$ which leads to about 95.87 e-folds of inflation in the CHI model. Figure 6.7 shows the potential and the phase-space plot for the CHI model. We can see in the phase-space plot that as the field approaches the point of

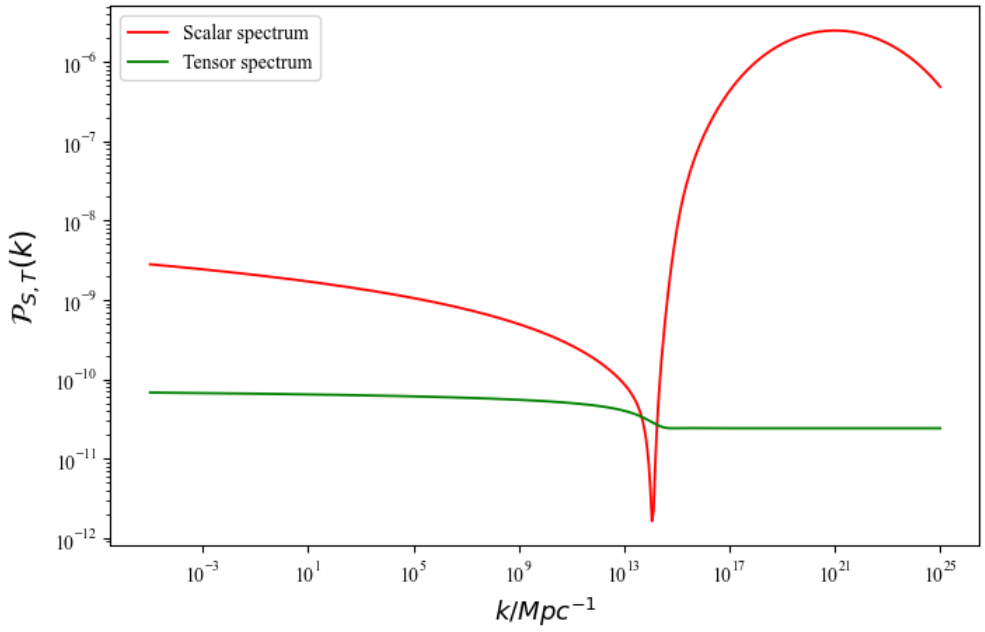

Figure 6.9: Scalar and tensor power spectra in the CHI model. We observe that due to the inflection point in the potential, the scalar power spectrum is amplified at small scales i.e. for large values of the comoving wavenumber k.

inflection, $d\chi/dN$ decreases and then approaches zero which reflects in the slow-roll parameters as well. Figure 6.8 shows the evolution of the first two slow-roll parameters. We see that ϵ_1 take a dip which corresponds to the time when the field crosses the inflection point in the potential.

Now let us see how the power spectra is affected by this. We shall assume that the mode corresponding to pivot scale leaves the horizon about 68 e-folds before inflation ends. The scalar and tensor power spectra for the CHI model is plotted in figure 6.9. We see that for the parameters chosen, $n_S \simeq 0.9629$ at the pivot scale and $r_{0.002} \simeq 0.028$ which agrees well with the observational constraints. But the scalar power spectrum shows a huge amplification at small scales, that is, for large values of k. All this is due to an inflection point in the potential!

The amplification of the scalar power spectrum at small scales has great applications in the formation of primordial black holes (PBHs) [38]. Since the perturbations at small

scales are amplified, when these modes reenter the horizon later in the radiation or matter dominated epoch, they lead to huge density fluctuations which collapse to form structures and PBHs. Also at higher order perturbation theory, the scalar and tensor perturbations do not evolve independently and the amplified primary scalar perturbations source the secondary tensor perturbations which may have left their imprints on the CMB [37, 39]. Therefore, inflection points lead to interesting inflationary dynamics!

6.3 UNITARITY CONCERNS

The unitarity problem is of crucial importance for an inflationary theory especially Higgs inflation that we are primarily focused on. The large non-minimal coupling constant ξ reduces the cut-off scale Λ of the Higgs inflation far below the inflationary energy scale which makes Higgs inflation *unnatural* and calls the self-consistency of Higgs inflation into question. But, what is this cut-off scale Λ? A theory which does not satisfy certain conditions (like a non-renormalizable theory) will have an ultraviolet cut-off Λ and the theory will only be an effective field theory (EFT) i.e. a low-energy approximation of a deeper fundamental theory [29]. In such cases, the traditional perturbative methods that we employ fall apart above this UV cut-off scale Λ.

Consider this. The Planck mass $M_{\rm Pl}$ is considered to be energy scale for the inflationary regime in an expanding universe. However, since the theories should hold up locally, this Planck cut-off scale for our theories must be a fixed value. Now, in an expanding universe, there are certain physical wavelengths that were initially smaller than the Planck length or in other words the physical wavenumbers k associated with those physical wavelengths were larger than the Planck scale $M_{\rm Pl}$. As the universe expanded, these wavelengths were stretched and their energy scales went below the Planck scale. Now, the Hilbert space in quantum mechanics (a low-energy theory yet) is made up of only the modes k below the Planck scale since we do not know what new physics or fundamental theory governs the evolution of universe above the Planck energy scale. However, as the universe expands

the value of physical k of these modes decrease (the corresponding physical wavelengths increase) and the Hilbert space keeps changing. This may lead to a non-unitary evolution of the modes. Moreover, as these modes escape below the Planck scale during inflation, we do not know about their evolution before and so imposing initial conditions is yet another challenge.

This is the reason we look for theories that push the cut-off scale Λ above the Planck scale. Now, it was shown that this cut-off depends on the background value of the field in an inflationary theory. For the theory of Higgs inflation in the Jordan frame that we have discussed so far [29]:

$$\Lambda(\bar{\phi}) = \frac{M_{\rm Pl}^2 + \xi\bar{\phi}^2 + 6\xi^2\bar{\phi}^2}{\xi\sqrt{M_{\rm Pl}^2 + \xi\bar{\phi}^2}}. \tag{6.10}$$

So, there are three limits:

- Low field region: For $\bar{\phi} \ll M_{\rm Pl}/\xi$, it corresponds to a cut-off of $\Lambda \simeq M_{\rm Pl}/\xi$ which is far below the Planck mass.
- Intermediate field region: For $M_{\rm Pl}/\xi \ll \bar{\phi} \ll M_{\rm Pl}/\sqrt{\xi}$, we get a cut-off given by $\Lambda \simeq \xi\bar{\phi}^2/M_{\rm Pl}$ which is again below the Planck mass.
- Large field region: $\bar{\phi} \gg M_{\rm Pl}/\sqrt{\xi}$, we get a cut-off of $\Lambda \simeq \sqrt{\xi}\bar{\phi}$ which is above the Planck mass.

Now, what do these three cases correspond to? The large field region corresponds to the beginning of inflation. The intermediate field region corresponds to when the field oscillates about the minimum of the potential which corresponds to the era of reheating. The low field region corresponds to when the field sits at the minimum of the potential that is, the universe today. Now, the cut-off scales show that even if unitarity is not a problem at the beginning of the inflation, it certainly is towards the end of inflation and especially during the reheating era which leads to a violent decay of the inflaton field during reheating.

There have been different proposals to solve this problem which mainly involve additional

degrees of freedom in the theory. One of these proposals was the addition of an R^2 term to the theory of non-minimal coupling of the Higgs to R. The R^2 term introduces a scalaron degree of freedom which pushes the UV cut-off of the theory above the Planck scale and therefore unitarizes the Higgs inflation theory. Other proposals include the addition of R^3 term instead of R^2 which all are conformally equivalent to two-field models of inflation in the Einstein frame or a single-field inflationary theory driven by a non-canonical scalar field and so on. Nevertheless, a UV complete theory is our ultimate goal!

CHAPTER 7

SUMMARY

The objective of this thesis has been to study inflationary dynamics in modified theories of gravitation and theories of gravitation coupled non-minimally to a scalar field.

In chapter 1, we introduced the idea of inflation and how we can drive inflation with the cosmological constant and scalar fields. We saw that using scalar fields to drive inflation provides a scenario where inflation ends at some point in time and the universe transitions to a radiation dominated epoch.

In chapter 2, we discussed the cosmological perturbation theory and the origin and evolution of primordial perturbations in the framework of single-field inflationary models in general relativity. We also discussed slow-roll inflation and computed the background dynamics and the primordial power spectra for two specific models: the quadratic potential and the axion monodromy model.

In chapter 3, we briefly discussed the theoretical landscape of modified gravity and studied in detail the evolution of universe in an $f(R)$ theory of gravitation. We also discussed how inflation occurs from a purely gravitational origin in these theories as well as the origin and evolution of primordial perturbations in a spatially flat $f(R)$ FLRW universe during inflation. We saw that the equations of motion governing the metric perturbations have the exact same form as in the framework of general relativity and that an $f(R)$ theory is conformally equivalent to a theory of general relativity coupled minimally to a canonical scalar field in the metric formalism thus introducing the Einstein and Jordan frames.

In chapter 4, we investigated one of the earliest proposed $f(R)$ theories: the Starobinsky

model. We studied how inflation occurs without any scalar field in this model and saw that the dynamics of perturbations during inflation agrees with the observational constraints from Planck data. Through explicit numerical computations, we also showed that the primordial power spectra and hence the scalar and tensor perturbations are equivalent in the Einstein and Jordan frames which means that we cannot distinguish which is the physical frame just from the CMB observations.

In chapter 5, we discussed the Higgs inflation model, why we need the non-minimal coupling of Higgs to gravitation and that the inflationary dynamics not only agrees well with the observational constraints but also allows for the self-coupling of Higgs to be within the observational constraints from the electroweak measurements. Once again, through explicit numerical computations we showed the equivalence of the perturbations in the Einstein and Jordan frames. We also showed that for suitable choice of parameters, the Starobinsky model is completely equivalent to the Higgs model.

In chapter 6, we first discussed modifications to the Higgs model due to radiative corrections to the tree potential as per the Coleman-Weinberg approximation which is applicable for massless scalar fields. We then, incorporated the running of the couplings of λ and ξ governed by the renormalised group equations (RGE) which leads to Critical Higgs Inflation (CHI). In the CHI model, we saw that an inflection point in the potential during inflation can lead to amplification of the scalar power spectrum which has applications in PBH formation and generation of secondary gravitational waves. Lastly, we discussed the unitarity problem, a very important issue and different proposals over the years to resolve it.

APPENDIX A

ADM FORMALISM

The ADM formalism is the Hamiltonian formulation of general relativity to view it as an initial value problem and to analyse the dynamics as the evolution of three-dimensional hyperspaces where all the fields are then defined. The idea is to split the spacetime into 3 + 1 dimensions, define and derive the dynamics in these three-dimensional space-like hypersurfaces and then connect two hypersurfaces in time using lapse and shift functions. The derivation of the ADM action for general relativity is rather complicated (see Refs.[40, 41] for full derivation) and we will directly move to the derivation of Eq.(2.18).

In ADM formalism, the spacetime metric is expressed in terms of the lapse function N, the shift functions N_i and the spatial metric h_{ij} and is given by:

$$ds^2 = -N^2 dt^2 + h_{ij}(dx^i + N^i dt)(dx^j + N^j dt). \tag{A.1}$$

The ADM formulation of the Einstein-Hilbert action minimally coupled to a scalar field in terms of the above metric then turns out to be [42]:

$$S = \frac{1}{2}\int dt d^3\mathbf{x}\sqrt{h}\left[NR^{(3)} - 2NV + N^{-1}\left(E_{ij}E^{ij} - E^2\right) + N^{-1}\left(\dot{\phi} - N^i\partial_i\phi\right)^2 - Nh^{ij}\partial_i\phi\partial_j\phi\right], \tag{A.2}$$

where $R^{(3)}$ denotes the intrinsic three-curvature of the space-like hypersurfaces, V denotes the potential of the scalar field ϕ and

$$\begin{aligned} E_{ij} &= \frac{1}{2}\left(\dot{h}_{ij} - \nabla_i N_j - \nabla_j N_i\right), \\ E &= E^i_i. \end{aligned} \tag{A.3}$$

The extrinsic curvature is $K_{ij} = N^{-1}E_{ij}$. We can now write the Hamiltonian from the action given above. We have the Lagrangian and hence we can obtain the Hamiltonian describing general relativity. In ADM formalism, we treat the quantities ϕ and h_{ij} as the

dynamical variables and the quantities N and N_i as the Lagrange multipliers. So, we first choose a convenient gauge to work in. Here, we shall choose the gauge [42, 43]:

$$\delta\phi = 0, \qquad h_{ij} = a^2 e^{2\mathcal{R}}\delta_{ij}. \tag{A.4}$$

This corresponds to the comoving gauge and $\mathcal{R}$ is the physical degree of freedom associated with the scalar curvature perturbations. For now, we shall ignore vector and tensor perturbations. Now, to derive the action governing the equation of motion for the scalar curvature perturbation $\mathcal{R}$, the method is rather straightforward. We first solve the Hamiltonian constraints corresponding to the Lagrange multipliers N and N_i, then substitute the results back in the action (A.2) and after simplifying, we get the final result we want. The Hamiltonian and momentum constraints corresponding to N and N_i respectively turn out to be:

$$\begin{aligned} N^2 &= \frac{E_{ij}E^{ij} - E^2 + \dot{\phi}^2}{R^{(3)} - 2V}, \\ \nabla_i[N^{-1}(E^i_j - \delta^i_j E)] &= 0. \end{aligned} \tag{A.5}$$

For the gauge conditions we have chosen, we get:

$$R^{(3)} = a^{-2}e^{-2\mathcal{R}}(-4\partial_i\partial_i\mathcal{R} - 2(\partial_i\mathcal{R})(\partial_i\mathcal{R})) = -4\partial_i\partial^i\mathcal{R} - 2(\partial_i\mathcal{R})(\partial^i\mathcal{R}). \tag{A.6}$$

Now, to get an action which is to the quadratic order, we solve the above equations (A.5) for N and N_i to linear order by setting: $N = 1 + N_1$ and $N_i = \partial_i\psi + N^T_i$ where $\partial_i N^i_T = 0$. Therefore, to the linear order, we get,

$$\begin{aligned} E_{ij} &= \frac{\dot{h}_{ij}}{2} - \nabla_i\nabla_j\psi - \frac{1}{2}\left(\nabla_i N^T_j + \nabla_j N^T_i\right), \\ E^i_j &= (H + \dot{\mathcal{R}})\delta^i_j - \nabla^i\nabla_j\psi - \frac{1}{2}\left(\nabla^i N^T_j + \nabla_j N^i_T\right), \\ E_{ij}E^{ij} &\approx 3H^2 + 6H\dot{\mathcal{R}} - 2H\nabla_i\nabla^i\psi, \\ E &= h_{ij}E^{ij} \approx 3(H + \dot{\mathcal{R}}) - \nabla_i\nabla^i\psi, \\ E^2 &\approx 9H^2 + 18H\dot{\mathcal{R}} - 6H\nabla_i\nabla^i\psi. \end{aligned} \tag{A.7}$$

Using these approximations, we can solve the constraint equations. Solving the momentum

constraint to the linear order, we get the following results:

$$N_1 = \frac{\dot{\mathcal{R}}}{H}, \qquad \partial^2 N_T = 0. \tag{A.8}$$

That takes care of N. Now, we use the above results and the background equation $3H^2 = V + \dot{\phi}^2/2$ in the Hamiltonian constraint:

$$\begin{aligned}
&\left(1 + 2\frac{\dot{\mathcal{R}}}{H}\right)(R^{(3)} - 6H^2 + \dot{\phi}^2) = -6H^2 - 12H\dot{\mathcal{R}} + 4H\nabla_i\nabla^i\psi \\
\implies &\nabla_i\nabla^i\psi \approx \partial_i\partial^i\psi \approx -\partial_i\partial^i\left(\frac{\mathcal{R}}{H}\right) + \frac{\dot{\phi}^2\dot{\mathcal{R}}}{2H^2} \\
\implies &\psi = -\frac{\mathcal{R}}{H} + \chi \quad \text{where} \quad \partial_i\partial_i\chi = a^2\dot{\phi}^2\dot{\mathcal{R}}/(2H^2).
\end{aligned} \tag{A.9}$$

Note that we have approximated the covariant derivative ∇_i to the partial derivative ∂_i since the connections Γ^i_{jk} are proportional to the derivatives of $\mathcal{R}$ and we have considered only linear-order terms. That takes care of the constraint equations. Now, we just have to substitute these results back in the action, consider terms only to the quadratic order and then integrate by parts:

$$\begin{aligned}
\mathcal{S}_2[\mathcal{R}] = &\frac{1}{2}\int dtd^3\mathbf{x}\left[ae^{\mathcal{R}}\left(1 + \frac{\dot{\mathcal{R}}}{H}\right)(-4\partial_i\partial_i\mathcal{R} - 2(\partial_i\mathcal{R})^2) - 2Va^3e^{3\mathcal{R}}\left(1 + \frac{\dot{\mathcal{R}}}{H}\right)\right] \\
&+ \frac{1}{2}\int dtd^3\mathbf{x}\left[\frac{a^3e^{3\mathcal{R}}}{\left(1 + \frac{\dot{\mathcal{R}}}{H}\right)}(\dot{\phi}^2 - 6(H + \dot{\mathcal{R}})^2)\right] \\
\implies = &\frac{1}{2}\int dtd^3\mathbf{x}\left[ae^{\mathcal{R}}\frac{(H + \dot{\mathcal{R}})}{H}(-4\partial_i\partial_i\mathcal{R} - 2(\partial_i\mathcal{R})^2)\right] \\
&+ \frac{1}{2}\int dtd^3\mathbf{x}\left[a^3e^{3\mathcal{R}}(\dot{\phi}^2\left(1 + \frac{\dot{\mathcal{R}}}{H} + 1 - \frac{\dot{\mathcal{R}}}{H} + \left(\frac{\dot{\mathcal{R}}}{H}\right)^2\right) - 12H(\dot{\mathcal{R}} + H))\right] \\
\implies = &\frac{1}{2}\int dtd^3\mathbf{x}\left[-(ae^{\mathcal{R}})\frac{d}{dt}\left[\frac{-4\partial_i\partial_i\mathcal{R} - 2(\partial_i\mathcal{R})^2}{H}\right] + (a^3e^{3\mathcal{R}})\left[4\dot{H} + \frac{\dot{\phi}^2\dot{\mathcal{R}}^2}{H^2} + 2\dot{\phi}^2\right]\right] \\
\implies = &\frac{1}{2}\int dtd^3\mathbf{x}\left[-(ae^{\mathcal{R}})\frac{\dot{H}}{H^2}\left[4\partial_i\partial_i\mathcal{R} + 2(\partial_i\mathcal{R})^2\right] + (a^3e^{3\mathcal{R}})\left[-2\dot{\phi}^2 + \frac{\dot{\phi}^2\dot{\mathcal{R}}^2}{H^2} + 2\dot{\phi}^2\right]\right] \\
\implies = &\frac{1}{2}\int dtd^3\mathbf{x}\left[(a^3e^{3\mathcal{R}})\left[\frac{\dot{\phi}^2\dot{\mathcal{R}}^2}{H^2}\right] - (ae^{\mathcal{R}})\frac{\dot{\phi}^2}{H^2}\left[(\partial_i\mathcal{R})^2\right]\right],
\end{aligned} \tag{A.10}$$

where we have used the Friedmann equations (1.20) and set $M_{\rm Pl}$ to unity in the derivation.

The subscript i represents sum over i and $(\partial_i \mathcal{R})^2 = \partial_i \mathcal{R} \partial_i \mathcal{R}$. Now, shifting from cosmic time coordinate to the conformal time coordinate, we get:

$$\mathcal{S}_2[\mathcal{R}] = \frac{1}{2} \int \mathrm{d}\eta \int \mathrm{d}^3\boldsymbol{x} \frac{a^2 \dot{\phi}^2}{H^2} \left[(\mathcal{R}')^2 - (\partial \mathcal{R})^2 \right], \tag{A.11}$$

which is the action to the quadratic order governing the scalar curvature perturbation. Similarly, we can derive the action governing the tensor perturbations by working in the gauge [42]:

$$\delta\phi = 0, \quad h_{ij} = a^2(\delta_{ij} + \gamma_{ij}), \quad \partial_i \gamma_{ij} = 0, \quad \gamma_{ii} = 0, \tag{A.12}$$

where γ_{ij} are the physical degrees of freedom associated with the tensor perturbations and are transverse and traceless. Using the above method, the action governing the tensor perturbations turns out to be:

$$\mathcal{S}_2\left[\gamma_{ij}\right] = \frac{M_{\mathrm{Pl}}^2}{8} \int \mathrm{d}\eta \int \mathrm{d}^3\boldsymbol{x} a^2 \left[(\gamma_{ij}')^2 - \left(\partial \gamma_{ij}\right)^2 \right]. \tag{A.13}$$

Note that we have not made any slow-roll approximations in the derivation of these actions.

BIBLIOGRAPHY

[1] Guth, Alan H., *Inflationary universe: A possible solution to the horizon and flatness problems*, Phys. Rev. D **23**, 347–356, (1981).

[2] Will Kinney, An Infinity of Worlds: Cosmic Inflation and the Beginning of the Universe, The MIT Press, (2022). ISBN:9780262046480.

[3] L. Sriramkumar, *An introduction to inflation and cosmological perturbation theory*, arXiv:0904.4584 [astro-ph.CO], (2009).

[4] L. Sriramkumar and T.R. Seshadri, Vignettes in Gravitation and Cosmology, World Scientific, (2012). ISBN:978-981-4322-07-2.

[5] Bruce A. Bassett, Shinji Tsujikawa, and David Wands, *Inflation dynamics and reheating*, Rev. Mod. Phys.**78**, 537, (2006).

[6] David Wands, Lectures on *Cosmological Perturbation Theory*, School on *Physics of the Early Universe*, ICTS, (2022).

[7] S. Weinberg, *Cosmology*, Oxford University Press, Oxford, England, (2008).

[8] Scott Dodelson, *Modern Cosmology*, Academic Press, Amsterdam, (2003).

[9] D. H. Lyth and A. R. Liddle, *Cosmological Inflation and Large-Scale Structure*, Cambridge University Press, Cambridge, England, (2009).

[10] Antonio Riotto, *Inflation and the Theory of Cosmological Perturbations*, arXiv:hep-ph/0210162v2, (2002).

[11] S. Shankar Sastry, *Introductory methods of numerical analysis*, (1984).

[12] Y. Akrami et al, *Planck 2018 results. X. Constraints on inflation*, arXiv:1807.06211 (astro-ph), (2018).

[13] Raphael Flauger, Liam McAllister, Enrico Pajer, Alexander Westphal, Gang Xu, *Oscillations in the CMB from Axion Monodromy Inflation*, JCAP,**1006**,009, (2010).

[14] Debika Chowdhury, V. Sreenath and L. Sriramkumar, *The scalar-scalar-tensor inflationary three-point function in the axion monodromy model*, arXiv:1605.05292 [astro-ph.CO], (2016).

[15] David Lovelock, *The Einstein Tensor and Its Generalizations*, J. Math. Phys. **12**, 498–501 , (1971).

[16] Alessandra Silvestri, Lectures on *Dark energy and modified gravity*, School on *Physics of the Early Universe*, ICTS, (2022).

[17] Shinji Tsujikawa, Antonio De Felice, *f(R) theories*, Living Rev. Relativ. **13**, 3, (2010).

[18] Shin'ichi Nojiri, Sergei D. Odintsov, *Unified cosmic history in modified gravity: from F(R) theory to Lorentz non-invariant models*, Physics Reports: Volume 505, Issues 2–4, Pages 59-144, (2011).

[19] Starobinsky, A.A., *A new type of isotropic cosmological models without singularity*, Phys. Lett. B **91(1)**, 99–102, (1980).

[20] Jai-chan Hwang, *Quantum generations of cosmological perturbations in generalized gravity*, Class. Quantum Grav. **14**, 3327–3336, (1997).

[21] Thomas P. Sotiriou, *6+1 lessons from f(R) gravity* , J. Phys.: Conf. Ser. **189**, 012039, (2009).

[22] Benedict J. Broy, *The Starobinsky Model*, URL: `https://indico.desy.de/event/8990/attachments/59128/71734/Starobinsky.pdf`.

[23] Sagarika Tripathy, Debika Chowdhury, Rajeev Kumar Jain, L. Sriramkumar, *Challenges in the choice of the nonconformal coupling function in inflationary magnetogenesis*, Phys. Rev. D **105**, 063519, (2022).

[24] David J. Griffiths, *Introduction to Elementary Particles, 2nd, Revised Edition*, Wiley-VCH, (2008). ISBN:978-3-527-40601-2.

[25] L. N. Granda, D. F. Jimenez, W. Cardona, *Higgs inflation with non-minimal derivative coupling to gravity*, Astroparticle Physics **Volume 121**, 102459, (2020).

[26] R. Fakir and W.G. Williams, *Improvement on cosmological chaotic inflation through nonminimal coupling*, Phys. Rev. D **41**, 1783-1791, (1990).

[27] Swagat S. Mishra, Varun Sahni, and Alexey V. Toporensky *Initial conditions for inflation in an FRW universe*, Phys. Rev. D **98**, 083538, (2018).

[28] Swagat S. Mishra, Daniel Müller, Aleksey V. Toporensky, *Generality of Starobinsky and Higgs inflation in the Jordan frame*, Phys. Rev. D **102**, 063523, (2020).

[29] F. Bezrukov, A. Magnin, M. Shaposhnikov and S. Sibiryakov, *Higgs inflation: consistency and generalisations*, JHEP **1101**,016, (2011).

[30] Sidney Coleman and Erick Weinberg, *Radiative Corrections as the Origin of Spontaneous Symmetry Breaking*, Phys. Rev. D **7**, 1888, (1973).

[31] J.G. Rodrigues, Micol Benetti, Marcela Campista and Jailson Alcaniz, *Probing the seesaw mechanism with cosmological data*, JCAP **07**,007, (2020).

[32] Jamerson G. Rodrigues, Micol Benetti and Jailson S. Alcaniz, *Possible discrepancies between cosmological and electroweak observables in Higgs Inflation*, JHEP **11**, 091, (2021).

[33] Jamerson G. Rodrigues, Micol Benetti, Rayff de Souza and Jailson Alcaniz, *Higgs Inflation: constraining the top quark mass and breaking the $H_0 - \sigma_8$ correlation*, arXiv:2301.11788 [astro-ph.CO], (2023).

[34] Giuseppe Degrassi, Stefano Di Vita, Joan Elias-Mir´o, Jos´e R. Espinosa, Gian F. Giudice, Gino Isidori and Alessandro Strumia, *Higgs mass and vacuum stability in the Standard Model at NNLO*, JHEP **08**, 098, (2012).

[35] Dhong Yeon Cheong, Sung Mook Lee, and Seong Chan Park, *Progress in Higgs inflation*, J. Korean Phys. Soc. **78**, 897–906, (2021).

[36] Gennaro Corcella, *The Top-Quark Mass: Challenges in Definition and Determination*, Front. in Phys. **7**, 54, arXiv:1903.06574 [hep-ph], (2019).

[37] Manuel Drees, Yong Xu, *Overshooting, Critical Higgs Inflation and Second Order Gravitational Wave Signatures*, Eur. Phys. J. C **81**, 182, (2021).

[38] Jose Mar´ıa Ezquiaga, Juan Garc´ıa-Bellido and Ester Ruiz Morales, *Primordial Black Hole production in Critical Higgs Inflation*, Phys. Lett. B **776**, 345-349, (2018).

[39] H. V. Ragavendra and L. Sriramkumar, *Observational imprints of enhanced scalar power on small scales in ultra slow roll inflation and associated non-Gaussianities*, Galaxies, **11**(1), 34, (2023).

[40] Alejandro Corichi and Dario Núñez, *Introduction to the ADM formalism*, arXiv:2210.10103 [gr-qc], (2022).

[41] Alessandro Danieli, ADM formalism: a Hamiltonian approach to General Relativity, thesis, (2020).

[42] Juan Maldacena, *Non-Gaussian features of primordial fluctuations in single field inflationary models*, arXiv:astro-ph/0210603 [astro-ph], (2005).

[43] Hael Collins, *Primordial non-Gaussianities from inflation*, arXiv:1101.1308v2 [astro-ph.CO], (2014).